Distribution Agreement

In presenting this thesis or dissertation as a partial fulfillment of the requirements for an advanced degree from Emory University, I hereby grant to Emory University and its agents the non-exclusive license to archive, make accessible, and display my thesis or dissertation in whole or in part in all forms of media, now or hereafter known, including display on the world wide web. I understand that I may select some access restrictions as part of the online submission of this thesis or dissertation. I retain all ownership rights to the copyright of the thesis or dissertation. I also retain the right to use in future works (such as articles or books) all or part of this thesis or dissertation.

Signature:

_____ _____

Kristie M. Garza Date

Lights, Gamma, Action: Gamma Visual Flicker Activates Neuroimmune Signaling

By Kristie M. Garza

Doctor of Philosophy
Graduate Division of Biological and Biomedical Science Neuroscience

---

Annabelle C. Singer, Ph.D.
Advisor

James Lah, M.D., Ph.D.
Committee Member

Machelle Pardue, Ph.D.
Committee Member

Malu Tansey, Ph.D.
Committee Member

Levi Wood, Ph.D.
Committee Member

Accepted:

Lisa A. Tedesco, Ph.D.
Dean of the James T. Laney School of Graduate Studies

Date

Lights, Gamma, Action: Gamma Visual Flicker Activates Neuroimmune Signaling

By

Kristie M. Garza

B.S., The University of Texas at Austin, 2014

Advisor: Annabelle C. Singer, PhD

An abstract of

A dissertation submitted to the Faculty of the

James T. Laney School of Graduate Studies of Emory University in partial fulfillment of the

requirements for the degree of Doctor of Philosophy

in Graduate Division of Biological and Biomedical Sciences Neuroscience

2021

Abstract

Lights, Gamma, Action: Gamma Visual Flicker Activates Neuroimmune Signaling

By: Kristie M. Garza

Many neurodegenerative and neurological diseases are rooted in dysfunction of the neuroimmune system. Therefore, the ability to manipulate this system has strong therapeutic potential. Prior work has shown that exposing mice to flickering lights at 40Hz drives gamma frequency (~40Hz) neural activity and recruits microglia, the primary immune cells of the brain. This stimulation, termed gamma visual flicker or 40Hz flicker, provides a novel method to manipulate the neuroimmune system. However, the biochemical signaling mechanisms between 40Hz neural activity and immune recruitment remain unknown. This gap in the literature presents a barrier to develop this stimulation to its full therapeutic potential. In this thesis, we exposed wild-type mice to gamma visual flicker or control flicker stimulations for durations ranging from five to sixty minutes. Following flicker exposure, we assessed cytokine and phosphoprotein networks known to play roles in immune functioning. Using these methods, we found, for the first time, that gamma visual flicker leads to increases in the expression of cytokines known to be involved in microglial recruitment. To identify possible mechanisms underlying cytokine expression, we quantified the effect of the flicker on intracellular signaling pathways known to regulate cytokine levels. We found 40Hz flicker upregulates phospho-signaling within the nuclear factor κ-light-chain-enhancer of activated B cells (NFκB) and mitogen-activated protein kinase (MAPK) pathways. We next used inhibitors of these pathways to prove that activity of these pathways is necessary for the increased cytokine profile seen following gamma visual flicker. Last, we use an established microglia depletion paradigm to show these cytokine signals are not fully dependent on microglia. We then provide evidence to suggest a neuronal origin for our observed neuroimmune signaling changes. The results presented in this thesis are the first to address a possible mechanism underlying the neuroimmune impacts of gamma visual flicker. These results provide a major contribution to the field and will be essential for the use of flicker as a therapeutic for brain disease.

Lights, Gamma, Action: Gamma Visual Flicker Activates Neuroimmune Signaling

By

Kristie M. Garza
B.S., The University of Texas at Austin, 2014

Advisor: Annabelle C. Singer, PhD

A dissertation submitted to the Faculty of the

James T. Laney School of Graduate Studies of Emory University

in partial fulfillment of the requirements for the degree of

Doctor of Philosophy

in Neuroscience

2021

Acknowledgments

I completed this work with the support of many people whom I would like to acknowledge here:

Annabelle, thank you for taking a chance on me. At a time when I was told I could not be a scientist, you not only reminded me this was wrong, but showed me how my personality made me a better scientist. Through watching you, I have learned to be a better teacher, writer, risk-taker, and a more confident woman. Thank you for allowing me to make mistakes and trusting that I would learn from them. Thank you for laughing at my awkward humor and reigniting my excitement for science. I feel incredibly lucky to have had the privilege of working with you.

Levi, thank you for welcoming me into your lab as one of your own and giving me the freedom to fearlessly explore science in your lab. My most joyful moments in graduate school were spent in your lab space.

To my committee members, it has been an honor to learn from each of you. Machelle, thank you for putting as much care into my journey as a person as you did into my science. When I first came to GT, it was so nice to see a fellow neuroscience member in the hallways. Jim, thank you for reminding me my work had clinical value. Your lighthearted humor at my committee meetings challenged me and encouraged me to have more fun with my science. Malu, thank you for your stable mentorship through my entire graduate school experience. I am not sure I would have been able to continue if it had not been for your support during a tough time. Thank you for being the strong Hispanic female role model I didn't know I needed.

My neuroscience friends, thank you for supporting me through the lows and celebrating with me through the highs. Maria Briscione, Archana Venkataraman, and Stephanie Foster: I do not have an older sister, but each of you served the role of one for me during this time. I will be forever grateful for your guidance and friendship. I am a better person for knowing each of you.

My Georgia Tech friends, I used to think changing labs in the middle of graduate school would be terrible. I have since learned things have a funny way of working out. Thank you for always answering SOS calls around IBB and taking pre-covid coffee breaks. Veronica Montgomery, thank you allowing me to be unapologetically myself and laughing along the way. Sitara Sankar, I could not have completed this without your guidance and support both in and out of the lab. Alyssa Pybus, you helped change my life when I first arrived at Tech; thanks for being part of the dream team. I am so grateful to have formed life-long friendships with each of you.

To my family, thank you for your continued loved and support. My future in-laws, Mark and Bonita Davis, Aunt Dee and Uncle Gene, thank you for the countless dinners and providing me a family in Atlanta. Tia Blanca, your phone calls always remind me of home. Thank you for always being there for me. Guelita y Guelito, verlos pasar por tiempos dificies en estos años me ha enseñado lo que es importante en la vida. Cuando estaba pasando por momentos dificiles en la escuela, pensando en ustedes me hacia siguir adelante, gracias. Jenny and Kevin, thank you for reminding me to never take myself too seriously.

Mom and Dad, we did it! I used to be scared to go to school because I could not speak English, and now I have written a whole dissertation. I could not have done it without you two. Thank you for you love, guidance, support, and for instilling in me a love for learning.

Doug, words cannot describe how much your love, support, and encouragement have meant to me these past 11 years. Thank you for going on this journey with me, for being both a shoulder to cry on and a dance partner to laugh with, for the countless trips you took to see me during graduate school and for always talking to me when I needed you, even through different time zones. Can you imagine going back in time and telling the newly dating high-school version of us that one day we will have PhDs and be engaged to be married. I have loved growing up with you.

TABLE OF CONTENTS

Tables & Figures

List of Symbols and Abbreviations

5XFAD - Five familial Alzheimer's disease mutations

a.u.- Arbitrary units

Akt- Protein kinase B

ANOVA- Analysis of Variance

APOE4 - Alipoprotein e4

APP- Amyloid Precursor Protein

ATF - Activating transcription factor

Aβ - Amyloid-beta

AD - Alzheimer's Disease

BCA – Bicinchoninic acid

BSA - Bovine serum albumin

BL/6J- black 6 Jackson laboratory

CNS - Central Nervous System

CX3CL1 - Fractalkine

CXCL- C-X-C Motif Chemokine Ligand

CXCR- CXC chemokine receptor 2

DAMP - Danger-associated molecular patterns

DAPI- 4′,6-diamidino-2-phenylindole

DBS - Deep brain stimulation

DMSO - Dimethyl sulfoxide

Elk - E26 transformation-specific like proein

ERK - Extracellular signal-regulated kinase

FADD - Fas-associated protein with death domain

G-CSF - Granulocyte-macrophage colony-stimulating factor

GFAP - Glial fibrillary acidic protein

GDP- Guanosine diphosphate

GM-CSF - Granulocyte-macrophage colony stimulating factor

GTP- Guanosine triphosphate

HSP- Heat shock protein

Hz – Hertz

IBA - Allograft inflammatory factor 1

IFN- Interferon

IHC – Immunohistochemistry

IL- Interleukin

IP- Intraperitoneal

IP-10 - Interferon- inducible protein-10

IR- Infrared

JNK - c-Jun N-terminal kinase

KC- Keratinocytes-derived chemokine

LED - Light-emitting diode

LIF- Leukemia inhibitory factor

LOOCV- Leave one out cross validation

LPS- Lipopolysaccharide

LV - Latent variable

M-CSF - Macrophage Colony Stimulating Factor

MAPK - Mitogen-activated protein kinase

MCP - Monocyte chemoattractant protein

MEK1- MAPK/ERK kinase

MIG - Monokine induced by gamma interferon

MIP - Macrophage inflammatory protein

mRNA-Messenger ribonucleic acid

ms - Millisecond

MSK1- Mitogen and stress activated protein kinase

n - Number

NFκB - Nuclear factor kappa-light-chain-enhancer of activated B cells

NMDA - N-methyl-D-aspartate

p - Phosphorylated

PAM - Pathogen-associated molecular patterns

PBS - Phosphate-buffered saline

PEG - Polyethylene glycol

PFA - Paraformaldehyde

PKC - Protein kinase C

PLSDA - Partial least squares discriminant analysis

PLX - Pexidartinib

PTSD - Post-traumatic Stress Disorder

RANTES - Regulated on Activation, Normal T Cell Expressed and Secreted

RM - Repeated measures

RNA- Ribonucleic acid

SAPE - phycoerythrin-conjugated streptavidin

SEM - Standard error of the mean

SD- Standard deviation

Tg3xAD Mouse - Triple transgenic alzheimer's disease mouse model

TGF - Transforming growth factor

TNF - Tumor necrosis factor

TNFR - Tumor necrosis factor receptor

VEGF - Vascular endothelial growth factor

VEH- Vehicle

WT - Wildtype

Chapter 1: Introduction

The beauty of neuroscience occurs through the amalgamation of various disciplines into one study of the brain. At its core, neuroscience is a network connecting different fields of study, as it takes a wide range of knowledge to understand how molecular interactions become human behavior. While studying each individual component of the nervous system is informative, some of the most influential discoveries in the field lie in the bridges connecting different disciplines.

Two key fields that have advanced the scope of neuroscience are electrophysiology and neuroimmunology. Electrophysiology studies the electrical activity of neurons to understand the function and dysfunction of cellular communication. Through studying electrophysiology in neuroscience, we have learned how groups of neurons interact within and between brain regions to orchestrate behavior. This field uses electrical recordings and complex analysis techniques to understand how animals integrate sensory input, synthesize it, and ultimately convert it to behavioral output. Through manipulating systems electrophysiology in neuroscience, we have the potential to directly influence the brain.

Neuroimmunology has come to focus as we discover the involvement of the immune system in many brain disorders. Neuroimmunology studies how the brain interacts with the immune system to maintain homeostasis, and how this fails in disease. The field of neuroimmunology involves a complex orchestra including many cellular and protein instruments. Neuroimmunology typically uses molecular assays to visualize and quantify protein and cell dynamics. While neuroscience studies have uncovered many facets of the neuroimmune system, it is a quickly growing subfield, as its role in many neurological processes is actively being elucidated.

Both fields discussed above have been crucial in the development of neuroscience and have recently gained increased attention. However, due to the differences in expertise required for methodologies and techniques, the fields of electrophysiology and neuroimmunology are rarely studied together. As stated earlier, the biggest discoveries in neuroscience happen when bridging two fields, and there is little known about how electrical activity in neurons interacts with immune functions in the brain.

Recent studies show sensory stimulation modulates neuronal activity and recruits the brain's immune cells, but the mechanism of how sensory modulation impacts microglial cells is uncharacterized. The goal of this thesis is to address this gap by elucidating the signaling mechanism by which gamma visual flicker modulates the neuroimmune environment. As such, our predominant hypothesis is that gamma visual flicker induces increases in cytokine expression through neuronal phosphosignaling pathways. The ability to non-invasively modulate the brain's immune environment holds strong therapeutic potential for disorders involving the neuro-immune system, such as Alzheimer's disease, Parkinson's disease, and depression. To continue building on the existing previous literature on the specific topic of sensory gamma entrainment, this thesis will focus mostly on how this potential therapeutic could apply to Alzheimer's disease.

1.1 Scope and Organization

The aims of this dissertation are to establish a mechanism which describes how light flashing at 40Hz frequency activates the neuroimmune system. To establish these aims, we asked what molecular pathways are responsible for activating the neuroimmune system after sensory

stimulation and which cells these signals arise from. This work contributes to the field by providing a bridge that explains two fields, molecular neuroimmunology and electrophysiology. Chapter 1 will serve as an introduction to the current state of exogenous modulation of neuro-electrophysiology, the field of neuroimmunology, and the use of sensory stimulation to modulate the brain. In Chapter 2, I describe the key materials and methodology used for experiments conducted for this thesis. In Chapter 3, I discuss a unique finding from this work, which found that 40Hz sensory stimulation and other frequencies uniquely modulate cytokines in the brain. This 40Hz flicker effect is then compared to other models of neuro-inflammation. In Chapter 4, I characterize the effect of 40Hz flicker on phospho-signaling pathways and confirm these signaling pathways are necessary for the downstream cytokine effects described in Chapter 3. I then provide evidence that these observed signals are localized to neuronal cells and that they do not depend entirely on microglia in Chapter 5. Chapter 6 summarizes the findings of this thesis and follows with a discussion on the major contributions of these outcomes as well as provide future considerations for the work of sensory modulation of the brain's immune environment. At the conclusion of this document, an appendix is used to detail other work completed in the duration of this thesis.

1.2 Gamma Oscillations

Organisms are able to navigate the world through the use of sensory systems. External sensory stimuli trigger coordinated activity in the brain to allow detection of patterns in our environment. The coordinated firing of neurons in specific brain regions allows for proper signal detection and integration. Coordinated neuronal firing is especially important in the visual system, where groups of neurons temporarily synchronize their activity. In a seminal 1989 study,

Gray and Singer made use of visual light sensory stimulation to enhance groups of neuronal firing in the visual cortex [1]. The authors found that the neuronal firing occurred in a synchronous, oscillatory pattern at a frequency of 35-50Hz, suggesting that 1) visual cortex neurons are organized in unique groups of activity and 2) the 35-50Hz frequency range is crucial for visual response. Synchronization of neuronal activity proved to be an important component of sensory processing.

Sensory stimulation leads to evoked rhythms, the coordinated firing of a population of neurons. Experimental external flashing lights, termed flicker, are used to better understand this synchronization of neuronal activity [2]. Flicker leads cells to engage in stimulus-locked activation patterns, 200-300ms after a stimulus onset, up to 50Hz frequency. Coincidently, 300ms is the duration of a single flash response, after which, a stable oscillatory pattern emerges [2].

The stable oscillatory pattern fires in the gamma frequency range, the driving of neural oscillations between 30-80Hz. While there are different ranges of neuronal oscillations, such as theta (~4-10Hz) and alpha (~8-13Hz), gamma oscillations are of particular interest because they are associated with a wide range of perception and cognitive tasks. Until the 1990s, gamma oscillations were thought to be strictly tied to sensory perception. However, in the late 1990s, new research emerged which correlated spontaneous, non-evoked gamma oscillations to cognitive functions. For example, gamma oscillations are involved in facial recognition, attention, and memory [3,4]. The involvement of gamma oscillations in cognitive processes is of particular importance because many neurological and psychiatric disorders show gamma deficits.

1.2.1 Gamma Deficits and Alzheimer's Disease

The role of gamma oscillations in cognition has revealed the importance of gamma deficits in many neurological and neuropsychiatric disorders. Oscillations are crucial for proper brain communication both within and between regions. Deficits in gamma oscillations may account for the lack of integration of communication between brain regions, a critical component of a healthy brain. While gamma oscillations are increasingly found to play an important role in many brain disorders, gamma deficits in Alzheimer's disease (AD) have been a focus of the field. It is important to focus on Alzheimer's disease, as it is the primary form of dementia, and its prevalence is expected to only increase with our aging population.

Changes in gamma oscillations have been found through multiple methods of studying Alzheimer's disease. First, in a non-pathological state, there is indeed a decrease in gamma activity correlated with increased ageing in humans [5,6]. It follows that humans with AD have decreased gamma band synchrony [7]. Similar results have been found when examining evoked gamma responses, with AD patients showing delayed cognitive gamma activity after a sensory stimulation [8]. It should also be noted that there is discrepancy in the field as to the direction of gamma changes associated with AD, and there is little literature clarifying this. For example, other studies have found an increase, rather than decrease in gamma activity in patients with AD, when compared to healthy controls [9,10]. While the direction of gamma changes is unclear, it is evident that there is a change in gamma oscillations associated with Alzheimer's disease.

Animal models of Alzheimer's disease have been used to confirm gamma deficits. In the apolipoprotein E4 (ApoE4) mouse model of AD, there is an attenuation of gamma activity that is suggested to align with observed cognitive deficits [11]. The 5XFAD mouse model of AD shows a decrease in gamma power, when compared to wildtype (WT) littermate controls [12]. Similar

effects are seen in both the APP and the 3xTg AD mouse models [13–15]. Changes in gamma in AD mouse models are thought to underly many of the behavioral deficits seen in these models, specifically related to learning and memory. Gamma activity plays an important role in memory processes in both humans and animals [16–18]. Indeed, increases in gamma oscillations predict successful memory encoding [19]. Changes in gamma appear to predate more traditional pathological measures of AD, such as amyloid pathology [20]. For these reasons, modulating gamma oscillations has strong therapeutic potential.

1.2.2 Gamma Entrainment

Oscillations occur naturally in the brain and are linked to crucial neuronal functions. The ability to modulate brain oscillations, termed entrainment, has provided the ability to ask question of causation, rather than correlational, between brain oscillations and cognitive outcomes. Indeed, it is possible to use gamma entrainment to modulate memory.

Modulation of brain oscillations is accomplished using a variety of methods. Deep brain stimulation (DBS), the direct electrical stimulation of brain tissue, has been used with the hope of improving memory in humans, with mixed results. While some studies show that DBS at 50Hz frequency during a period of learning enhances memory, other studies find that this stimulation actually impairs memory retrieval [21,22]. DBS involves an invasive neurosurgery and is usually done in patients with neurological disorders, such as epilepsy and depression. The invasive nature along with the mixed results of DBS, make it a questionable method to pursue therapeutically.

Optogenetics used in animal provides a more direct method for gamma entrainment. While optogenetic techniques are also invasive and cannot be used therapeutically, the precision

of these experiments has helped understand gamma entrainment more scientifically. Optogenetic stimulation restores gamma oscillations and improves memory in mice with plaque depositions [18]. Optogenetically-induced gamma also reduces plaque in mouse models of AD [12]. These studies provide strong evidence for the use of gamma modulation therapeutically in humans.

In order to have a strong therapeutic, it is important to develop a non-invasive, easy to implement strategy, as optogenetics and DBS would not be viable options for most humans. For this, the field returned to previous findings on the use of sensory stimulation techniques, as described earlier in this section. Using light stimulation to entrain gamma has similar effects to optogenetic stimulation [12]. Sensory stimulation, termed flicker, entrains gamma, reduces amyloid beta, and improves memory in mouse models of AD [12,23]. Using sensory stimulation to evoke gamma oscillations has since been more studied in both humans and animals.

It has become clear that gamma entrainment does ameliorate behavioral and pathological consequences of AD. While more research has been done to make sensory modulation of gamma a promising therapeutic, most of this research is in the field of neuro-electrophysiology. With this, we know that sensory flicker successfully leads to gamma entrainment, but we have little understanding of how gamma entrainment helps alleviate AD-like symptoms.

To fully understand how gamma entrainment could be a therapeutic for AD, it is important to focus on how it impacts the brain's immune system, as this has been poorly understood. AD triggers complex changes in the immune system, such as increased cytokine expression and cell death [24]. Further, as mentioned earlier, AD is not the only disorder gamma entrainment could help. Many neuro-diseases associated with gamma deficits in humans also show deficits in neuroimmune function, such as depression and schizophrenia [25–28]. For these

reasons, it is important to have a thorough understanding of the brain's immune system to fully incorporate into a potential use of gamma entrainment as a therapeutic.

1.3 The Neuroimmune System

Neuroscience and immunology have long been separate fields. However, the two systems have been found to not only communicate, but their bi-directions interactions are crucial for proper brain function. While the brain communicates with the body's peripheral immune system, the brain also has its own immune system, the neuroimmune system. The neuroimmune system is utilized for local central nervous system (CNS) issues, and it is implicated in many diseases and disorders of the CNS. Importantly for this thesis, gamma entrainment also modulates the neuroimmune system.

1.3.1 Cells of the Neuroimmune System

This section will focus on cells classically involved in immune mechanisms in the brain, including immune response, signaling, and healing. It is important to note that all cells in the brain, by nature of being a part of the nervous system, are likely to be involved in many neuroimmune processes.

Brain cell types are classified as either neurons or glial cells, with glial cells further diving into macro- and microglia. Macroglia include oligodendrocytes and astrocytes. While oligodendrocytes have long been established as myelin-producing for neurons, the role of astrocytes has been less clear. Astrocytes are involved in maintaining the neuronal environment, with newly elucidated roles. They release immune proteins and activate to accompany neuronal damage and microglial response, allowing them to be classified as immune cells [29,30]. The role of astrocytes is constantly expanding, and current research is actively finding they play an

important role in many brain functions. A discussion on the potential involvement of astrocytes in gamma entrainment will be further explored in the Chapter 5 of this thesis.

Microglia, known as the brain's resident immune cells, are traditionally thought to play the largest role in the brain's immune functions. Microglia, like macrophages, are derived from myeloid cells. This similarly in origin may explain why the two cell types are so alike. In fact, microglia are so similar to macrophages, it took 150 years for them to be classified as their own distinct cell type. However, microglia do play a distinct role in responding to the central nervous system's unique environment.

Microglia use their processes to actively observe and sense changes in the environment. When microglia detect an aberration in the brain's ecosystem, they respond in various ways. The correct vocabulary to describe this microglial response has been controversial. Some researchers will refer to responding microglia as "activated" versus "resting." When "activated", some microglia are said to take on an M1 or M2 phenotype, terms originated for describing macrophages. M1 describes pro-inflammatory microglia, while M2 describes anti-inflammatory microglia. These types of bimodal distinctions in describing microglia are controversial because they limit the proper study of microglia as dynamically changing cells [31].

A key component of a microglial response involves a change in microglial morphology, which some researchers have used to classify microglia. Using morphological measures may be a more accurate way of describing microglia, as this allows for a more dynamic view of a microglial response. Importantly, changes in microglial morphology allow researchers to detect differences in microglial response, without having to classify microglial type.

From examining differences in microglia, it is clear they respond to changes in the brain's environment. While there is still much to discover in this field, a microglial response

entails a range of consequences, involving modulating neuron and synaptic behavior [32]. Importantly, microglia are also responsible for clearing pathology from the brain [33,34]. When microglia sense a dysfunction in the neuronal environment, they migrate to the region and use signaling mechanisms to recruit other immune cells in an attempt to fix the issue. This function is of special relevance when focusing on AD, as microglia phagocytose toxic amyloid plaques related to AD [33,34]. While the action of microglia is an adaptive feature of the human brain, chronic microglial reactive activity, leading to prolonged neuroinflammation, is harmful to the overall health of the brain.

Another key role of glial cells is communication with neurons. While neurons are categorically separate from glial cells, their role in the immune system must not be disregarded. It has long been evident that bi-directional communication between and within cell types is crucial, particularly between microglia and neurons [35]. While neurons are not traditionally thought of as immune cells, recent research has elucidated their role in immune interactions.

1.4 Neuroimmune Signaling Mechanisms

Interactions within and between cell types in the neuroimmune system are crucial to the proper functioning of the larger system. Neuroimmune signaling mechanisms are especially important in responding to abnormalities in the brain. For example, microglia are recruited to sites of irregularity upon sensing signals, such as danger-associated molecular patterns (DAMPs), pathogen-associated molecular patterns (PAMs), and cytokine signaling [36]. A phosphorylation cascade is triggered in immune cells to lead to a further release of signals to recruit more cells and remove or fix the irregularity in the brain. It is important to note here the many mechanisms of positive and negative feedback within neuroinflammatory pathways,

causing signals to further amplify of themselves, often making it difficult to delineate the origin of signaling pathways.

1.4.1 Phosphoprotein Pathways

Inflammatory activity is usually mediated by intracellular signaling cascades. These protein sequences lead to an array of downstream effects, and the pathways are composed of many sub-components. Phosphoprotein pathways are therefore easy to modulate, allowing a cell to quickly respond to a rapidly changing extracellular environment. Key pathways involved in the brain's immune response include the the nuclear factor kappa-light-chain-enhancer of activated B cells (NFκB) pathway and the mitogen-activated protein kinase (MAPK) pathway.

1.4.1.1 NFκB

The NFκB pathway is a more traditionally established pathway for inflammation throughout the body. The NFκB pathway responds to signals of cell stress or injury. The activation of the NFκB pathway ultimately leads to an immune or inflammatory response through the control of gene transcription. At rest, the NFκB dimer (composed of p50 and RelA) is in the cytoplasm bound to an IKKα/β protein unit (Figure 1.1). After an external signal triggers the start of the NFκB pathway, IκB Kinase (IKK) is recruited, and phosphorylates the IKKα/β unit. These phosphates mark the IKKα/β for ubiquitination and ultimately degradation, leaving NFκB alone and able to translocate to the nucleus and act as a transcription factor to induce changes in gene transcription.

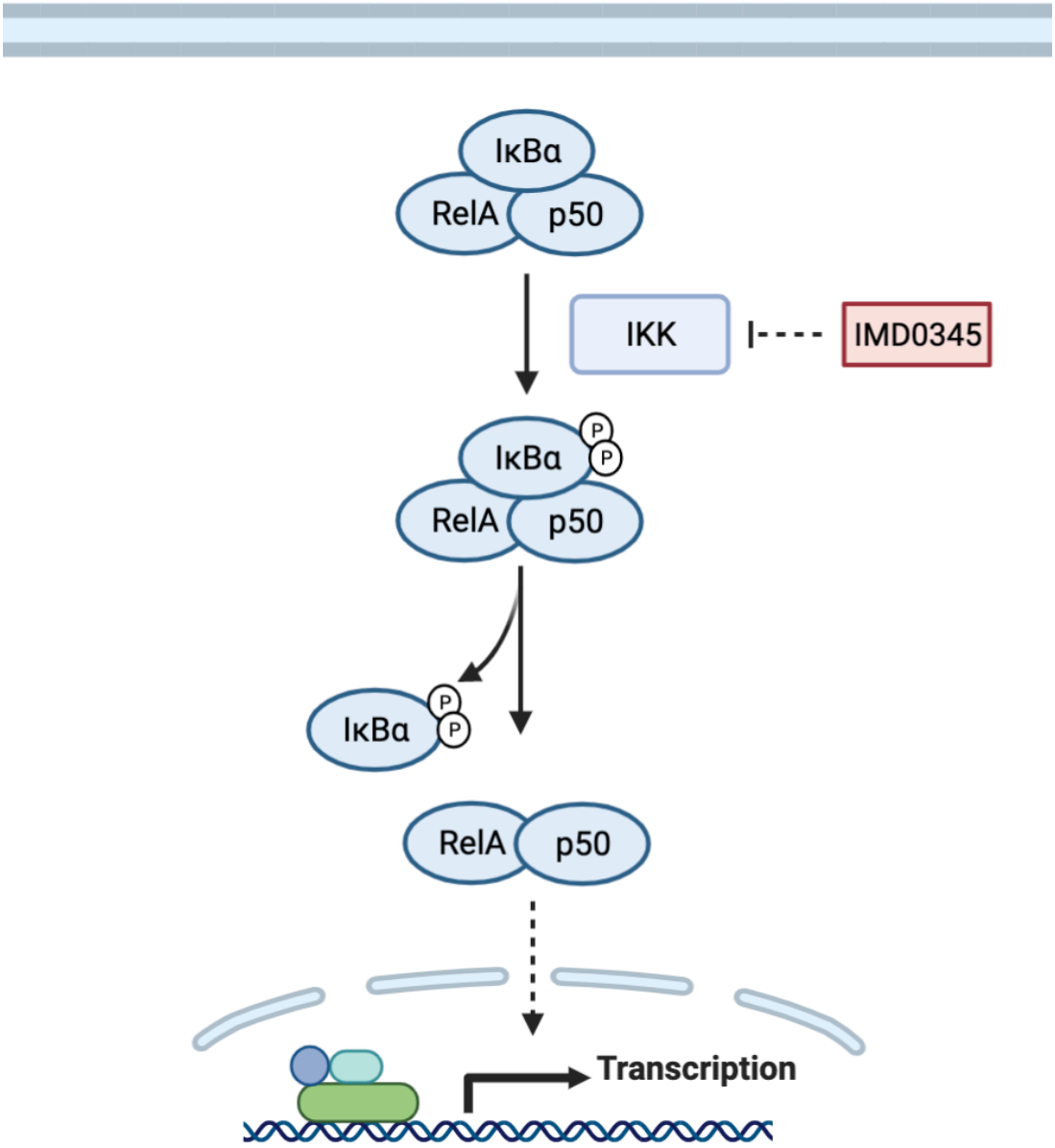

***Figure.0.1.1**: **Simplified diagram of the NFκB pathway**.*

The NFκB dimer is compose of p50 and RelA. At rest, it is in the cytoplasm. Upon activation, IKK, a kinase, is recruited, and phosphorylates the IKKα/β unit(IκBα), removing it from the complex. NFκB is then translocate to the nucleus and acts as a transcription factor. Inhibiting the IKK kinase is a potential mechanism for inhibiting this pathway. This is done by the IMD0345 drug, represented in red.

Due to its involvement in neuroinflammation, the NFκB pathway is highly associated with chronic inflammation, and as such, many neurodegenerative disorders, including AD [37–39]. In fact, post-mortem analysis of the brains of patients who suffered from AD show an increase in NFκB activity in cells located near amyloid beta plaques [40]. This, along with similar work, suggest NFκB is either a consequence of the amyloid beta plaques, works to fight off the amyloid plaques, or more likely, a mixture of both. Further, amyloid plaques have been shown to stimulate both the NFκB and MAPK pathways to elicit the production of proinflammatory cytokines [41]. Thus, both the NFκB and MAPK pathways function as intracellular signaling pathways to change cell behavior, and this is done through the change in downstream gene transcription.

1.4.1.2 MAPK

The MAPK pathway is composed of a series of serine/threonine MAP kinases that function to phosphorylate the next kinase. The pathway is usually triggered by an extracellular event, such as stress to the cell. This extracellular signal leads to the activation of a MAP Kinase Kinase Kinase (MAP3K). The MAP3K phosphorylates a MAP kinase kinase (MAP2K), ultimately phosphorylating a MAPK. There are different pathways that compromise MAPK signaling (Figure 1.2). These pathways are named after the last MAP regulatory kinase. Three of these sub pathways are extracellular signal-regulated kinase (ERK), c-Jun N-terminal kinase (JNK), and p38 (Figure. 1.2). Each of these functions as a MAPK, acting as a kinase to activate downstream proteins involved in a wide array of functions, ultimately leading to the change in transcription of proteins in the cell nucleus involved in cell functions, such as cell growth and proliferation, apoptosis, and inflammation.

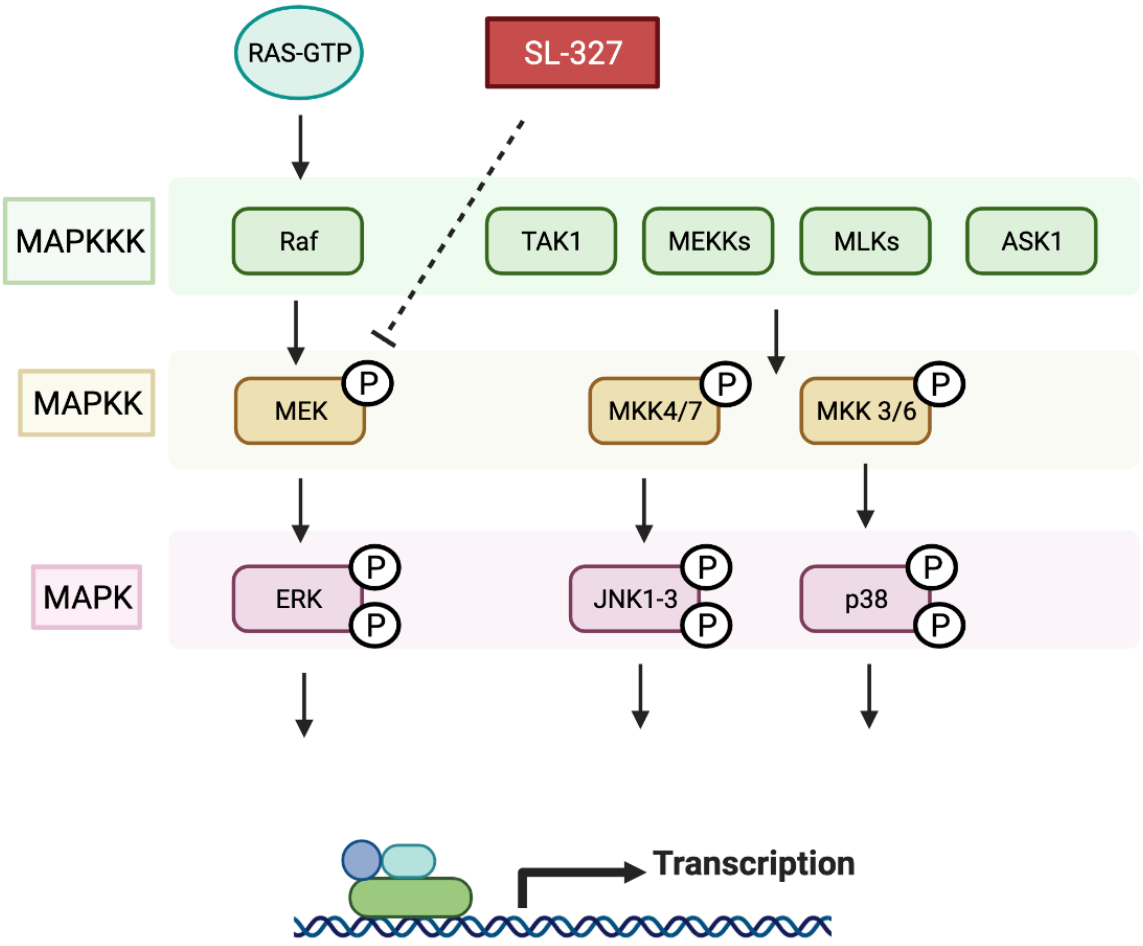

Figure 1.2: Simplified diagram of the MAPK pathway.

The three main nodes of the MAPK pathway, ERK, JNKN, p38, are represented on the pink. This thesis focuses on the ERK pathway, which is inhibited using SL-327, represented in red. SL-327 inhibits MEK phosphorylation.

Of these sub-pathways the ERK pathway is the best characterized. The MAPK ERK pathway in the brain is involved in crucial brain functions, such as learning and memory [42].

More recently, the ERK pathway has also been implicated in immune functions, and treatments to reduce neuroinflammation do so through the MAPK ERK pathway [43]. Interestingly, dysregulations in the MAPK ERK pathway are also associated with neurodegenerative disorders, such as AD [44,45].

1.4.2 Cytokines

Cytokines are critical upstream activators of and downstream products of phosphoprotein pathways. Cytokines are small immune proteins that function as signals in the brain. They both signal to initiate the activation of phosphoprotein cascades as well as are initiated by these pathways.

Cytokines are categorized into several major groups, based on their function. Cytokine groups usually include proinflammatory cytokines, anti-inflammatory cytokines, growth factors, and chemokines. Pro-inflammatory cytokines function to induce inflammation and increase immune activity, while anti-inflammatory cytokines typically function to suppress pro-inflammatory cytokines and activity. Growth factors are cytokines which promote cell proliferation and differentiation. Chemokines are often classified separately from cytokines as they are strong regulators of immune cell migration and recruitment. Chemokines function as chemotaxic signals to actively recruit immune cells to a site of injury. Several chemokines types are upregulated in the brains of AD patients [46–48].

Classifying cytokines by a key function helps identify their broad role in many systems. However, most cytokines serve multiple roles and have a place in multiple groups, depending on the circumstance, concentration, and environment. Therefore, like classification of microglia,

this may be another instance where categorizing biological entities hurts rather than helps progress knowledge.

Further, cytokines are found in most neuroinflammatory and neurodegenerative disease. In an AD mouse model, for example, cytokine levels directly correlate with levels of amyloid beta [49]. Therefore, the ability to modulate cytokines is of special importance for therapeutic potential.

1.4.3 Neuroinflammation

A common thread through the components of the neuroimmune system is their involvement in neuroinflammation. Neuroinflammation is a general term referring to the activation of the neuroimmune system. Like other body parts, the brain becomes inflamed to fight off infection and injury.

A neuroinflammatory response is classically characterized as either pro-inflammatory or anti-inflammatory, which is why cell types and proteins often get classified in similar ways. Pro-inflammatory responses typically consist of the activation of immune cells and the release of pro-inflammatory cytokines. Anti-inflammatory responses in the brain work to alleviate or prevent an inflammatory response. Again, there is nuance in these classifications. Neither pro- nor anti-inflammatory should be thought of as “good” or “bad”. The proper homeostatic balance of the two given the situation (at rest, acute injury, chronic injury) is crucial for proper brain health.

Both of these types of neuroinflammatory responses are critical for proper brain functioning. It is important to note, that although typically thought of as negative, pro-inflammatory responses are a necessary part of the brain’s immune system. A proinflammatory response is a sign that the brain is actively working to fight off a threat. Usually, this is a helpful and necessary

component of a healthy brain. However, chronic inflammation, as is associated with many neurodegenerative disorders, is damaging to brain function. Because inflammation is necessary for brain function but, under certain conditions, can be harmful, just how much neuroinflammation is optimal in the brain is still an open research question.

The neuroimmune system's primary responsibility is to maintain a healthy homeostatic neural environment. Still, recent research has shown the involvement of this system in many aspects of brain function. For this reason, the proper functioning of the neuroimmune system is critical for brain health and function, and the ability to modulate this system holds large therapeutic potential.

1.5 Gamma Entrainment and the Neuroimmune system

As stated earlier, the field of neuro-electrophysiology and the neuroimmune field are rarely examined together. However, recent studies show that the external modulation of neuronal activity leads to immune system recruitment [12,23]. This is specifically relevant when considering the therapeutic relevance of gamma entrainment. Gamma entrainment could help restore gamma oscillations in the brain, deficits in AD, while simultaneously triggering the brain's immune system. This interaction would allow for a multi-modal therapeutic that could prompt a response from two critical biological systems involved in AD, neural activity and neuroimmunology. Research using gamma entrainment to modulate the brain has seen a steep increase in the past couple of years. The first support for this idea was showing that gamma entrainment, through optogenetics, lead to changed microglia morphology, a decrease in amyloid plaques, and an increase in colocalization of microglia and amyloid [12].This research then drew from earlier work in the field to show that using flickering lights, at 40Hz frequency, termed

flicker, also induced very similar electrophysiological and microglial changes [12]. This ground-breaking finding was revolutionary to the field, but also opened the door to many more questions utilizing this technique.

Since the 2016 original finding, more work has been done to expand on the validity of flicker. In 2019, flicker was found to drive gamma in deeper sub-cortical brain regions, making it more applicable to studying it for AD [23]. Flicker was also proven to improve learning and memory as well as decrease synaptic loss in a mouse models of neurodegeneration [23,50]. Last, the effect of flicker on the brain's immune environment has further been confirmed and expanded on. 40Hz flicker leads to changes in microglia, astrocytes, and vasculature, as well as reduces neurodegeneration and inflammatory gens within the brain [23,50]. This past research provides rational for studying flicker as a therapeutic for neurodegenerative disease, especially AD. However, it is incomplete, as the mechanism underlying these changes is still unknown. It is important to understand how 40Hz flicker is impacting cellular and molecular changes to fully understand its clinical value as well as further its scientific understanding.

1.6 Thesis Objectives and Hypothesis

This introduction has presented research spanning two very different fields and concludes with an overview of recent studies that have demonstrated an interaction between the two fields. From previous research, it is clear that visual gamma entrainment recruits microglial cells, which are suggested to be responsible for the uptake of amyloid beta. However, this discovered interaction between neural activity and microglial recruitment opens the door to many more questions, such as how exogenously driving gamma neural activity activates the neuroimmune system. Thus, the purpose of this thesis is to understand the mechanism between visual flicker

stimulation at 40Hz and the immune response. As such, the objectives of this thesis are to 1) characterize the immune response following gamma visual flicker, 2) establish the molecular mechanism driving this response, and 3) determine which cells generate the response to 40Hz flicker. The primary hypothesis is that 40Hz visual stimulation (gamma flicker) leads to an increase in neuronal phosphosignaling pathway activity, which triggers a release of cytokines (Figure 1.3).

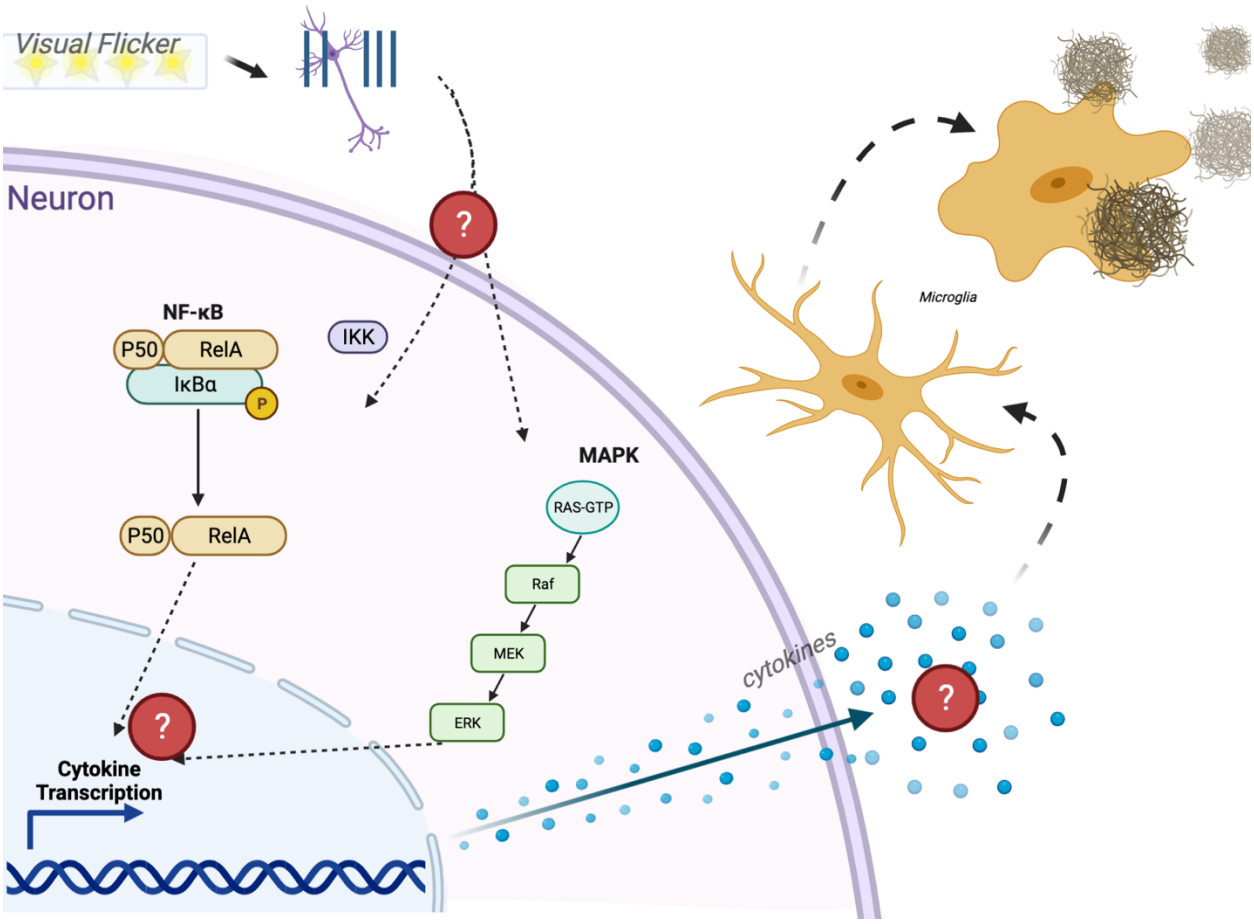

Figure 1.3: Hypothesize Mechanism Explored in Dissertation.

Gamma visual flicker leads to gamma entrainment, represented here by modulation in neuronal spike patterns. We hypothesize gamma visual flicker leads to changes in activity of phosphoprotein pathways in neurons, which causes an increase in cytokine transcription, ultimately changing the neuroimmune environment after flicker. Red question mark circles represent questions explored in this dissertation.

Chapter 2: Materials and Methods

P*ortions of this chapter were adapted from the following publication:*

Garza, K. M., Zhang, L., Borron, B., Wood, L. B., & Singer, A. C. (2020). Gamma Visual Stimulation Induces a Neuroimmune Signaling Profile Distinct from Acute Neuroinflammation. Journal of Neuroscience, 40(6), 1211-1225.

2.1 Animals

All animal work was approved by The Georgia Tech Institutional Animal Care and Use Committee. Adult (2-3 month old) male C57BL/6J mice were purchased from The Jackson Laboratory. Mice were pair housed upon arrival and allowed to acclimate to the environment for at least 5 days before experiments began.

For all animals, food and water were provided ad libitum. All experiments were performed during the light cycle of the animals. For experiments with flicker durations of less than 1 hour, animals undergoing the same stimulation condition were interspersed with animals undergoing different conditions, to ensure circadian rhythms did not impact results. For experiments with duration of flicker exposure at 1 hour, we conducted multiple experiments, at different times of day, with varying order of stimulus presentation, to ensure results remained consistent (data not shown).

To assess changes in cytokine profile induced by chronic inflammation, we used female 5XFAD transgenic animals, an aggressive model of amyloid beta pathology. For this experiment, 7-8-month-old 5XFAD mice were compared to wildtype (WT) littermate controls with 7 mice

per group. Animals were anesthetized and visual cortex was micro- dissected, as described below.

2.2 Visual Stimulation Exposure

To habituate and reduce visual stimulation, mice were placed in a dark room in the laboratory, for at least one hour, before beginning each experiment. To commence the experiment, mice were transferred from their home cage to a similar cage without bedding, termed a flicker cage. The flicker cage was covered in dark material on all but one side, which was clear and faced a strip of light-emitting diode (LED) lights. Animals remained in the dark room, where they were exposed to either LED lights flashing at 40Hz frequency (12.5ms light on, 12.5ms light off), 20Hz frequency (25ms light on, 25ms light off), a random frequency which averaged at 40Hz (12.5ms light on, variable duration light off), or constant light on stimulation, utilizing a dimmer to ensure the same total lux (about 150 lux) as 40Hz light flicker [51]. These conditions allowed us to control for light stimulation (light), light stimulation flashes (random), and frequency specific stimulation (20Hz). Animals were exposed to visual stimulation for 5 minutes, 15 minutes, or 1 hour.

Immediately after stimulation exposure, mice were anesthetized with isoflurane, and within 3 minutes mice were decapitated and brains were removed. The left hemisphere's visual cortex was micro-dissected, placed in an Eppendorf tube, and flash frozen using liquid nitrogen.

2.3 Lipopolysaccharides (LPS) Stimulation

Animals were intraperitoneal (IP) injected with 5mg/kg LPS (n=6), diluted in saline (Sigma lot #039M-4004V) or saline (veh) (n=5). 3 hours after injection, mice were anesthetized

with isoflurane, and within 3 minutes mice were decapitated and brains were removed. The left hemisphere's visual cortex was micro-dissected, placed in an Eppendorf tube, and flash frozen using liquid nitrogen. Cytokine analysis was conducted as described below.

2.4 Phosphoprotein Inhibitors

To test if our flicker-induced cytokine increase is dependent on the identified increase in NFκB and MAPK phosphoprotein pathways, we inhibited both of these pathways individually. To inhibit the NFκB pathway, we used IKK inhibitor, IMD0354, at 10mg/kg combined with Curcumin (S1848) at 100mg/kg. To inhibit the MAPK pathway, we used MEK inhibitor, SL327, at 100mg/kg and JNK inhibitor, SP600125, at 15mg/kg. All drugs were dissolved in a combination of Dimethyl sulfoxide (DMSO), Polyethylene glycol (PEG), and sterile 1X Phosphate Buffered Saline (PBS). Drugs were delivered to animals through intraperitoneal (IP) injection 30 minutes before the start of flicker stimulation. A combination of DMSO, PEG, and PBS was used as the vehicle injection.

2.5 Microglia Depletion

Microglia were depleted using Pexidartinib (PLX3397), purchased from MedChem. PLX3397 was incorporated into the Open Standard Diet with 15Kcal% fat by Research Diets, INC, at a dose of 290mg/kg. A control diet of the Open Standard Diet with15Kcal%, without PLX3397. Depending on pre-assigned groups, mice were fed either the PLX Diet or the control diet for 3 weeks. Weight was monitored to ensure mice were not losing or gaining unexpected weight.

2.6 Immunohistochemistry (IHC) and Microscopy

Immunohistochemistry (IHC) was performed to visualize protein expression in the visual cortex of mice exposed to flicker conditions. Immediately after decapitation and brain removal, each brain was cut into left and right hemisphere. The right hemisphere was immediately drop-fixed into cold 4% paraformaldehyde (PFA). 24 hours later, brain hemispheres were rinsed with 1X Phosphate Buffered Saline (PBS) and placed in .02% sodium azide (NaN_3). Three days before sectioning, each hemisphere was rinsed and placed in 30% sucrose. Three days later, each hemisphere was frozen and sagittal sections at 30-40 microns (30 microns for phosphoprotein detection and 40 microns for microglia detection) were obtained using a Leica cryostat.
Two sections per animal were rinsed 3 times for 10 minutes each in 1XPBS on a shaker. Sections were then blocked for 1 hour in blocking buffer consisting of 0.2% Triton X, 5% Normal Goat/Donkey Serum, and 1XPBS. After blocking, sections were left overnight at 4C in 350 μL of primary antibody diluted in blocking buffer at antibody combination and concentrations shown in Table 2.1. The next day, sections were washed in 1X PBS 3 times for 10 minutes each. Following washes, sections were incubated on shaker at room temperature for 2 hours in secondary antibody solution diluted in blocking buffer with antibody combinations and dilutions shown in Table 2.1. Sections were then washed in 1X PBS 3 times for 10 minutes each, and nuclei were stained with 4′,6-diamidino-2-phenylindole (DAPI) for 1 minute. Sections were then mounted on a glass slide using Vectashield. Images displaying microglia were taken on a Nikon Crest Spinning Disk Confocal Microscope with a 40x objective.

Table 2.1: Antibodies and Dilutions

Primary Antibody	**Secondary Antibody**
anti-pNFκB in rabbit (ab8629) (1:500)	Goat antirabbit 555 1937183 (1:5000)
anti-NeuN in mouse (ab1042240) (1:500)	Goat antimouse 488 A11001 (1:5000)
anti-mCSF in rabbit (PA542557) (1:500)	Goat antirabbit 555 1937183 (1:5000)
Anti-IBA1 in rabbit (PA527436) (1:500)	Goat antirabbit 555 1937183 (1:5000)

2.7 Cytokine and phospho-protein assays

For signaling and cytokine analysis, the visual cortex was thawed on ice and lysed using Bio-Plex lysis buffer (Bio-Rad). After lysing, samples were centrifuged at 4C for 10 minutes at 13,000 RPM. Protein concentrations in each sample were determined using a Pierce BCA Protein Assay (Thermo Fisher). Total protein concentrations were normalized in each sample using Bio-Plex lysis buffer (Bio-Rad). For MAPK and NFκB pathway analysis, 1.5 μg of total protein was loaded, and 6μg was loaded for cytokine analysis. Preliminary experiments determined these protein concentrations fell within the linear range of bead fluorescent intensity versus protein concentration for detectable analysis. Multiplexed phospho-protein analysis was conducted by adapting the protocols provided for the Milliplex MAP MAPK/SAPK Signaling Magnetic Bead 10-Plex (p-ATF2, p-Erk, p-HSP27*, p-JNK, p-c-Jun, p-MEK1, p-MSK1, p-p38*, p-p53*) kit and the Milliplex MAP NFκB Signaling Magnetic Bead 6-Plex Kit(c-Myc*, p-FADD, p-IκBα*, p-IKKα/β, pNFκB, TNFR1) (Figure 2.1). Cytokine analysis was conducted by adapting protocols provided for the Milliplex Mouse MAP Mouse Cytokine/Chemokine Magnetic Bead Panel 32-Plex Kit (Eotaxin, G-CSF, GM-CSF, IFN-γ, IL-1α, IL-1β, IL-2, IL-3,

IL-4, IL-5, IL-6, IL-7, IL-9, IL-10, IL-12p40, IL-12p70, IL-13, IL-15, IL-17, IP-10, KC, LIF, LIX, MCP-1, M-CSF, MIG, MIP-1α, MIP-1β, MIP-2, RANTES, TNF-α, and VEGF) (Figure 2.1). All kits were read on a MAGPX system (Luminex, Austin, TX).

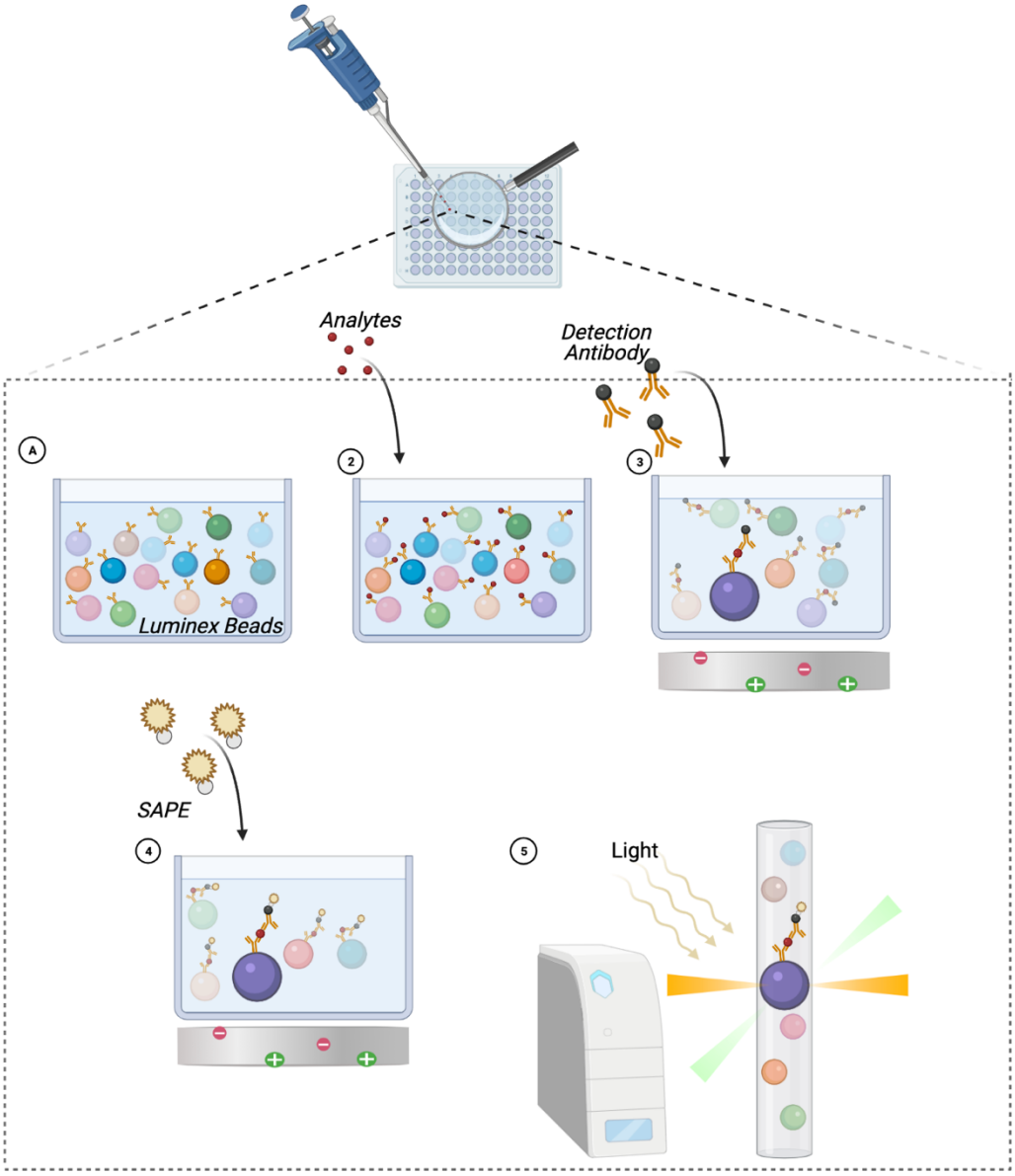

Figure 2.1 Schematic displaying the main steps of the Luminex assay. *Step 1: Fluorescently tagged beads are attached to antibodies for identification. Step 2: Biological tissue is placed in a well with antibodies for each protein of interest. Step 3: Detection antibodies are added to the samples to form an*

antibody-antigen sandwich. Step 4: SAPE (phycoerythrin-conjugated streptavidin) is added to bind to the detection antibody to allow for enhanced visual signal. Step 5: A Luminex instrument reads each bead using a combination of colored illumination.

2.8 Partial least squares discriminant analysis

Data was z-scored before analysis. A partial least squares discriminant analysis (PLSDA) was performed in MATLAB (Mathworks) using the algorithm by Cleiton Nunes (Mathworks File Exchange) [52]. To identify latent variables (LVs) that best separated conditions, an orthogonal rotation in the plane of the first two latent variables (LV1-LV2 plane) was performed. Error bars for LV1 figures represent the mean and standard deviations after iteratively excluding single samples (a leave-one-out cross validation), one at a time, and recalculating the PLSDA 1000 times.

To test different flicker conditions and durations, phosphoprotein experiments were performed over several cohorts and samples were normalized by removing batch effects. We performed a batch effects analysis (limma package in R v 3.5.2) to remove any between-experiment-variability before conducting the PLSDA. Outliers from the phosphoprotein experiments were removed by performing a principle component analysis on the data and iteratively removed data points which fell outside of a 99.5% confidence ellipse (mahalanobisQC in R v 3.5.2).

Last, for analyzing the effect of 40Hz flicker after microglia depletion, the data from three cohorts was combined by performing a batch-effects analysis (limma package in R version 3.5.2) to remove any between-experiment variability before conducting the PLSDA.

2.9 Animal behavior assays

To analyze animal behavior, mice were placed in a polycarbonate cage (210 x375 x 480mm), covered on all sides but one with 100% polyester black material (similar to cage in visual flicker experimental protocol cage described above, but larger and without cage top). In order to record the mice in the dark, an infrared (IR) light was placed above the cage. To record mice, without the flicker stimulation affecting behavior tracking, a Basler Ace monochrome IR-sensitive camera with Gigabit Ethernet interface with attached IR-only filter was used for recording. Ethernet connection from the camera to the computer allowed for Ethovision to record and analyze the experiment in real time.

After three days of handling, each mouse was placed in the behavior cage to habituate for five minutes. On the fourth day, each mouse was recorded individually for an hour and five minutes while receiving one of four flicker treatments (40Hz, 20Hz, random, light). Behavior assays were conducted using a total of six animals, with a within-subjects design. Each mouse received each treatment separated by 1 day in a randomized order. Experimenter was blinded to treatment type during experiment and analysis.

Ethovision XT version 14.0 was used to track and analyze behavior. First, the arena was defined, and a zone group defined which split the bottom of the cage in to two halves, front and back. A second zone group defined as center consisted of half of the total area in the center of the cage. Detection settings were made using Ethovision's automatic detection function and were adjusted after preliminary analysis. Automated video analysis recorded the animals' center point and all recordings were checked and manually corrected through software interpolation for any time points in which the mouse could not be automatically detected. Activity level was designated as active or inactive with inactive indicating freezing. Inactivity was determined to be

less than 0.01% of the total arena having activity and lasting for a duration longer than half a second. Data for each variable was exported and analyzed using GraphPad. A one-way analysis of variance (ANOVA) was conducted to assess differences between groups for each variable of interest.

2.10 Experimental design and statistical analysis

Animals were randomly assigned to flicker exposure groups and experimenters were blind to flicker exposure conditions during analysis for all experiments. Sample sizes were determined on preliminary data with a 0.80 power and alpha of 0.05, and samples sizes were adjusted based on high variability. Control groups (20Hz, random, and light) were based on prior experiments and preliminary data.

For multi-plex analysis, either a one-way ANOVA (more than two groups) or two-tailed unpaired t-test (two groups) was used to determine if there was a significant LV1 separation between groups. The top correlated cytokines and/or phospho-proteins on the LV1 were isolated and an ANOVA or two-tailed unpaired t-test was performed using GraphPad Prism 8 (GraphPad Software, La Jolla, CA) to determine statistical significance between groups. These tests were followed by a post-hoc Dunnett's multiple comparisons test to determine differences between specific groups or a Tuckey's multiple comparisons test to compare differences in phosphorylation levels across time. Levels of significance were set to *$p<0.05$, ** $p<0.01$, ****$p<0.001$.

To further confirm significant differences between groups using PLSDA, a permutation analysis was conducted, which randomly assigned animals into experimental groups and ran the PLSDA based on these shuffled values 1000 times [53]. For each test, true group assignment

showed $p_{permute}<0.05$ compared to the randomly permuted distribution, further confirming the validity of our data.

For analyzing changes in animal behavior, a one-way repeated measures analysis of variance (RM-ANOVA) was to compare results between different stimulation types.

For comparing between LPS-treated and 40Hz-stimulated animals, each group was normalized to control. Specifically, each cytokine level in each animal was divided by the mean cytokine level in the related control group (vehicle for LPS and random for 40Hz). Multiple t-tests were then conducted to compare each stimulation to its control; multiple comparisons were corrected using the Holm-Sidak method.

Last, for comparing individual cytokine expression in the microglia depletion and flicker experiment, a one-way ANOVA was used, following by multiple comparisons using the Tukey method.

Chapter 3: Gamma Visual Flicker Induces Cytokine Expression in the Brain

Portions of this chapter were adapted from the following publication:

Garza, K. M., Zhang, L., Borron, B., Wood, L. B., & Singer, A. C. (2020). Gamma Visual Stimulation Induces a Neuroimmune Signaling Profile Distinct from Acute Neuroinflammation. Journal of Neuroscience, 40(6), 1211-1225.

3.1 Introduction

Interactions between the brain and immune system play critical roles in neurological and neuropsychiatric disorders [54,55] . The neuroimmune system, including glial cells and immune signaling molecules, offers a unique target to treat disease and improve brain health. However, little is known about how to non-pharmacologically manipulate the brain's immune system. Recent research has shown that exogenously stimulating neural electrical activity at gamma frequency (30-50Hz), through sensory stimulation, promotes microglial activity, a component of the neuroimmune system, and decreases amyloid-beta (Aβ), one of the key proteins that build up in Alzheimer's disease (AD) [56,57]. While this recent research shows that neural electrical activity manipulates a component of the neuroimmune system and has therapeutic implications, a broader understanding of how exogenous stimulation of neural activity affects neuroimmune function is required. Indeed, the immediate effects of exogenous gamma stimulation on biochemical signals that control immune function in the brain are unknown. While the previous literature in this area has focused on Alzheimer's disease pathology, it is important to understand these basic biological interactions between neural activity and immune function in healthy animals outside the context of AD. Furthermore, while 40Hz visual stimulation is hypothesized

to recruit the immune system, the effects of different frequencies of visual stimulation on immune signaling remains unknown. Determining how different frequencies of visual stimulation affect the immune system in the brain will enable new strategies to manipulate brain function.

Cytokines, extracellular soluble signaling proteins of the immune system, are a main communication signal between neurons and immune cells [58,59]. Chemotactic cytokines, or chemokines, are responsible for attracting immune cells to a site of injury and pro- and anti-inflammatory cytokines promote or reduce inflammation, respectively. While molecular signaling between neurons and microglia has been largely attributed to neuronal expression of the cytokine fractalkine (CX3CL1), which attenuates microglial over-activation [60], many other cytokines play a role in signaling between neurons and microglia. For example, glial-derived TNF-α is necessary for proper neuronal synaptic scaling and is also a modulator of microglia neuronal phagocytosis [61–63]. Besides regulating microglial activation and recruitment, cytokines are also involved in diverse neuronal and synaptic functions. Still, little is known about how neuronal electrical activity affects cytokine expression.

In the present study, we determined how 40Hz visual stimulation affects expression of key cytokines involved in the brain's immune response, synaptic plasticity, and neuronal health. We tested this by exposing mice to varying durations of light emitting diode (LED) light strips flickering at 40Hz, which is known to induce gamma neuronal activity, as well as several control conditions [51,56,57,64]. Our analysis showed that 1 hour of 40Hz flicker stimulation induces protein expression of diverse cytokines. Interestingly, 20Hz flicker, random flicker, and constant light each induced unique cytokine expression profiles, revealing that different frequencies of visual stimulation induce unique immune signaling patterns.

We next determined if the cytokine response after 40Hz flicker differed from that due to models of both acute and pathological inflammation induced by lipopolysaccharides (LPS) administration or the 5XFAD AD model, respectively. We found that the cytokine profiles of acute inflammation due to LPS administration and due to 5XFAD genetics were both distinct from the cytokine response to 40Hz flicker. Furthermore, different frequencies of stimulation induced unique cytokine expression patterns. Thus, our results suggest that stimulation of different patterns of activity are used to regulate expression of genes that promote neuronal health, synaptic plasticity, and healthy immune activity.

3.2 Results

3.2.1 40Hz Visual Flicker Induces Increases in Cytokine Expression Profile

Given previous findings showing that exposing mice to 40Hz light flicker leads to morphological changes in microglia, we speculated that 40Hz flicker affects neuroimmune signaling. Specifically, since cytokines are key regulators of immune activity in the brain, we hypothesized that 40Hz light flicker promotes cytokine expression in the visual cortex. To test this, we exposed animals to 1 hour of 40Hz flickering light, light flickering at a random interval averaging at 40Hz (random), 20Hz flickering light (20Hz), and constant light (light) (Figure 3.1). After visual stimulation, mice were euthanized, and the visual cortex was rapidly (<3min) micro-dissected and flash frozen. Using a Luminex multi-plex immunoassay we quantified expression levels of thirty-two cytokine proteins in the visual cortex (Figure 3.1B). To account for the multi-dimensional nature of the data, we used a PLSDA to identify profiles of cytokines that distinguished the effects of 40Hz stimulation from the control groups (Figure 3.1C) [52].

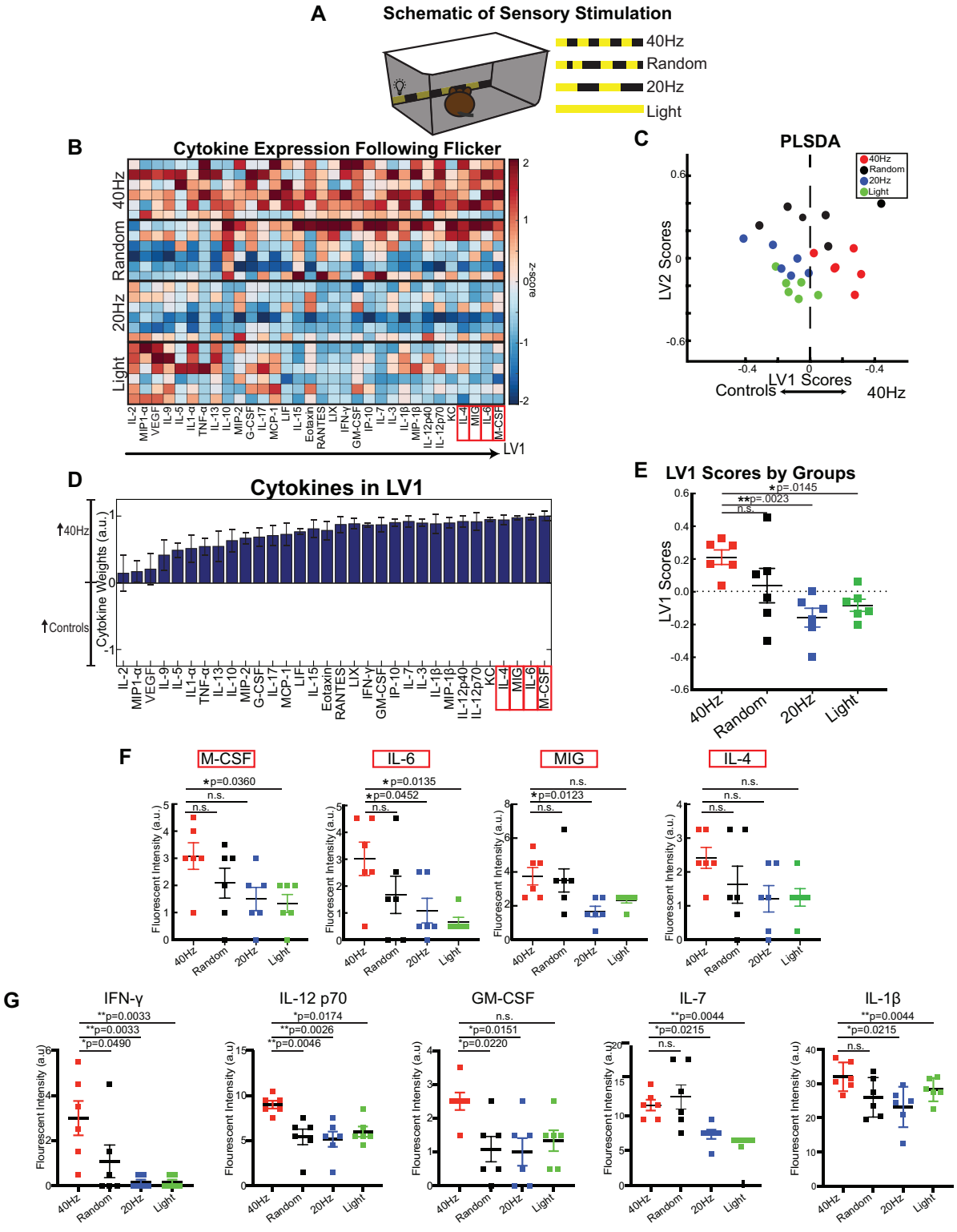

Figure 3.1: One hour of 40Hz flicker increased cytokine expression in visual cortex.

A*, Experimental configuration for presenting visual stimulation.* ***B****, Cytokine expression in visual cortices of mice exposed to 1 h of visual stimulation. Each row represents one animal (n = 6). Cytokines*

(columns) are arranged in the order of their weights on the LV1 in D. Color indicates z-scored expression levels for each cytokine. Top four cytokines from LV1 are boxed in red. ***C****, PLSDA identified LV1, the axis that separated 40Hz flicker-exposed animals (red) to the right, 20Hz flicker (blue) and constant light (green)-exposed animals to the left and random (black) flicker-exposed animals toward the middle (dots indicate individual animals for all graphs in this figure). LV2 separated 20Hz, random, and light conditions.* ***D****, The weighted profile of cytokines that make up LV1 based on which cytokines best correlated with separation of 40Hz (positive) versus flicker control groups (negative). (mean ± SD from a leave-one-out cross-validation).* ***E****, LV1 scores were significantly different for the 40Hz group compared with controls (mean ± SEM; F(3,20) = 5.855, p = 0.0049, one-way ANOVA). Each dot represents one animal. Results were confirmed with shuffling analysis (see Materials and Methods).* ***F,*** *There were significant differences in expression of most of the top four analytes, M-CSF, IL-6, MIG, and IL-4 when assessed individually. The p values for comparisons between groups are listed in the figure. For one-way ANOVA comparisons across all groups: M-CSF: F(3,20) = 2.970, p = 0.0564; IL-6: F(3,20) = 3.775, p = 0.0269; MIG: F(3,20) = 4.532, p = 0.0140; and IL-4: F(3,20) = 2.051, p = 0.1391.* ***G****, There were significant differences in the expression of IFN-γ, IL-12p70, GM-CSF, IL-7, and IL-1β as well.*
The p values for comparisons between groups are listed in the figure. For one-way ANOVA comparisons across all groups: IFN-γ: F(3,20) = 6.32, p = 0.0034; IL-12p70: F(3,20) = 6.428, p = 0.0032; GM-CSF: F(3,20) = 4.13, p = 0.0197; IL-7: F(3,20) = 9.541, p = 0.0004; and IL-1β: F(3,20) = 3.404, p = 0.0377. SEM, standard error of the mean.

We observed overall higher cytokine expression levels across animals exposed to 40Hz flicker compared to other groups. PLSDA identified a latent variable 1 (LV1), consisting of a weighted linear combination of cytokines, as being most upregulated in 40Hz (higher LV1 scores) or from all control conditions ((negative) (lower LV1 scores), Figure 3.1D). LV1 best separated 40Hz from all control groups (Figure 3.1C, Figure 3.1D). LV1 scores differed

significantly between groups confirming the groups were statistically separate, specifically, 40Hz flicker versus light and 20Hz stimulation were best separated (F (3, 20) = 5.855, p=0.0049, one-way ANOVA) (Figure 3.1E). LV2 significantly separated control groups from each other (F(3,20)=21.77, p<0.0001, Figure 3.1C, Figure 3.2B).

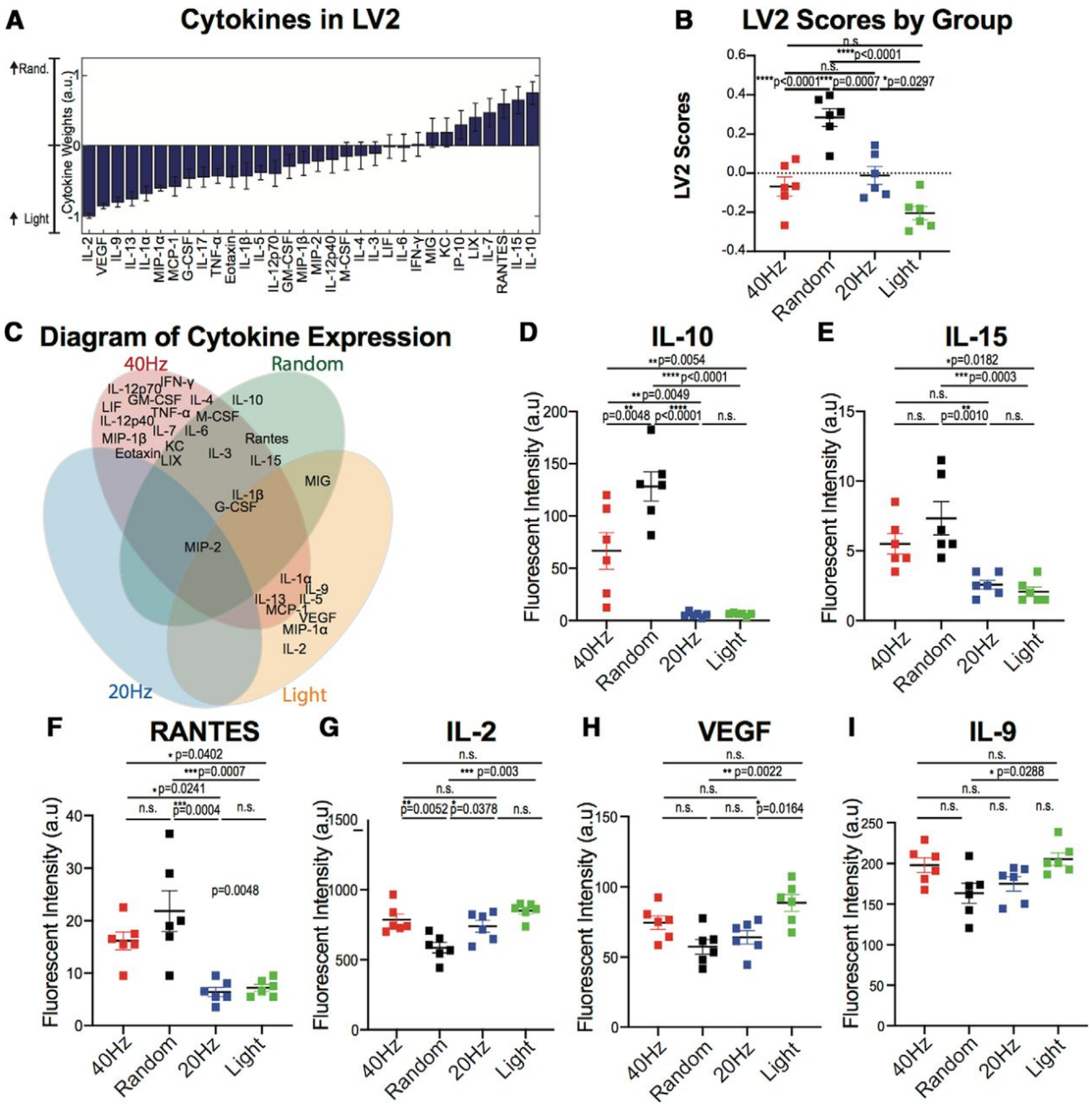

Figure 3.2: Flicker control conditions each lead to unique cytokine expression.

***A**, The weighted profile of cytokines that make up LV2 based on which cytokines best correlated with separation of random (positive) versus 20Hz versus light flicker control groups (negative; mean ± SD from a leave-one-out cross-validation). **B**, LV2 scores were significantly different for all four groups (mean ± SEM; $F(3,20) = 21.77$, $p < 0.0001$, one-way ANOVA). Each dot represents one animal. The p values from Tukey's multiple-comparison test are listed. **C**, Diagram of cytokine expression, with each cytokine name arranged based on increased expression per stimulation group. **D**, One-way ANOVA displays significant difference in IL-10 expression across groups (mean ± SEM; $F(3,20) = 27.29$, $p < 0.0001$, one-way ANOVA). The p values from Tukey's multiple-comparison test are listed. **E**, As in D for IL-15 expression across groups (mean ± SEM; $F(3,20) = 11.33$, $p = 0.0001$, one-way ANOVA). **F**, As in D for RANTES expression across groups (mean ± SEM; $F(3,20) = 11.48$, $p = 0.0001$, one-way ANOVA). **G**, As in D for IL-2 expression across groups (mean ± SEM; $F(3,20) = 9.366$, $p = 0.0005$, one-way ANOVA). **H**, As in D for VEGF expression across groups (mean ± SEM; $F(3,20) = 6.790$, $p = 0.0024$, one-way ANOVA). **I**, As in D for IL-9 expression across groups (mean ± SEM; $F(3,20) = 4.076$, $p = 0.0207$, one-way ANOVA). SD, standard deviation*

The top four identified by the PLSDA to contribute to differences between groups were M-CSF, IL-6, MIG, and IL-4 (Figure 3.1F). Of these top upregulated cytokines, IL-6 and MIG were significantly different between groups when each one was analyzed individually (IL-6: $F(3,20)=3.775$, $p=0.0269$; MIG: $F(3,20)=4.532$, $p=0.0140$, one-way ANOVA) (Figure 3.1F). We found IL-6 had significantly higher expression in 40Hz than 20Hz flicker and light; and MIG had significantly higher expression in 40Hz than 20Hz flicker (IL-6: 40Hz versus 20Hz: mean difference =1.917, adjusted p=0.0452; IL-6: 40Hz versus light: mean difference= 2.33, adjusted p=0.0135; MIG: 40Hz versus 20Hz: mean difference =2.083, adjusted p=0.0123, Dunnett's test). M-CSF expression was higher in 40Hz flicker than light exposed animals (mean difference = 1.750, adjusted p=0.0360. Dunnett's test). We found no significant differences in IL-4 between

groups although expression levels trended towards being higher in 40Hz flicker animals ($F(3,20)=2.051, p=0.1391$, one-way ANOVA). Based on observed differences between groups in a heatmap of these cytokines (Figure 3.1B), we ran additional analysis on a subset of cytokines and found significant differences in IL-12p70, IL-1β, IFN-γ, GM-CSF, IL-7 between 40Hz flicker and control conditions (see Figure 3.1G). These findings show that 1 hour of 40Hz flicker drives a significant neuroimmune signaling response, and this response is distinct from other flicker 40Hz frequencies or exposure to constant light.

3.2.2 Flicker Frequencies Each Induce Unique Cytokine Profiles

Interestingly, while animals exposed to 40Hz flicker showed a higher cytokine expression profile, we also observed distinct cytokine expression profiles for random, 20Hz, and light stimulation conditions (Figure 3.1B, Figure 3.2C). Indeed, our analysis revealed a second latent variable (LV2), which best separated these three control groups (Figure 3.1C, Figure 3.2A). Quantification of these effects showed constant light leads to an upregulation of a subset of cytokines, unique from those upregulated by 40Hz flicker. For example, when analyzed individually, IL-2, VEGF, IL-9, IL-1α, and IL-13 all showed significant differences in expression levels between groups, with higher upregulation after light exposure than at least one other group (IL-2: $F(3,20)=9.366, p=0.0005$; VGEF: $F(3,20)=6.790$, $p=0.0024$; IL-9: $F(3,20)=4.076, p=0.0207$; IL-1α:$F(3,20)=4.399$, $p=0.0157$; IL-13: $F(3,20)=3.802$, $p=0.0263$; one-way ANOVA, Dunnett's multiple comparisons method was used to control for 3 comparisons, (Figure 3.2E-2I) In contrast, random stimulation uniquely upregulated IL-10 across all samples, when compared to other stimulation types ($F(3, 20) =27.29$, $p<.0001$, Figure 3.2D) These results highlight that while 40Hz flicker modulated cytokine activity, 20Hz, random, and light exposure also led to distinct cytokine activity.

3.2.3 Animal Behavior is similar across flicker stimulations

Given our findings indicating cytokine and phospho-protein upregulation induced by 40Hz flicker, we sought to determine if behavioral differences during flicker could explain these results. We assessed both overall activity levels, measured as percent time active and total distance traveled, as well as exploratory versus anxiety-like behavior, assess by the percent of time animals spent in the center of the environment versus along the walls (perimeter). More anxious animals stay close to the walls of an enclosure. We recorded mice during 1 hour of either 40Hz flicker, random flicker, 20Hz flicker, or light and tracked mouse movement (Figure 3.3A). Our results revealed no significant differences between different flicker conditions in the amount of time spent in the center versus the perimeter of the enclosure, time spent active instead of freezing, time spent in the front (near the light source) versus the back half of the enclosure, and total distance traveled (Center versus perimeter: Figure 3.3B, $F(3,15)=0.8754$, $p=0.4757$, RM-ANOVA; Activity: (Figure 3.3C, $F(3,15)=0.9304$, $p=0.4502$, RM-ANOVA; Front versus Back: Figure 3.3D, $F(3,15)=0.1727p=0.9132$, RM-ANOVA; Distance: Figure 3.3E, $F(3,14)=0.3392$, $p=0.7973$, RM-ANOVA). These results show different visual stimulation conditions including different frequencies of flicker, periodic or aperiodic flicker, or constant or flickering light stimuli do not differentially affect animal behavior or induce an anxiety-like phenotype. Thus, the molecular changes we found in response to different visual stimulation conditions are not due to changes in animal behavior.

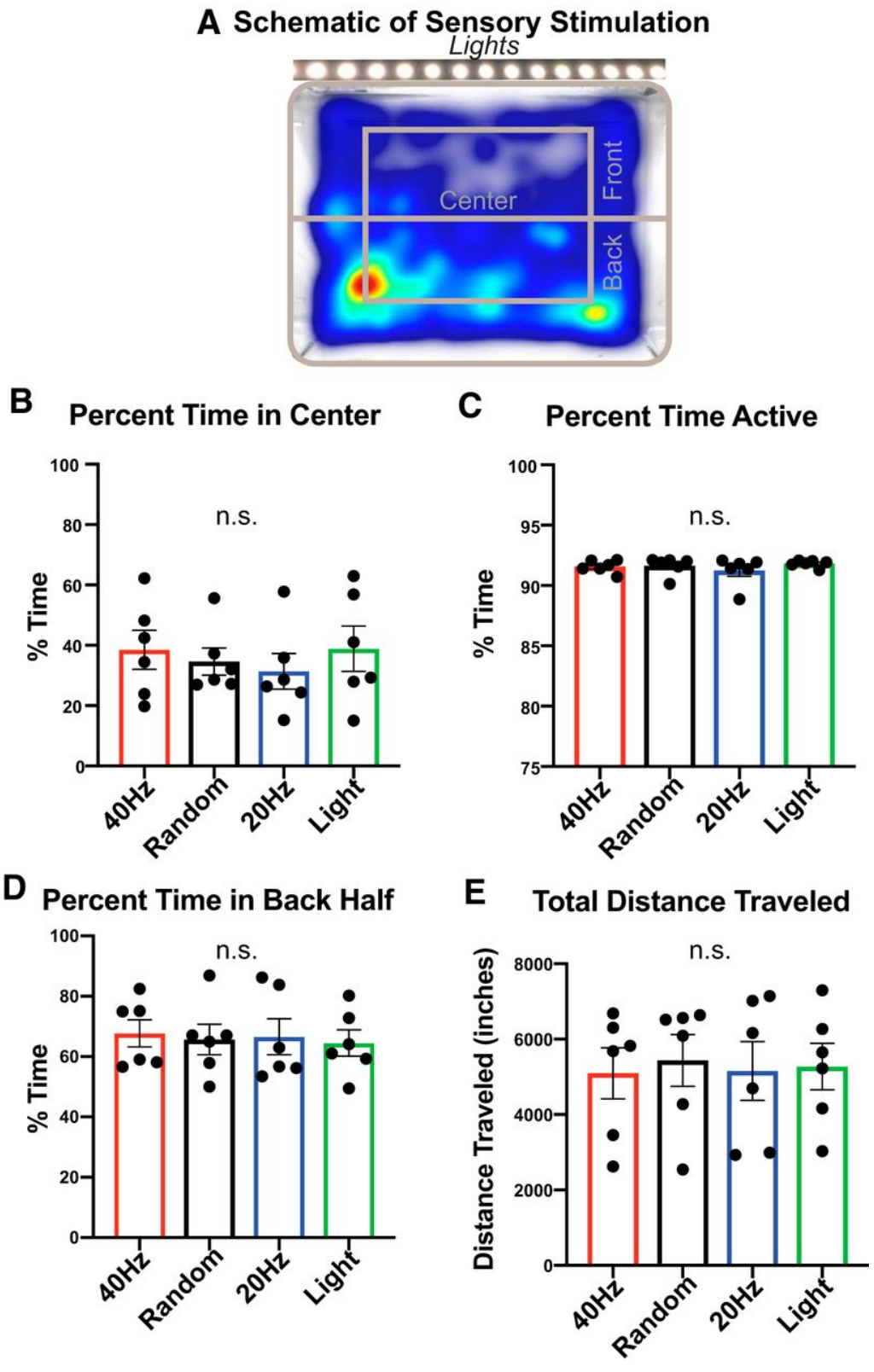
A Schematic of Sensory Stimulation
Lights
Center
Front
Back
B
Percent Time in Center
% Time
n.s.
40Hz
Random
20Hz
Light
C
Percent Time Active
% Time
n.s.
D
Percent Time in Back Half
% Time
n.s.
E
Total Distance Traveled
Distance Traveled (inches)
n.s.

Figure 3.3: Animal behavior is similar across conditions during exposure.

***A**, Example heatmap representing the amount of time spent in locations within the flicker enclosure. Delineations indicating the center, front, and back of the cage that were used for behavior analysis. **B**, Total percentage of time animals in each group spent in the center of the cage ($F_{(3,15)} = 0.8754$, $p = 0.4757$, RM-ANOVA). Error bars indicate the mean ± SEM. Five animals total were used, represented by dots indicating individual animals for all bar graphs in this figure (red = 40Hz, black = random, blue = 20Hz, green = light). **C**, Total percentage of time animals in each group spent active ($F_{(3,15)} = 0.9306$, $p = 0.4502$, RM-ANOVA). **D**, Total percentage of time animals in each group spend in the back half of the cage ($F_{(3,15)} = 0.1727$, $p = 0.9132$, RM-ANOVA). **E**, Total distance animals in each group travelled during stimulation ($F_{(3,15)} = 0.3392$, $p = 0.7973$, RM-ANOVA).*

3.2.4 40Hz Flicker induces neuroimmune profile distinct from acute and chronic pathological inflammation

Next, we wondered how the cytokine profile in response to 40Hz flicker differed from acute inflammation. Thus we assessed cytokine expression in the visual cortex of animals intraperitoneally injected with lipopolysaccharides (LPS), a traditional, acute model of inflammation [65–67]. As in our flicker experiments, we characterized cytokine expression in visual cortex of mice injected with LPS versus vehicle injection and separated these differences using a PLSDA (Figure 3.4). The latent variable that best separated LPS- and vehicle-injected animals (LV1, orange) was most heavily weighted by expression of MIG, IP-10, IL-3, and IL-17 (Figure 3.4A). The profile of cytokines weights that separated LPS from vehicle injected animals (LV1, orange) differed from the profile that separated 40Hz versus random stimulation exposed animals (LV1, blue, Figure 3.4A). These results show that 40Hz flicker and LPS stimulation led to distinct immune profiles.

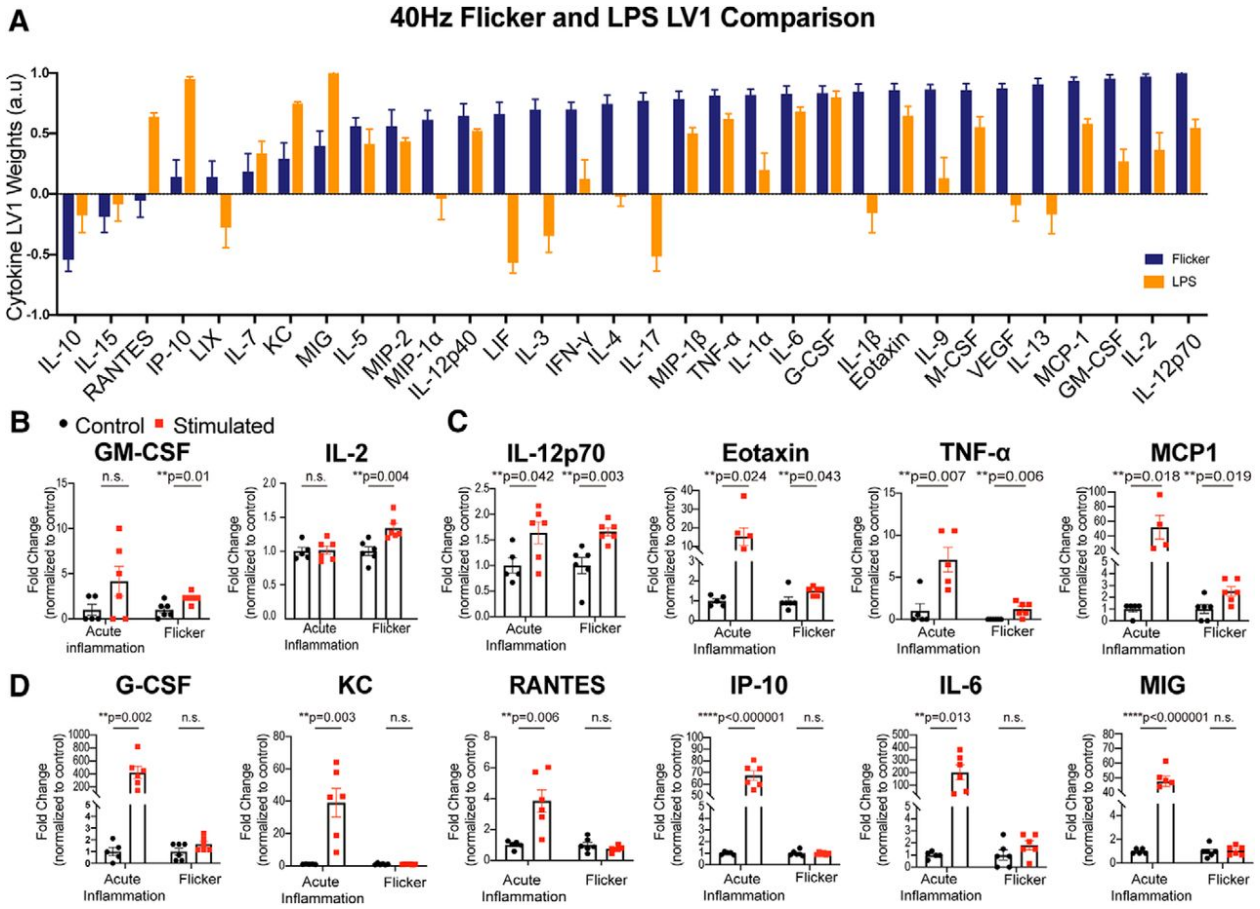

Figure 3.4: The 40Hz flicker cytokine response differs from LPS-induced acute inflammation.

A, *The weighted profile of cytokines that make up LV1 following 40Hz flicker (blue) or LPS (orange; mean ± SD from a leave-one-out cross-validation, n = 6).* ***B****, GM-CSF and IL-2 expression levels significantly differed in 40Hz versus random ("Flicker") but not LPS versus vehicle ("Acute Inflammation"). Error bars indicate the mean ± SEM. The p values for t test comparisons between groups are listed in the figure.* ***C****, IL-12p70, Eotaxin, TNF-α, and MCP1 expression levels significantly differed for both 40Hz versus random and LPS versus vehicle. Error bars indicate the mean ± SEM. The p values for t test comparisons between groups are listed in figure.* ***D****, G-CSF, KC, RANTES, IP-10, IL-4, and MIC expression levels significantly differed for LPS versus vehicle but not for 40Hz versus random flicker. Error bars indicate the mean ± SEM. The p values for t test comparisons between groups are listed in figure.*

We further analyzed the differences between LPS and 40Hz flicker by comparing individual cytokines following LPS or 40Hz flicker relative to their controls. These comparisons revealed that most cytokines differed between LPS and 40Hz flicker, both in terms of whether or not each cytokine was modulated by the stimulus and in terms of the magnitude of the response relative to control (Figure 3.4B, C, D). For example, GM-CSF and IL-2 significantly differed between animals exposed to 40Hz flicker versus random stimulation but did not differ between animals injected with LPS or vehicle (40Hz versus random: GM-CSF: $t(10)=3.114$, $p=0.011$; IL-2: $t(10)=3.613$, $p=0.0047$; LPS versus vehicle: GM-CSF: $t(9)=1.646$, $p=0.134$; IL-2: $t(9)=0.167$, $p=0.871$) (Figure 3.4B). In contrast, G-CSF, KC, MIG, RANTES, IP-10, and IL-6 significantly differed between LPS and vehicle but not between 40Hz and random (LPS versus vehicle: G-CSF: $t(9)=4.069$, $p=0.003$; KC: $t(9)=3.883$, $p=0.004$; MIG: $t(9)=12.16$, $p<0.000001$; RANTES: $t(9)=3.502$,$p=0.007$; IP-10: $t(9)= 14.86$, $p<0.000001$: IL-6: $t(9)= 3.107$, $p=0.013$; 40Hz versus random: G-CSF: $t(10)=1.661$, $p=0.128$; KC: $t(10)=0.450$, $p=0.662$, MIG: $t(10)=0.2928$,$p=0.776$; RANTES: $t(10)=1.335$,$p=0.212$, IP-10: $t(10)=0.3421$, $p=0.739$; IL-6: $t(10)=1.437$, $p=0.1813$) (Fig. 7C). Lastly, there was a subset of cytokines, IL-12p70, Eotaxin, TNF-α, and MCP1, that significantly differed in both LPS versus vehicle and 40Hz versus random (LPS versus vehicle:IL-12p70: $t(9)=2.359$,$p=0.043$;Eotaxin: $t(9)=2.710$,$p=0.024$;TNF -α: $t(9)=3.561$, $p=0.007$; MCP1: $t(9)= 2.884$,$p=0.018$; 40Hz versus random: IL-12p70 :$t(10)=3.729$, $p=0.004$; Eotaxin:$t(10)= 2.318$,$p=0.043$;TNF-α: $t(10)= 3.512$,$p=0.006$; MCP1: $t(10)= 2.785$,$p=0.019$) (Figure 3.4D). For those cytokines that significantly increased expression in response to both LPS and 40Hz stimulations relative to controls, the scale of the difference between the two comparisons was usually much larger when comparing LPS versus vehicle. For example, the

difference in expression of MCP1 was over 10-fold larger between LPS and vehicle than between 40Hz and random, though both differences were significant (Figure 3.4D).

We also assessed how 40Hz flicker compares to a chronic pathological state. To do this, we assessed how the immunological profile of brains from aged, female 5XFAD mice compared to mice which were acutely flickered for hour. Amyloid beta plaques are already present in visual cortex of the 5XFAD mouse model at this age; however prior neuroimmune characterization in this model has traditionally been in frontal cortex and hippocampus [12,68,69]. Therefore, to compare cytokine responses to 40Hz light flicker in visual cortex to a model of chronic inflammation, we first characterized cytokine expression in visual cortex of 5XFAD mice and WT littermates. Interestingly, we found some cytokines were more elevated in the 5XFAD group, like MIG, M-CSF, IP-10, and IL-1α, while other cytokines were more elevated in the WT-littermates, like RANTES, VEGF, IL-12p40, and GM-CSF (Figure 3.5D). Using a two-tailed t-test, we found that the LV1 score generated by the PLSDA was significantly different between the two groups ($t(12)=4.713, p=0.0005$, Figure 3.5B,5C). The cytokine expression profile in 5XFAD mice differed from the profile following 1 hour of 40Hz flicker. Specifically, 5XFAD mice had lower expression of several cytokines while 40Hz licker led to an increase in almost all cytokines (Figure 3.1A, Figure 3.5E). Some cytokines, namely M-CSF, MIG, IP-10, IL-1α, and IL-5, were elevated in both 5XFAD mice and following 40Hz flicker and provided similar contributions to LV1 scores for both the 5XFAD and 40Hz PLSDA models (Figure 3.5E), cytokines that fall along the line of equality, dashed).

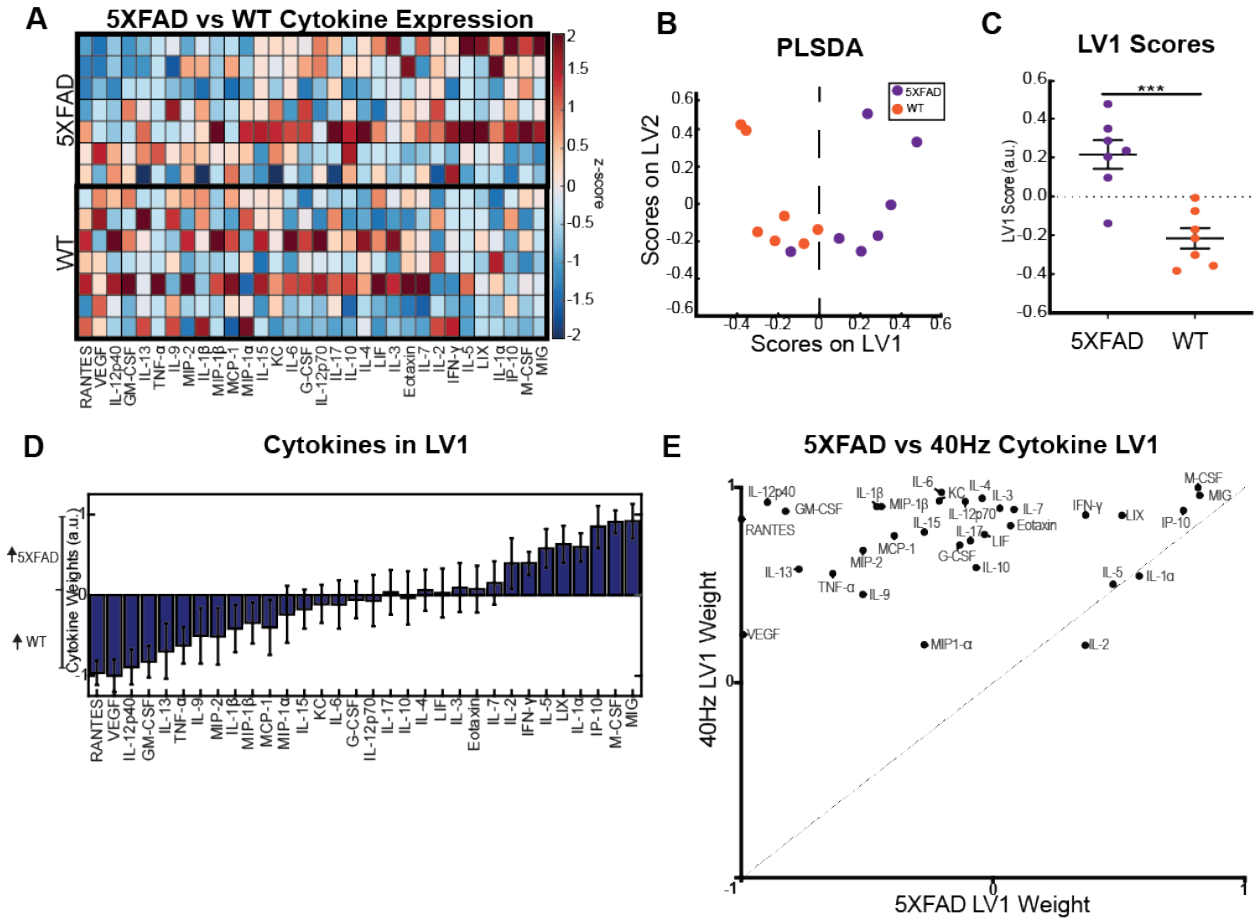

Figure 3.5: 5XFAD mice show distinct cytokine profiles when compared with 40Hz flicker.

A*, Cytokine expression in visual cortex of 5XFAD mice or wild-type littermates (z-scored). Each row represents one animal with groups separated by the thicker black horizontal line, n=6. Cytokines (columns) are arranged in order of increased expression based on LV1 score in (B).* ***B****,PLSDA identified the LV1 axis that separated 5XFAD (purple) mice to the right and WT (orange) mice to the left. Dots indicate individual animals for all graphs in this figure.* ***C****, Plot of LV1 scores per group revealed that 5XFAD mice were significantly different from WT controls (mean±SEM; t(12)=4.713, p=0.0005, two-tailed t-test).* ***D****, The weighted profile of cytokines that make up LV1 based on which were upregulated in 5XFAD mice (positive) or WT controls (negative) (mean ± SD from a leave one out cross validation).* ***E****, LV1 cytokine weights for the 5XFAD model versus the 40Hz model.*

However, most cytokines made different contributions to LV1 scores for both the 5XFAD and 40Hz PLSDA models, including (Il-2, LIX, IFN-γ, MIP-1α, Eotaxin, IL-10, G-CSF, LIF, IL-17, IL-3, IL-7, IL-4, IL-12p70, IL-6, KC, IL-15, MIP-2, TNF-α, IL-9, IL-13, VEGF, MCP-1, IL-1β, MIP-1β, GM-CSF, RANTES, IL-12p40) (Figure 3.5E). Thus, while there are similarities present between the two models, the entirety of the LV1 profile is different between 40Hz flicker and 5XFAD mice (Figure 3.1D, Figure 3.5D, Figure 3.5E). Overall, these results show that both acute inflammation via LPS and chronic inflammation due to Alzheimer's-like pathology produce different immune responses than 40Hz flicker.

3.3 Discussion

3.3.1 40Hz flicker-induces a unique cytokine profile in the visual cortex

Because nothing is known about the effect of gamma oscillatory activity on cytokine expression levels, we used a multi-plex approach to determine the global impact of this activity on the brain's main immune signals. Our results establish that 40Hz flicker upregulated a combination of cytokines in the visual cortex resulting in a neuroimmune profile distinct both from other types of flicker stimulation and from acute inflammation induced by LPS. Interestingly, LV1 better separated 40Hz stimulation from 20Hz and light than from random stimulation. This point is reinforced by our finding that the top LV1-contributing cytokines did not differ significantly between 40Hz and random stimulation. However other cytokines, such as IFN-γ, IL-12p70, and GM-CSF, showed significant differences between 40Hz and random stimulation (Figure 3.1G). Thus, random stimulation leads to an immune profile with an overlap in expression of some cytokines to that of 40Hz but distinct expression levels of other cytokines (Figure 3.2). While random stimulation does not induce gamma oscillations, randomized pulses

of light slightly alter neural activity in visual cortex over a much broader ranges of frequencies than gamma frequency light flicker [12].Therefore, random flicker has some similar and some different effects on cytokines as 40Hz flicker but taken together this still produces a distinct immune profile.

Random flicker, 20Hz flicker, and light stimulation each induce expression of unique subsets of cytokines (Figure 3.2). When comparing cytokine expression, LV1 best separated 40Hz stimulation from the other controls. In contrast, LV2 best separated all of the control groups from each other. Interestingly, while LV1 separated animals stimulated with 20Hz and light stimulation from those stimulated with 40Hz visual flicker, these groups were not as well separated by LV2. In fact, LV2 best separated animals stimulated with random visual flicker from other groups. When examining individual cytokines, plotted in Figure 2, there is a significant difference in expression of IL-10 and RANTES between 40Hz and 20Hz flicker, and significant difference in expression of IL-10, IL-15, and RANTES between 40Hz flicker and light. Together, these results demonstrate that 40Hz stimulation leads to increased expression of the many cytokines in the visual cortex compared to other conditions, but each of our control stimulations produces its own unique profile of cytokine expression.

3.3.2 40Hz flicker-induced cytokines have neuroprotective functions

We found that 40Hz flicker is upregulating a unique combination of cytokines, and we hypothesize that no one cytokine in particular is responsible for neuroprotective function, but rather the combinatory profile is necessary. This effect would coincide with what is known about gamma oscillations, that no one neuron is responsible for gamma oscillations, but rather the combination of neuronal activity.

By focusing on the functions of the top five cytokines distinguishing 40Hz flicker from all other groups M-CSF, IL-6, MIG, IL-4, and KC (also known as CXCL1), it becomes apparent that each cytokine's unique immune function contributes to an overall neuroprotective effect (Figure 3.1)., M-CSF (encoded by Csf1) transforms microglia morphologically and has been reported to enhance phagocytosis of amyloid beta [70,71]. Furthermore, the primary receptor for M-CSF, CSF1R, is primarily expressed by microglia in the brain [72]. Thus, we hypothesize M-CSF is responsible for previously observed morphological transformation of microglia in 5XFAD mice (after 1 hour of 40Hz light flicker stimulation followed by 1 hour of no stimulation) because those microglial changes are associated with engulfment [12].

Interestingly, IL-6, the second top cytokine that increased following 1 hour of 40Hz flicker, is a pleiotropic cytokine with both protective and pathogenic effects. The potential pathogenic effects of IL-6 include stimulating amyloid precursor protein expression (APP) [73]. In contrast, the neuroprotective effects of IL-6 include increasing synaptic density and inhibiting macrophage expression of TNF-α, a cytokine known to have pro-inflammatory and neurotoxic properties [74]. In our own work, increased expression of IL-6 was correlated with a resiliency to Alzheimer's pathology; defined as human subjects with no neuronal loss or cognitive impairment even in the presence of plaques and tangles associated with Alzheimer's [75]. IL-6 is also important for neural progenitor cell health as IL-6 knockout significantly reduced neural progenitor cell density in multiple brain regions [76]. Furthermore, IL-6 levels correlate with improved learning and memory performance in both animals and humans [77–79].

The third flicker-upregulated cytokine, monokine induced by gamma interferon (MIG), is a chemokine involved in microglial recruitment via its receptor, CXCR3 [80]. In brain endothelial cells in vitro, MIG is released in response to the presence of other cytokines [81]. It

is specifically responsible for recruiting T-cells to the brain and responds to interferon gamma (IFN-γ), suggesting MIG is released to combat infection. Indeed, injecting mice with an anti-MIG treatment leads to increased viral infection and pathology [82].

Finally, the fourth and fifth top cytokines, IL-4 and KC (CXCL1) signal to microglia [83–85]. IL-4 has been shown to reprogram microglia to stimulate neurite outgrowth after spinal cord injury [85]. In addition, adeno-associated vrius mediated over-expression of IL-4 in APP mice reduced Aβ plaque load [86]. KC (CXCL1) is a chemokine involved in recruiting neutrophils, a type of white blood cell, signaling to microglia [83,84]. Finally, KC signals to the receptor CXCR2, which is expressed on microglia and has been reported to mediate microglial recruitment [87]. In total, our data show that 40Hz light flicker stimulates expression of diverse cytokines with both immunomodulatory and neuro-protective properties.

It is important to note that our results were based on experiments done with male mice. We chose to focus on males because we wanted to assess how 40Hz flicker, which induces gamma oscillations, impacts neuroimmune signaling, building on previous papers that have only studied this effect in male mice [12,23,50]. However, we acknowledge that this is a limitation of this study because there are effects of sex on immune response and ovarian hormones have been shown to impact cytokine expression [88,89]. Future studies should further explore how this effect differs between the sexes.

3.3.3 Behavior is similar across different visual stimulation conditions

Cytokine expression are modified by an animal's behavioral state, for example when an animal is under stress [90,91]. While it is known that chronic 40Hz flicker does not affect anxiolytic behaviors over time, we wanted to ensure 40Hz flicker stimulation did not differentially affect animal behavior in real time over the timescales of our analyses when

compared to other stimulation types [92]. We measured total time spent in the center versus surround areas of the enclosure and time spent active versus freezing. We concluded that flicker stimulation did not invoke anxiety-like behavior or changes in overall activity levels. To assess if one stimulation type was more aversive than others, we analyzed time spent in the front of the cage where the lights were positioned versus the back and found no differences across stimulation conditions. Interestingly, animals across all conditions spent somewhat more time (~65%) in the back of the cage, which is not surprising considering that mice tend to stay in dark areas if given the choice [93]. Last, we measured the distance animals traveled within each stimulation type and found no differences across flicker conditions. In short, our analysis revealed no differences in any of our measured animal behaviors between stimulation conditions. Therefore, our observations show that induced phospho-signaling and cytokine expression after 40Hz light flicker cannot be explained by changes in animal behavior.

3.3.4 40Hz flicker cytokine response differs from acute pathological inflammation

We found that 40Hz flicker upregulates a profile of cytokines in a short period of time, similar to an acute pro-inflammatory stimulus. However, previous work has shown that 40Hz flicker has a neuro-protective effect. Therefore, we wanted to compare how 40Hz flicker induced cytokine expression differs from a known pro-inflammatory stimulus operating under a similar acute time period.

Our analysis showed that 40Hz flicker stimulates expression of diverse cytokines that differs from a model of acute inflammation. This difference was established by comparing the LV1 cytokine profile of gamma sensory stimulation and acute LPS inflammation. While there is an overlap in some cytokines that were elevated, the overall profiles are distinct between these

two stimulations due to the differences in magnitude of responses and the overall cytokines included. Two cytokines, GM-CSF and IL-2 significantly differed between 40Hz flicker and random stimulation but did not differ between LPS and vehicle administration. The specific response of these two cytokines to 40Hz flicker is especially interesting because GM-CSF is both neuroprotective and proinflammatory and low-dose IL-2 rescues cognitive and synaptic plasticity deficits in a mouse model of AD [94–96]. Furthermore, the combination of GM-CSF and IL-2 has been suggested to have synergistic effects. The combination of these cytokines has been used to prevent immune dysregulation in multiple models of disease [97–99]. Thus, there is evidence that shows the combination of these two cytokines following 40Hz flicker is neuroprotective.

Some cytokines significantly differed between both 40Hz versus random flicker and LPS versus vehicle administration. An interesting observation from our data is that while there was overlap in some of these cytokines, there was a noticeable difference in the scale of separation between LPS and vehicle versus 40Hz and random stimulation. While both were significantly upregulated by stimulation, LPS had a much larger effect when compared to control condition. The magnitude of the cytokine response has been suggested to alter a cytokine's effects [100,101]. Thus, we speculate this low-dose increase caused by 40Hz flicker is more responsible for the neuroprotective effect of 40Hz flicker.

Lastly, IL-12p70, the bioactive form of the p35 and p40 combined IL-12 subunits, was up-regulated in both LPS and 40Hz versus controls. In contrast, IP-10, which is downstream of IL-12, was significantly different between LPS and control but not 40Hz and random. IP-10 is induced by IFN- γ, which is a pro-inflammatory cytokine downstream of IL-12 [102]. This finding suggests that while both LPS and 40Hz flicker upregulate some similar cytokines, they

are leading to different downstream mechanisms, explaining why LPS is known to be neuro-toxic, while 40Hz flicker is neuroprotective[12,23].

3.3.5 40Hz flicker cytokine response differs from chronic, pathological inflammation

Our cytokine profiling analysis showed that 40Hz flicker stimulates expression of diverse cytokines, which are distinct from those expressed in a model of chronic inflammation, the 5XFAD amyloid mouse model [68,103,104] (Figures 3.1,3. 5). It is important to note that chronic inflammation does not necessarily imply all high levels of cytokines. In fact, we expect more subtle inflammatory signature in the visual cortex of 5XFAD mice because amyloid pathology develops more slowly in cortex [103]. Neuroinflammation, especially prolonged neuroinflammation, is believed to promote pathogenesis and plays an important role in Alzheimer's disease and many other neurodegenerative diseases [105,106]. In contrast, certain modes of inflammation are thought to be protective. For example, some protocols to stimulate neural immune responses via lipopolysaccharides have been shown to clear amyloid beta plaques and promote neuroprotection in mice [107–109]. Although the distinction between a protective versus deleterious immune responses remains unclear, our group has recently found that patients resilient to AD pathology (patients with plaques and neurofibrillary tangles, but no neuronal loss or cognitive impairment) had distinct cytokine profiles in post-mortem cortical tissues compared to patients diagnosed with AD [75]. Interestingly, patients resilient to AD pathology had increased expression of IL-1β, IL-6, IL-4, and IL-13, all of which were upregulated by 40Hz flicker in the current study. In contrast, AD cases had increased IL-5, and IP-10, which we found to be upregulated in 5XFAD mice. While there was overlap in some of the cytokines expressed in our model of chronic inflammation and 40Hz flicker, such as M-CSF and MIG, we

hypothesize an overlap in protective effects from both conditions. Together, these data suggest that 40Hz flicker stimulates an immune response associated with resilience to Alzheimer's pathology.

In total, our results show the diversity of cytokine and growth factors expressed in response to 40Hz stimulation suggests that flicker stimulation induces changes in various cell and tissue functions that include immune activity and neuronal and synaptic health. Furthermore, different forms of visual stimulation induced unique cytokine profiles. Thus, flicker stimulation is a rapid and non-invasive way to manipulate signaling and expression of genes that go beyond neural immune activity. Our analyses comparing flicker stimulations were conducted in wild-type animals, helping establish the effects of 40Hz flicker stimulation independent of disease pathology. We also compared the effects of 40Hz flicker to the cytokine response after LPS stimulation and the 5XFAD transgenes to show the effects of flicker differ from pathological states. Our work provides a foundation for flicker's therapeutic potential to other disorders involving the neuroimmune system.

Chapter 4: Gamma Visual Flicker Activates Phosphoprotein Pathways necessary for Cytokine Expression

Portions of this chapter were adapted from the following publication:

Garza, K. M., Zhang, L., Borron, B., Wood, L. B., & Singer, A. C. (2020). Gamma Visual Stimulation Induces a Neuroimmune Signaling Profile Distinct from Acute Neuroinflammation. Journal of Neuroscience, 40(6), 1211-1225.

4.1 Introduction

Cytokine expression and its effects on immune function are regulated by intracellular signaling, such as the nuclear factor kappa-light-chain-enhancer of activated B cells (NFκB) and the mitogen activated protein kinase (MAPK) immunomodulatory pathways. These pathways are activated through the subsequent phosphorylation of proteins in a cascade, or phospho-signaling, and they culminate in the activation of transcription factors, which regulate cytokine transcription, expression, and release from the cell. Both the NFκB and MAPK immunomodulatory pathways strongly regulate expression of diverse cytokines involved in immune responses, such as microglial activation and recruitment (e.g., M-CSF, MCP-1) [110–112]. These pathways also control expression of neurotrophic and synaptotrophic factors and are involved in mechanisms of learning and memory [113–116]. Recent studies show 40Hz flicker changes protein phosphorylation patterns after weeks of exposure compared to no stimulation, but the immediate effect of flicker on protein phosphorylation and the immediate effects of flicker on these two key phospho-protein pathways is still unknown [57].

NFκB rests in the cellular cytoplasm, maintained there by inhibitory kappa B (I IKKα/β) proteins. When the pathway is stimulated, the IKKα/β proteins are phosphorylated by the IKKαβ Kinase complex (IKK). This phosphorylation causes NFκB release, and it is translocated into the cellular nucleus, where it acts as a transcription factor for gene expression. Accordingly, inhibiting IKK blocks phosphorylation of IKKα/β proteins in the NFκB pathway, and therefore decrease NFκB role as a gene transcription factor. This inhibition is experimentally accomplished with the use of small molecular inhibitor, IMD0354, which blocks IKK activity and is proven to lead to a decrease in NFκB gene expression (Figure 1.1) [117].

The mitogen-activated protein kinase (MAPK) pathway is also highly involved in intracellular communication. When the MAPK pathway is activated, Ras, a GTP-binding protein, activates Raf, a serine/theronin kinase, causing a protein phosphorylation cascade. Raf phosphorylates MEK awhich then phosphorylates ERK1 (Figure 1.2). Phosphorylated ERK activates many transcription factors, such as activating protein 1 (AP-1), Elk-1, c-Myc, which culminate in the regulation of genes involved in immune responses [118,119].

MEK inhibition would decrease these downstream effects of the MAPK pathway. Phosphoprotein inhibition is experimentally accomplished using small molecular inhibitors, small molecules that modulate protein interactions. The MAPK inhibitor, SL-327 is a selective, noncompetitive inhibitor of MEK, which leads to decreased ERK phosphorylation, thereby inhibiting the MAPK pathway (Figure 1.2) [120].

Because cytokine expression is regulated by intracellular signaling, we assessed if the NFκB and MAPK phospho-signaling pathways change in mice exposed to 40Hz visual stimulation compared to control visual stimuli. Inhibition of the NFκB pathway affects downstream gene transcription response to an inflammatory stimulus, and this effect is stimulus dependent [121].

Inhibition of the MAPK pathway attenuates cytokine expression, specifically in an AD model [122]. Therefore, after confirming these pathways were increased after 40Hz flicker, we tested if these pathways are necessary for the downstream cytokine expression we observed after gamma visual flicker.

Our results show that 40Hz flicker induces NFκB phospho-signaling followed by MAPK phospho-signaling and increased cytokine expression distinct from inflammation. We also show that these two phosphoprotein pathways are necessary for cytokine expression after 40Hz flicker stimulation. Importantly, the cytokines assessed here, as well as the NFκB and MAPK pathways, play key roles in many different cellular functions involved in immune activity, learning and memory, and pathology.

4.2 Results

4.2.1 40Hz Flicker Induces NFκB and MAPK Signaling

Cytokine expression is regulated by several canonical intracellular phospho-signaling pathways, including the NFκB and MAPK pathways. Thus, to gain better insight into intracellular signaling changes that underlie changes in cytokine expression after visual stimulation, we examined how 40Hz flicker impacted these two phosphoprotein pathways. Because phospho-signaling is usually transient, we examined this signaling after 5, 15, and 60 minutes of 40Hz and random flicker [123]. We focused on random flicker as our control group for this comparison specifically because it controls for the average number of times the lights turn on and off, the percent of time the light is on, and the frequency of light presentation without inducing periodic neural activity [51,56,57]. As with cytokine experiments, immediately following flicker exposure, mice were euthanized, and visual cortex was rapidly micro-dissected.

We used Luminex assays and PLSDA to quantify differences in the NFκB and MAPK phospho-protein pathways in 40Hz versus random flicker exposure animals after different durations of flicker.

We found phospho-signaling in the NFκB pathway was significantly upregulated after 15 minutes, but not 5 or 60 minutes, of 40Hz versus random flicker. Experiments were performed across several cohorts and animals were removed based on an outlier analysis; data was z-scored according to batch-corrected data (see Chapter 2). Our analysis revealed a trend of increased phosphorylation after 5 minutes of flicker, driven specifically by increases in TNFR1 and pIKKα/β, but 40Hz and random groups were not significantly different ($t(21) = 2.056$, $p = 0.0525$, unpaired t-test, Figure 4.1B,E). After 15 minutes of flicker exposure, NFκB phosphorylation significantly differed between groups as indicated by significant separation of NFκB LV1 scores ($t(16) = 4.456$, $p = 0.0004$,unpaired t-test, Figure 4.1C,F). At 60 minutes, there was no significant difference between groups but phosphorylation of NFκB proteins appeared lower in 40Hz than random groups ($t(8) = 1.415$, $p = 0.1948$, unpaired t-test, Figure 4.1D,G). These results show that 40Hz flicker transiently upregulates the NFκB pathway after approximately 5 to 15 minutes and this difference in upregulation is no longer detectable after 60 minutes of flicker.

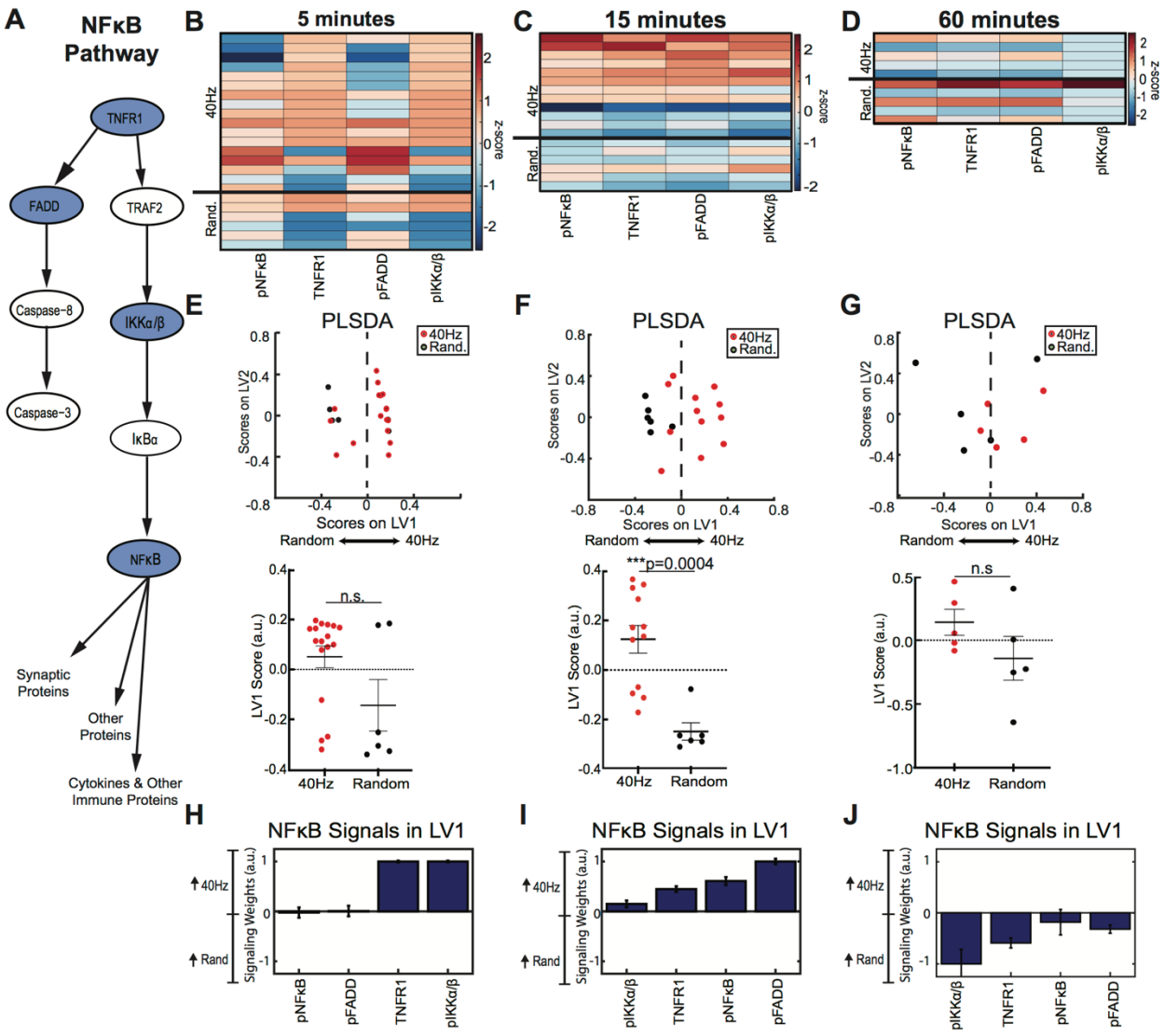

Figure 4.1: NFκB phosphoprotein signaling in visual cortex increased in response to 15 minutes of 40Hz flicker.

A, *Simplified diagram of NFκB signaling including phosphoproteins quantified in the present study (blue ovals).* ***B****, NFκB phosphoproteins quantified in visual cortex in mice exposed to 5 minutes of 40Hz or random flicker (z-scored). Each row represents one animal with groups separated by thicker black horizontal lines. Twenty-three total animals were analyzed, n = 17 in 40Hz group, n = 6 in random group; outliers removed through a principle component analysis on the data and iterative removal of data points outside a 99.5% confidence ellipse (mahalanobisQC in R version 3.5.2).* ***C****, As in B for mice*

exposed to 15 min of 40Hz or random flicker; 40Hz, n = 12; random, n = 6. ***D****, As in B for mice exposed to 60 min of 40Hz or random flicker; 40Hz, n = 6; random, n = 6.* ***E****, Top, PLSDA of phospho-signaling data from mice exposed to 5 min of flicker, separating 40Hz (red)-exposed animal to the right and random (black) to the left, along LV1. Bottom, Plots of LV1 scores between groups show a trend toward higher LV1 scores in 40Hz-exposed animals (difference between means ± SEM = −0.1943 ± 0.09455;* $t_{(21)}$ *= 2.065, p = 0.0525, two-tailed t test). Dots indicate individual animals for all graphs in this figure.* ***F****, Top, As in E for mice exposed to 15 min of 40Hz or random flicker. Bottom, Plot of LV1 scores between groups reveals significantly higher LV1 scores in 40Hz-exposed animals (difference between mean ± SEM values = −0.3721 ± 0.08351;* $t_{(16)}$ *= 4.456, p = 0.0004, two-tailed t test). Results were confirmed with permutation analysis (see Materials and Methods).* ***G****, Top, As in E for mice exposed to 60 min of 40Hz or random flicker. Bottom, Plot of LV1 scores between groups shows no significant difference (difference between mean ± SEM values = −0.2829 ± 0.2;* $t_{(8)}$ *= 1.415, p = 0.1948, two-tailed t test).* ***H****, The weighted profile of NFκB phosphoproteins that make up LV1 based on which phosphoproteins best correlated with 40Hz (positive) or random (negative) after 5 min of flicker exposure (mean ± SD from a leave-one-out cross-validation). pIKKα/β and TNFR1 most strongly contributed to separation between the groups.* ***I****, As in H for 15 min of flicker. pFADD expression in 40Hz flicker group and pNFκB in random group most strongly contributed to separation between groups. J, As in H for 60 min of flicker.*

We found that MAPK phosphorylation patterns were similar to those of NFκB but with different kinetics. MAPK phospho-signaling was significantly different between 40Hz and random groups after 60 minutes of flicker but not after 5 or 15 minutes. Phosphorylation of MAPK proteins following 5 minutes of 40Hz flicker did not significantly differ from random stimulation as indicated by no significant LV1 separation (t (32) =1.870, p=0.0707, unpaired t-test) (Fig. 4.2B,E). While phosphorylation of MAPK proteins also did not significantly differ following 15 minutes of 40Hz or random flicker (t(8.582)=1.99, p=0.2624, welch corrected

unpaired t-test), the heatmap of phospho-protein levels showed a trend for more phosphorylated MAPK proteins in 40Hz than random group (Figure 4.2C,F). MAPK phospho-signaling did significantly differ between 40Hz and random stimulation following 60 minutes of flicker exposure, as revealed by significantly separated LV1 scores (t(10)=3.709,p=0.004, unpaired t-test, Figure 4.2D,G). This effect was mostly driven by differences in phosphorylated MSK1, and MEK1 (Figure 4.2J). These results show that 40Hz flicker upregulates the MAPK pathway after approximately 60 minutes.

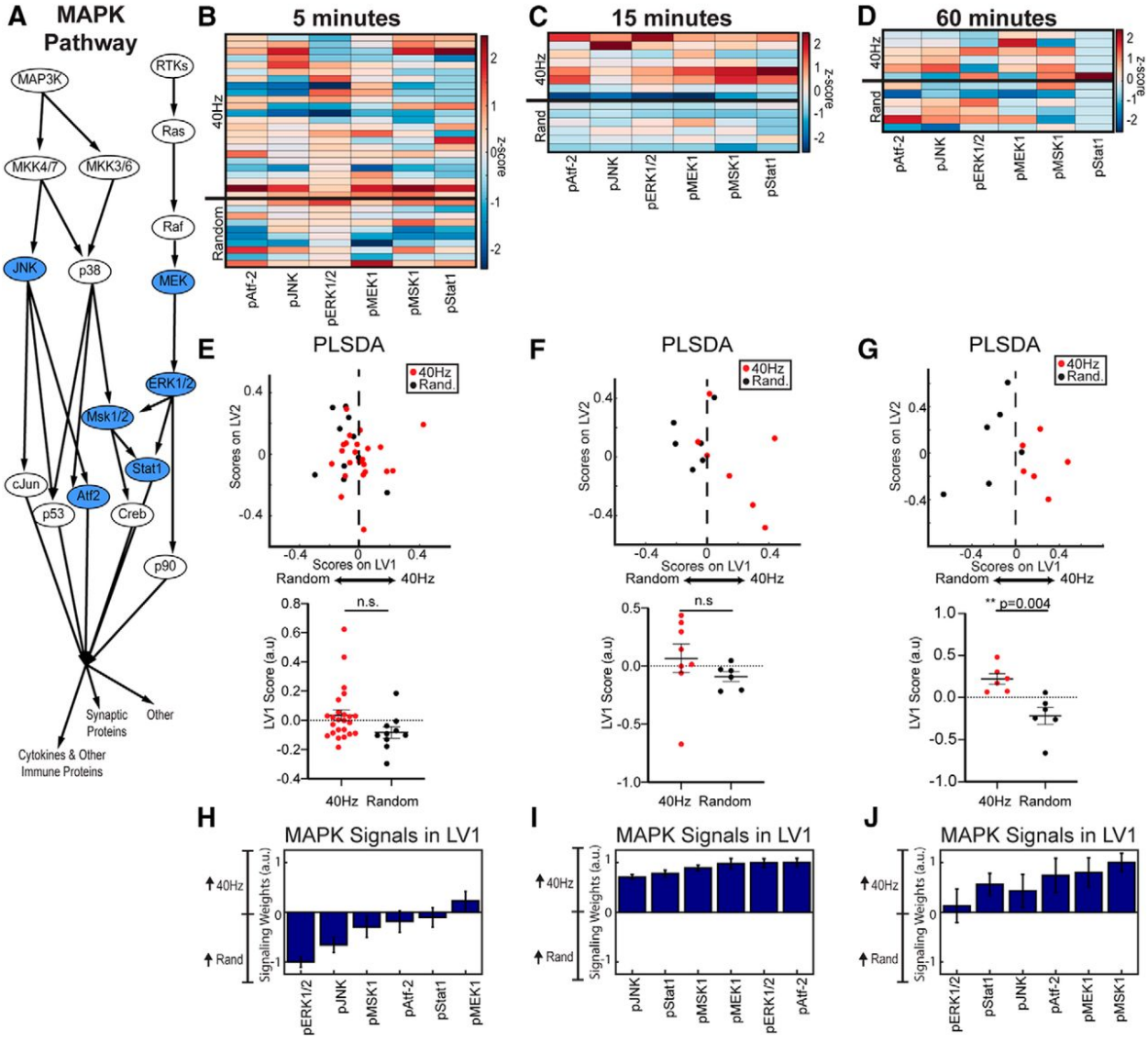

Figure 4.2: MAPK phosphoprotein signaling in visual cortex increased in response to 60 min of 40Hz flicker. ***A****, Simplified diagram of MAPK signaling including phosphoproteins quantified in the present study (blue ovals).* ***B****, MAPK phosphoproteins quantified in visual cortex in mice exposed to 5 min of 40Hz or random flicker (z-scored). Each row represents one animal with groups separated by thicker black horizontal lines. Thirty-four total animals were analyzed, n = 24 in 40Hz group, n = 10 in random group; outliers were removed through a principle component analysis on the data and iterative removal of data points outside a 99.5% confidence ellipse (mahalanobisQC in R version 3.5.2).* ***C****, As in B for mice exposed to 15 min of 40Hz or random flicker; 40Hz, n = 8; random, n = 6.* ***D****, As in B for mice exposed to 60 min of 40Hz or random flicker.* ***E****, Top, PLSDA on phospho-signaling data for mice exposed to 5 min of flicker did not separate 40Hz (red) samples and random (black) along LV1. Bottom, Plot of LV1 scores per group shows no significant differences between groups (difference between mean ± SEM values = −0.1181 ± 0.06318;* $t_{(32)}$ *= 1.870, p = 0.0707, unpaired two-tailed t test). Dots indicate individual animals for all graphs in this figure.* ***F****, Top, As in E, for mice exposed to 15 min of 40Hz or random flicker. Bottom, Plot of LV1 scores per group reveals a nonsignificant increase in 40Hz LV1 expression in 40Hz-exposed animals. (−0.1572 ± 0.1311; t (8.582) = 1.199, p = 0.2624, unpaired t test with Welch's correction).* ***G****, Top, As in E for mice exposed to 15 min of 40Hz or random flicker. Bottom, Plot of LV1 scores per group shows significantly higher LV1 scores in 40Hz-exposed animals (−0.4393 ± 0.1185;* $t_{(10)}$ *= 3.709, p = 0.0040, two-tailed t test).* ***H****, The weighted profile of MAPK phosphoproteins that make up LV1 based on which best correlated with 40Hz (positive) or random (negative) flicker after 5 min of flicker exposure (mean ± SD from a leave-one-out cross-validation).* ***I****, As in H for 15 min of flicker.* ***J****, As in H for 60 min of flicker. pMSK and pMEK expression in the 40Hz flicker group most strongly contributed to separation between groups.*

4.2.2 Phosphoprotein Network Correlations

Because phospho-signaling is transient, another way of assessing activity in these pathways is to measure coordinated phosphorylation among proteins. We thus hypothesized that activation of these pathways would lead to coordinated phospho-protein levels at time points prior to our observed increases in cytokine expression. Therefore, we examined how coordination both within and between NFκB and MAPK networks changed over the course of 40Hz flicker exposure. In order to do so, we utilized variability across animals and investigated protein co-variation across animals by calculating the correlation coefficients of each protein pair from NFκB and MAPK pathways after 5, 15 and 60 minutes of 40Hz flicker stimulation [124,125] (Figure 4.3). In other words, this analysis revealed protein phosphorylation levels that significantly increased or decreased together across animals (Figure 4.3, $q < 0.1$, false discover rate correction for 135 comparisons, Pearson correlation test).

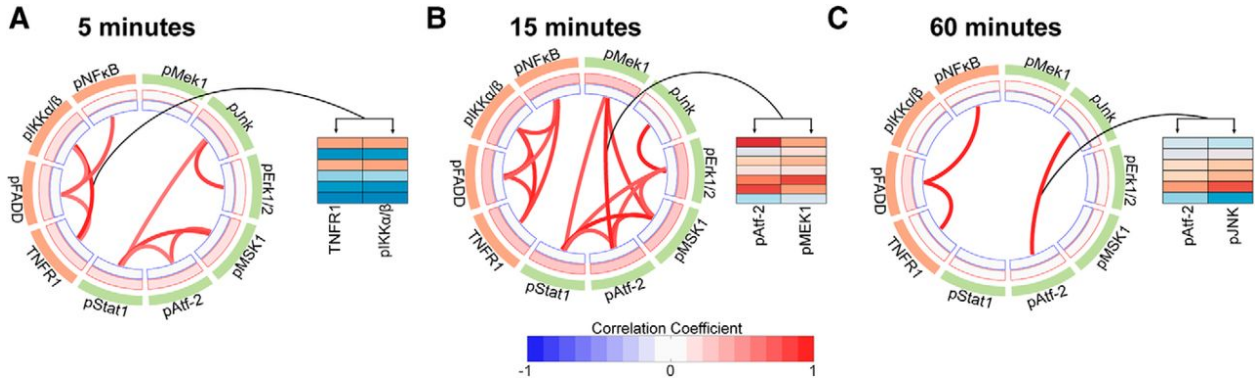

Figure 4.3: Phosphoprotein network correlations are highest after 15 min of 40Hz flicker exposure*. A, Significant correlations following 5 min of 40Hz flicker in NFκB (orange) and MAPK (green) phosphoprotein levels across animals displayed as links, with color indicating the strength of positive correlations (red) or negative correlations (blue). No negative correlations were found in these interactions. $q < 0.1$, false discovery rate correction for 135 comparisons, Pearson correlation test.*

Right, Example of correlated phosphoproteins. ***B****, As in A for 15 min of 40Hz flicker.* ***C****, As in A for 60 min of 40Hz flicker.*

Over the time points assessed, we found the number of significant correlations between proteins within each pathway was highest after 15 minutes of 40Hz flicker. After 5 minutes of 40Hz flicker, five proteins were significantly correlated within the NFκB pathway and four within the MAPK pathway (Figure 4.3A). After 15 minutes of 40Hz flicker, more protein correlations were found: 6 significant correlations in the NFκB pathway and 10 significant correlations in the MAPK pathway (Figure 4.3B). Interestingly, the proteins that were significantly correlated after 15 but not 5 minutes of flicker were farther downstream in the MAPK pathway: pERK1/2, pMSK1, pATF-2, and pSTAT1 (Figure 4.2A). After 60 minutes of 40Hz flicker, only 3 significant correlations were found in both pathways (Figure 4.3C). Of note, all significant correlations were within and not across NFκB and MAPK pathways in all time points assessed.

4.2.3 Cytokine signaling after 40Hz Flicker is dependent on both NFκB and MAPK pathways

We observed that 40Hz flicker induced an increased in NFκB and MAPK pathway phosphorylation. This increased pathway activation occurs before the observed flicker-induced cytokine effect (Figure 3.1). Therefore, we hypothesized that phosphoprotein pathway activation of the NFκB and MAPK pathways is necessary for the observed flicker-induced cytokine expression. To test this, we inhibited these pathways using NFκB or MAPK inhibitors via intraperitoneal injection (IP) before exposing animals to 40Hz or 20Hz flicker and compared to vehicle injected animals.

Inhibiting the NFκB and MAPK pathways before 40Hz flicker stimulation prevented the increased cytokine expression caused by 40Hz stimulation. LV1 significantly separated each of the four the groups ($F(3, 20) = 13.28$, $p<0.0001$, one-way ANOVA) (Figure 4.4). A post-hoc multiple comparison analysis of LV1 scores by group showed significant differences between LV1 scores of animals in groups exposed to 40Hz vehicle compared to each other group (Table 4.1; Figure 4.4D,).

Table 4.1 Analysis Group Comparisons

Groups Compared	**Mean Diff.**	**95.00% CI of diff.**	**Significance**	**Adjusted P Value**
40Hz Vehicle vs. MAPK Inhibitor	0.3177	0.1281 to 0.5073	**	0.0011
40Hz Vehicle vs. NFκB Inhibitor	0.2379	0.04827 to 0.4275	*	0.0125
40Hz Vehicle vs. 20Hz Vehicle	0.4592	0.2696 to 0.6489	****	<0.0001

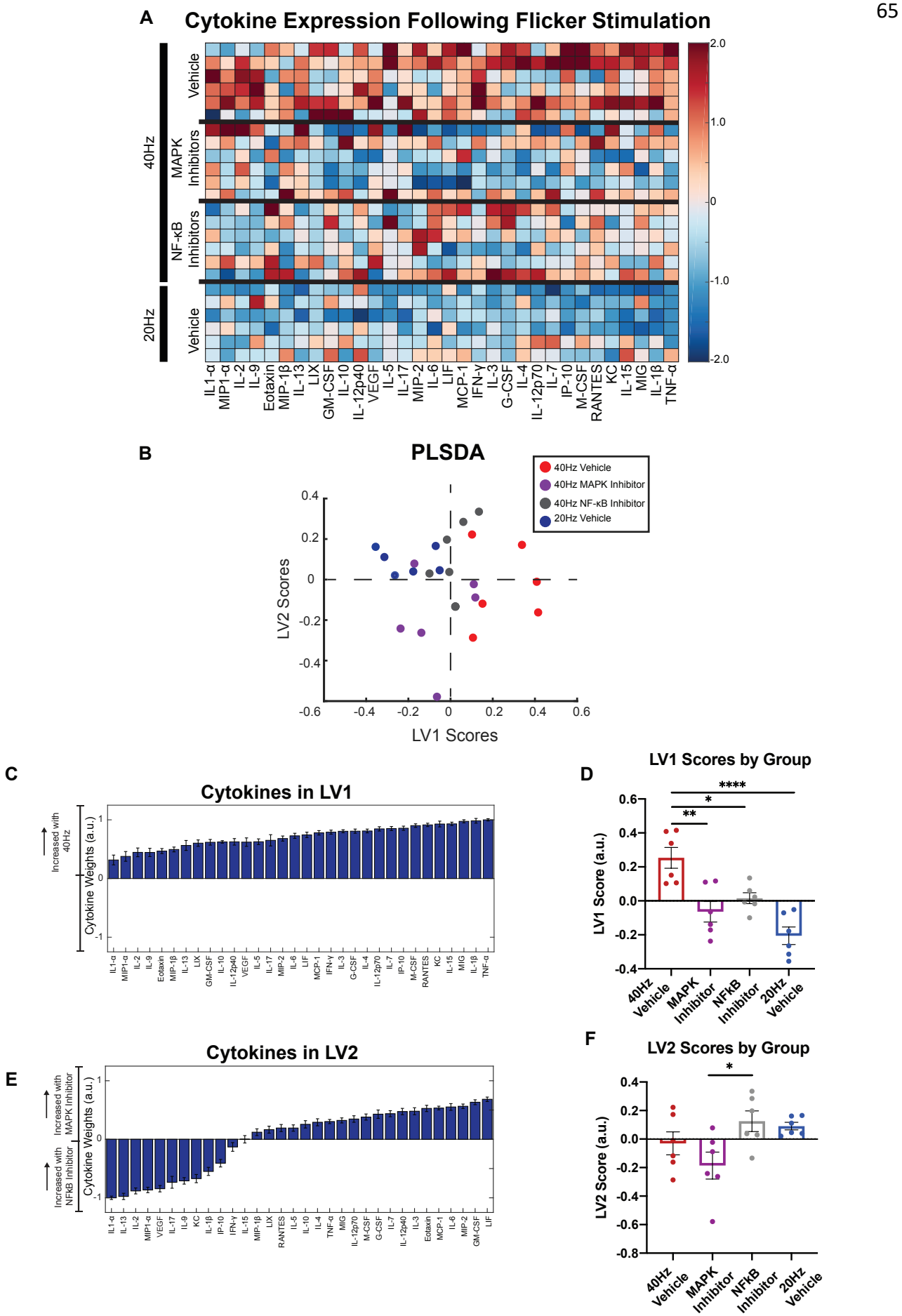
A
Cytokine Expression Following Flicker Stimulation
40Hz
20Hz
Vehicle
MAPK Inhibitors
NF-κB Inhibitors
Vehicle
2.0
1.0
0
-1.0
-2.0
IL1-α MIP1-α IL-2 IL-9 Eotaxin MIP-1β IL-13 LIX GM-CSF IL-10 IL-12p40 VEGF IL-5 IL-17 MIP-2 IL-6 LIF MCP-1 IFN-γ IL-3 G-CSF IL-4 IL-12p70 IL-7 IP-10 M-CSF RANTES KC IL-15 MIG IL-1β TNF-α
B
PLSDA
40Hz Vehicle
40Hz MAPK Inhibitor
40Hz NF-κB Inhibitor
20Hz Vehicle
LV2 Scores
LV1 Scores
C
Cytokines in LV1
Increased with 40Hz
Cytokine Weights (a.u.)
D
LV1 Scores by Group
LV1 Score (a.u.)
40Hz Vehicle
MAPK Inhibitor
NFkB Inhibitor
20Hz Vehicle
E
Cytokines in LV2
Increased with MAPK Inhibitor
Increased with NFkB Inhibitor
Cytokine Weights (a.u.)
F
LV2 Scores by Group
LV2 Score (a.u.)

Figure 4.4: NFκB and MAPK phospho-signaling pathways are necessary for gamma flicker-induced cytokine expression.

A*, Cytokine expression in visual cortices of mice injected with either phosphosignaling inhibitors or vehicle then exposed to 1 h of visual stimulation. Each row represents one animal (n = 6). Cytokines (columns) are arranged in the order of their weights on the LV1 in D. Color indicates z-scored expression levels for each cytokine.* ***B****, PLSDA identified LV1, the axis that separated 40Hz flicker-exposed animals (red) to the right, 20Hz flicker (blue) and inhibited animals to the left and random (purple and gray) (dots indicate individual animals for all graphs in this figure). LV2 separated the two inhibitor types (NFκB inhibited, gray; MAPK inhibited, purple).* ***C****, The weighted profile of cytokines that make up LV1 based on which cytokines best correlated with separation of 40Hz (positive) versus other groups (mean ± SD from a leave-one-out cross-validation).* ***D****, LV1 scores were significantly different for the 40Hz group compared with the comparison groups (mean ± SEM; F(3,20) = 13.28, p < 0.0001, one-way ANOVA). Each dot represents one animal.* ***E****, The weighted profile of cytokines that make up LV2 based on which cytokines best correlated with separation of the two inhibited groups MAPK inhibitor (positive) and NFκB inhibitor (negative) (mean ± SD from a leave-one-out cross-validation).****F****, LV2 scores were significantly different between the four groups (mean ± SEM; F(3,20) = 3.689, p = 0.0291, one-way ANOVA), with post-hoc analysis revealing a significant difference between animals injected with the MAPK versus NFκB inhibitors (p=0.0415) .*

Specifically, 40Hz and 20Hz vehicle groups were the highest separated by the PLSDA. Both groups injected with inhibitors before 40Hz expressed cytokines at levels between those of animals injected with vehicle and exposed to 40Hz and 20Hz (Figure 4.4 A). This general trend is also evident when analyzing specific cytokines. While not all of the following cytokines revealed significantly differences between groups with a one-way ANOVA, they all show a similar trend of increase in 40Hz and decrease in 20Hz, with the two inhibited groups between the two: IL-5, IL-9,IL-10, IL-12p70, LIF,IL-1β, IL-2, LIX, IL-15, IP, 10, KC MCP-1,MIP-1α,

M-CSF, MIP-2, MIG, RANTES, VEGF, TNF-α (Figure 4.5). Of these cytokines, TNF-α, IL-1β, MIG, and KC, most contribute to the effect (Figure 4.4A, C).

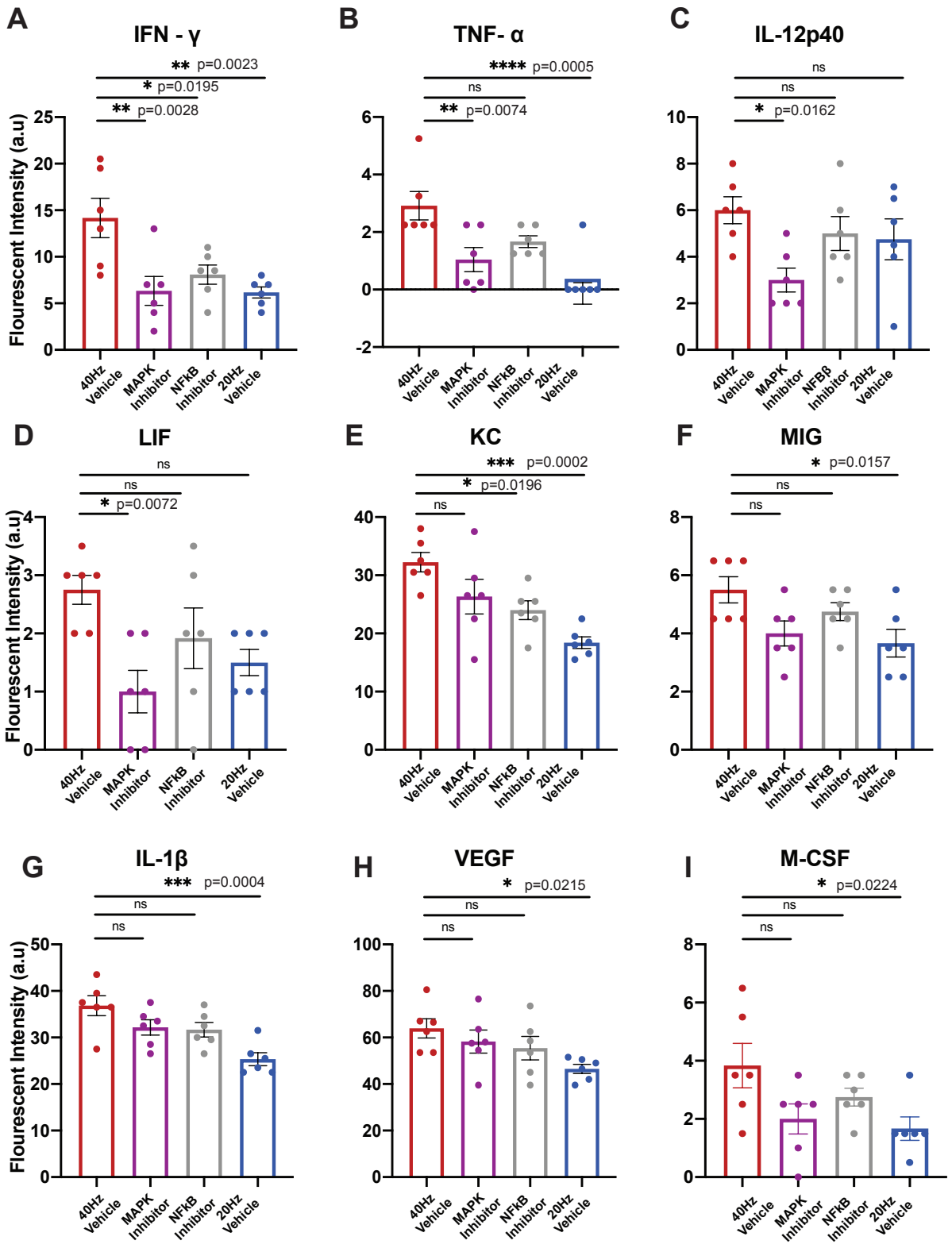
A
IFN - γ
** p=0.0023
* p=0.0195
** p=0.0028
Flourescent Intensity (a.u)
B
TNF- α
**** p=0.0005
ns
** p=0.0074
C
IL-12p40
ns
ns
* p=0.0162
D
LIF
ns
ns
* p=0.0072
E
KC
*** p=0.0002
* p=0.0196
ns
F
MIG
* p=0.0157
ns
ns
G
IL-1β
*** p=0.0004
ns
ns
H
VEGF
* p=0.0215
ns
ns
I
M-CSF
* p=0.0224
ns
ns
40Hz Vehicle
MAPK Inhibitor
NFkB Inhibitor
NFBβ Inhibitor
20Hz Vehicle

Figure 4.5: NFκB and MAPK inhibition suppressed expression of distinct cytokines following 40Hz stimulation. ***A****, One-way ANOVA displays significant difference in IFN-γ expression across groups, (mean ± SEM; F(3,20) = 6.787, p =0.0024, one-way ANOVA). The p-values from a Dunnett's multiple-comparison test are listed.* ***B****, As in A for TNF-α, (mean ± SEM; F(3,20) = 7.774, p =0.0012, one-way ANOVA).* ***C****, As in A for IL-12p40, (mean ± SEM; F(3,20) = 3.257, p =0.0431, one-way ANOVA).* ***D****, As in A for LIF, (mean ± SEM; F(3,20) = 4.225, p =0.0182, one-way ANOVA).* ***E****, As in A for KC, (mean ± SEM; F(3,20) = 8.57, p =0.0007, one-way ANOVA).* ***F****, As in A for MIG, (mean ± SEM; F(3,20) =3.782 , p =0.0268, one-way ANOVA).* ***G****, As in A for IL-1β, (mean ± SEM; F(3,20) =7.633 , p =0.0014, one-way ANOVA).* ***H****, As in A for VEGF, (mean ± SEM; F(3,20) =3.007, p =0.0545, one-way ANOVA).* ***I****, As in A for M-CSF, (mean ± SEM; F(3,20) =3.352 , p =0.0395, one-way ANOVA).*

Next, we found that each inhibitor significantly changes the cytokine profile uniquely. The second latent variable (LV2) identified by the PLSDA most clearly separates the animals injected with the inhibitors, and shows significant differences between groups (F(3,20)=3.689, p=0.0291, one-way ANOVA) (Figure 4.4B). A post-hoc analysis reveals that this difference indeed between the two groups injected with NFκB or MAPK inhibitor (t(20)=3.002,adjusted p-value=0.0415) (Figure 4.4 B,F). This effect is most driven by cytokines, LIF, GM-CSF, MIP-2, and IL-6 (Figure 4.4E). When the NFκB pathway is inhibited, IFN-γ and KC are both significantly decreased (p=0.0340) (Figure 4.5A, E). When the MAPK pathway is inhibited, GM-CSF is significantly decreased (p=0.0350), IFN-γ, TNF-α, IL-12p40, and LIF are all significantly decreased (Figure 4.5).

4.3 Discussion

Our data show that 40Hz gamma flicker stimulates NFκB and MAPK pathway signaling, which increased following 15 minutes or 60 minutes of 40Hz flicker, respectively. We show high correlations between phosphoproteins in each pathway, suggesting these pathways act independently. Last, we provide data to show the NFκB and MAPK pathways are required for downstream cytokine expression after gamma flicker.

These findings are consistent with the known transient kinetics of phospho-signaling and downstream gene and protein expression [123,126]. While the effect of 5 minutes of 40Hz flicker on the NFκB pathway were not significant, many of the animals did separate on LV1 and this was mostly driven by increases in TNFR1 and FADD phosphorylation. Interestingly, these two proteins are upstream in the NFκB pathway, and therefore we would expect these to become phosphorylated earlier than other proteins in the pathway. After 15 minutes of 40Hz flicker, all proteins in the NFκB pathway had elevated phosphorylation levels. Thus, we conclude that phosphorylation of the NFκB pathway begins after around 5 minutes of 40Hz flicker in some animals, but the full effects are not be detectable until after 15 minutes of 40Hz flicker. A similar trend is observed for the MAPK pathway, but it seems to be later, where 15 minutes of 40Hz flicker begins to upregulate the pathway and 60 minutes shows a distinct separation between 40Hz flicker and random groups. It is possible that later onset of MAPK pathway activation is related to increased expression of cytokines that act through the MAPK pathway.

For phosphoprotein analysis, we specifically compared 40Hz flicker and random flicker exposure. We chose random flicker as a key comparison because this stimulation type controls for the largest number of stimulation variables. However, we anticipate that if we compared 40Hz to 20Hz stimulation instead, we would see a bigger difference between groups, since 20Hz

had a more reduced cytokine expression profile in Figure 3.1. In contrast, we anticipate that light stimulation also upregulates signaling pathways because light stimulation uniquely upregulates some cytokines, distinct from 40Hz flicker.

Interestingly, our data show that the NFκB pathway is downregulated below random flicker after 1hour of 40Hz flicker stimulation, suggesting the effects of 40Hz flicker on these pathways are transient. Both NFκB and MAPK pathways are highly regulated via feedback mechanisms [127,128]. Given that our observed changes are occurring over the course of an hour, negative feedback mechanisms within the pathways are likely responsible for the downregulation of these pathways.

Our hypothesized time-course of pathway activity is further supported when examining correlations between phosphoproteins. After 5 minutes of 40Hz flicker, a pattern emerged within each pathway. Specifically, in the NFκB pathway, both pFADD and TNFR1 were highly correlated with phosphorylation of each other protein, aligning with increased expression patterns of these two phosphoproteins at the same time course. TNFR1 is upstream in the NFκB signaling pathway, suggesting 5 minutes of flicker begins to modulate the top of the pathway. 15 minutes of 40Hz flicker revealed more correlations among proteins, and these correlations included more proteins downstream in the pathway, suggesting the pathway is progressively activated with longer flicker exposure. However, after 60 minutes of 40Hz flicker, many correlations were no longer present. In fact, in the MAPK pathway, only pATF-2 and pJnk were correlated, downstream in the pathway. These correlation results help support our activation data. However, we note that the small sample size (6 animals), might account for the low significance associated with 60 minutes of stimulation at 40Hz. Further, while the analysis was designed to reveal correlations between any phosphoproteins, all significant correlations

remained within each pathway, supporting the idea that each pathway is operating with independent dynamics.

Inhibiting the NFκB and MAPK pathways prior to 40Hz flicker stimulation prevented the increased cytokine expression caused by 40Hz stimulation. These results show that both NFκB and MAPK pathways play a role in the increased cytokine expression after 40Hz flicker stimulation. IP-10 and KC both significantly decreased following NFκB inhibition only. Our findings align with previous research showing that both of these cytokines are indeed NFκB pathway dependent [129–132]. IL-12p70, LIF, MIP-2, and TNF-α significantly decreased following MAPK inhibition only. These results are supported by previous literature showing that expression of these cytokines are downstream components of the MAPK pathway [133–135].

IFN-γ was the only cytokine which significantly decreased following inhibition of both pathways. IFN-γ is of particular interest in this study because one of its main functions in the brain is to prime microglia recruitment, another effect of 40Hz flicker [12,136]. Further, IFN-γ has been considered the “master regulator”, suggesting that this cytokine acts as a checkpoint, thereby regulating expression of other cytokines [137]. Because both pathways inhibited this regulatory cytokine, it is possible that there would be more similarity in inhibition of cytokines after a longer duration of flicker exposure.

Other observed cytokines did not differ significantly between 40Hz and inhibitor groups but did show moderate decreases following inhibition of either pathway, suggesting that each pathway is not fully responsible for the effect. However, this conclusion is not in agreement with results from our correlation analysis, suggesting independent activity of both pathways (Figure 4.3). One possible explanation for this difference is unique temporal dynamics between both pathways after 40Hz flicker stimulation.

Both inhibitors decreased overall cytokine expression, but not to the level of 20Hz stimulation. While these results clearly show NFκB and MAPK signaling play a causal role in generating the cytokine expression following 40Hz flicker, questions remain as to why some cytokine expression remains. Several biological mechanisms could be responsible for the observed decrease as the effect varies by cytokines. First, as suggested above, each pathway may only be moderately responsible for the observed increase after 40Hz, and a combined cocktail of inhibitors would show a more decreased effect in cytokine expression. Second, both the NFκB and MAPK pathways are key cell signaling pathways, so inhibition of either pathway could lead to compensatory biological effects from other pathways. Other pathways, such as the Akt pathway have shown a biological relationship with these pathways, therefore it is possible that it increases in activation if one of these pathways is altered [138,139]. Last, the moderate decrease in cytokine expression when compared to 20Hz could be due to a possible downregulation of cytokine expression following 20Hz flicker exposure shown in Chapter 3, and the MAPK and NFκB inhibitors prevented the increase in cytokine expression after 40Hz flicker stimulation but did not bring it down to the downregulated levels following 20Hz stimulation.

Both the NFκB and MAPK pathways play key roles in immune function, synaptic plasticity, and learning and memory. NFκB and MAPK pathways regulate cytokine levels by activating transcription factors involved in cytokine expression [110–112]. Increased phosphorylation in the MAPK pathway occurs after spatial memory and is necessary for long-term memory formation [140]. The NFκB pathway is more traditionally known for its role in inflammation, but is also necessary for long-term potentiation and long-term depression and is increased following synaptic stimulation [141,142].

40Hz light flicker likely stimulates intracellular phospho-signaling and expression of diverse genes by driving neural activity. Several studies have shown that flickering light at a particular frequency drives that frequency neural activity in primary visual areas and 40Hz flicker induces neural activity around 40Hz [51,56,64]. Neuronal activity leads to calcium influx which in turn, stimulates multiple molecular signaling events, including activation of multiple isoforms of protein kinase C (PKC), which activates the NFκB and MAPK pathways. In fact, inhibition of calcium activity blocks NFκB activation [142]. These pathways provide a possible link between gamma frequency activity induced by 40Hz flicker, phospho-signaling, and downstream gene expression.

Chapter 5: Gamma Visual Flicker Induces Immune Signals in Non-Microglial Cells

5.1 Introduction

Communication is crucial for proper functioning of the neuroimmune system. As stated earlier, both cytokines and phosphoproteins are essential communication signals within this system. The research presented in the last chapter established that the MAPK and NFκB phosphoprotein pathways are responsible for the cytokines expressed after 40Hz flicker. As such and based on other research, it follows that these intracellular phospho-signaling pathways are occurring in the same cells that are releasing the cytokines [143,144]. To properly understand the mechanism of action of 40Hz flicker's effect on the immune system, it is important to know which cells types are responsible for the observed effect.

The most well-known immune regulating cells in the brain are microglia. Microglia are indeed well-known sources and targets of cytokines, as microglia are primarily responsible for sensing changes in the neuronal environment and releasing immune factors to both help neurons and recruit other cells to a site of injury [145]. For these reasons, microglia are the most likely cell to be responsible for increased immune proteins.

It would be reasonable to hypothesize that the observed increase in immune signals following flicker stimulation arises from microglia, however the quick timeframe of protein phosphorylation suggests otherwise. The increase in phosphorylation is happening within minutes, suggesting these signals are likely coming from the very cells being modulated by the sensory stimulus. 40Hz flicker is modulating neuronal activity [12,23,146]. Flicker produces gamma oscillations, which occur in the brain through an interaction of activity from pyramidal cells and interneurons [147]. Both the NFκB and MAPK phosphopathways are signaling

pathways in both of these types of neurons [148–151]. Due to the quick nature of the phospho-signaling, it is more likely that the observed phosphoprotein signaling and following cytokine release are arising from neurons.

Neurons are not well-known for releasing immune proteins, but there are abundant examples showing activation of NFκB and MAPK pathways in neurons, specifically in relation to learning and memory functions. For example, expression of NFκB in neurons is shown in various neuronal cell types in the adult mouse brain, and its expression is modulated by neuronal activity [152]. Further, both pathways interact in neurons to regulate expression of immune proteins involved in detecting cellular damage and responding with an immune response [153].

Neuronal secretion of cytokines is not as well studied as cytokine release from other cell types; however, it is not unheard of. IL-6 and IL-1β can both be expressed in neurons in a healthy brain, as well as after an ischemia for IL-6 [154,155]. TNF-α, a key inflammatory cytokine, is also expressed in neurons, under conditions such as after a hippocampal lesion or a focal ischemia, with suggestions to it being a neuromodulator [156–158]. More specific to flicker, M-CSF, one of the primarily expressed proteins after 40Hz light stimulation seen in Chapter 3, is expressed in neurons through the NFκB signaling pathway in response to amyloid beta [159]. This previous research provides evidence and support for a neuronal origin of immune signals following 40Hz flicker stimulation.

Thus, based on the rapid cascade of immune signals observed following flicker and prior work showing neurons release cytokines, we hypothesize flicker-induced cytokines arise from neurons. We expect that microglia also play a role in this signaling because microglia are the primary immune cells in the brain and are well-established to release cytokines. This chapter will investigate in which cell types the 40Hz flicker-elicited immune response arises, specifically

focusing on neurons and microglia. We will first determine the role of microglia in flicker-induced immune changes by testing the effect of 40Hz Flicker in microglia-depleted brains. Then, we use immunohistochemistry to stain for phosphoproteins and cytokines of interest to determine with which cell types they localize with. These phosphoprotein studies are focused on the NFκB pathway because this was the pathway we saw the greatest effect in after 40Hz flicker stimulation (see Chapter 3).

5.2 Results

5.2.1 Confirmation of Microglial Depletion

To create a neural environment devoid of microglia, we used a CSF1 receptor (CSF1R) inhibitor, PLX3397 (PLX), added to mouse chow. We first wanted to confirm the drug did indeed deplete microglia in our hands because we used a new drug supplier that has not been previously used in published research. We also wanted to compare microglial expression after 1-week and 3-weeks of animals being fed this drug. To do this, we fed a group of mice either PLX3397 (PLX) or a control diet. Mice were sacrificed and brains extracted either 1 week or 3 weeks after onset of diet presentation (Figure 5.1A). Representative images after immunohistochemistry for, microglial marker, allograft inflammatory factor 1 (IBA1) on brains after one week or three weeks duration of the PLX or control diet visually show a dramatic decrease in microglia present for animals fed the PLX versus control diet at both durations, with almost all microglia ablated after 3 weeks duration. (Figure 5.1B). This pattern persisted when quantifying microglial amount in three different brain areas, which all show significant differences between animals fed a PLX or control diet (Frontal Cortex: one-week ($t(15)=9.930$, $p<0.000001$), three-weeks ($t(15)=14.87$, $p<0.000001$) ; Hippocampus: one-week($t(8)=7.875$,

p=0.000049), three-weeks(t(8)=8.807, p=0.000043); Visual Cortex: one-week(t(8)=4.573, p=0.0018), three-weeks(t(8)=17.35, p<0.000001))) (Figure 5.1C). This data shows that PLX treatment significantly decreased microglia presence after both one-week and three-week feeding durations (Figure 5.1C). The microglia remaining after PLX treatment also reflects a reactive morphology, evidenced by differences in soma volume (Figure 5.1B). So, while both durations significantly decreased microglia, there were far more reactive microglia after one week diet duration than three weeks. Therefore, three weeks of PLX treatment was necessary to deplete microglia and ensure minimal reactive cells remained.

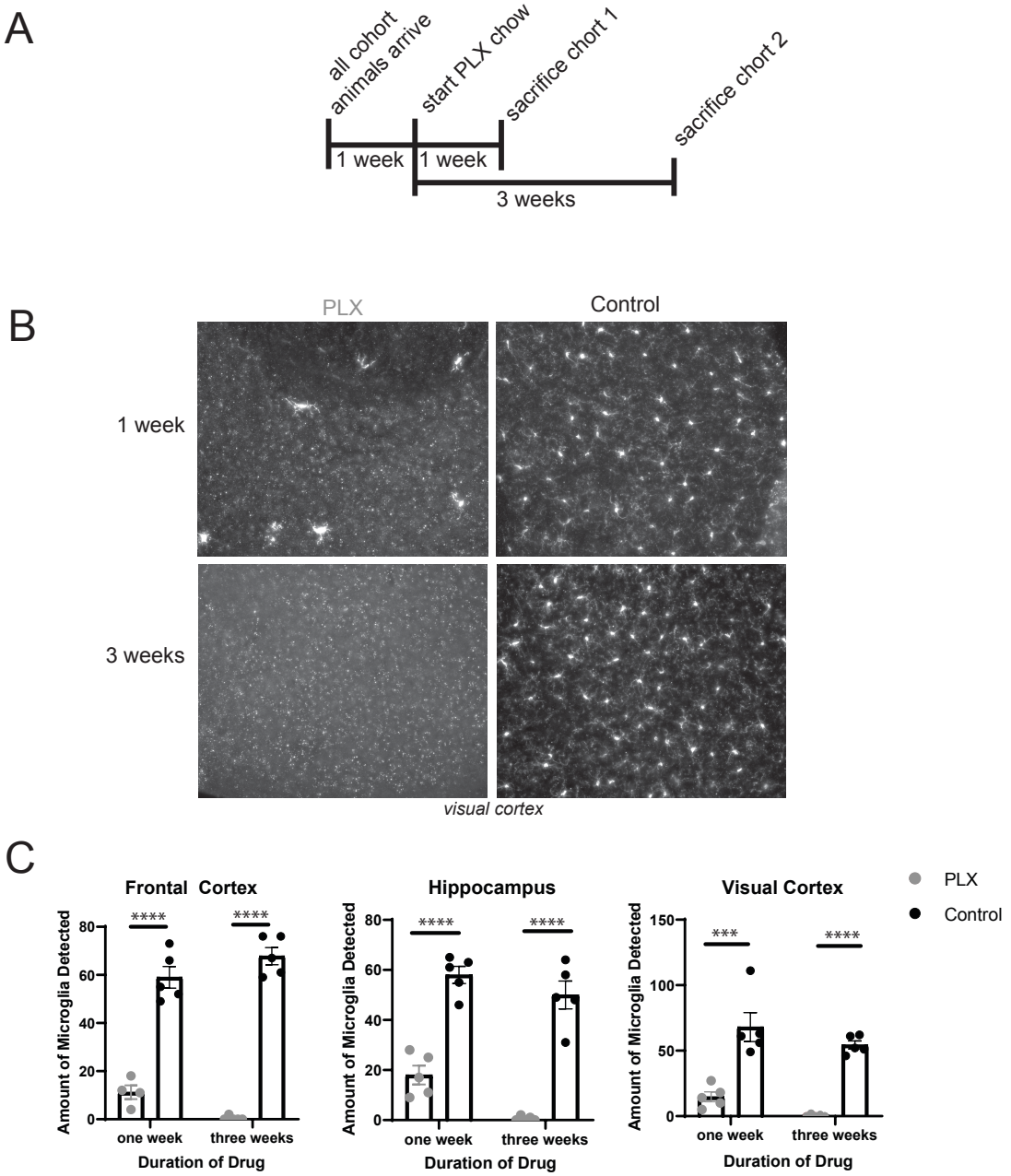

Figure 5.1: Three Weeks of PLX Diet Leads to Maximal Microglia Depletion.

A*, Experimental timeline for duration of diet after animal arrival.* ***B****, Representative immunohistochemistry in the visual cortex for IBA1 at both 1-week and 3-week PLX durations.* ***C****, Amount of microglia counted in three different brain regions with significant differences in microglial counts between PLX and control at both 1-week and 3-week durations.*

5.2.2 Microglia are not necessary for cytokine expression

We next confirmed that cytokines are expressed without microglia in the brain's environment. We fed a group of mice a diet with the drug PLX3397 or a control diet for three weeks. We then euthanized, removed the brain, and extracted the visual cortex from one hemisphere of the brain for multi-plex Luminex cytokine analysis and fixed the other hemisphere for immunohistochemistry of IBA1. This process is the same as what is done after flicker exposure, in an attempt to keep all variables consistent (see Chapter 2 for Methods).

We found that after three weeks of PLX treatment, and consequently microglial depletion, there is still cytokine expression in the visual cortex (Figure 5.2A). A PLSDA identified a latent variable (PLX LV1), which consisted of a weighted linear combination of cytokines most upregulated by the PLX diet. There was a significant separation between both groups along PLX LV1 ($t(25)=7.297$, $p<0.0001$, two-tailed t-test) (Figure 5.2B). T-tests conducted for individual cytokines revealed significant increases in expression of four cytokines after PLX treatment (IL-10: $t(25)=2.647$, $p=0.0139$; IL-12p40: $t(25)=2.665$, $p=0.0133$; M-CSF: $t(25)=4.608$, $p=0.001$; IL-1α: $t(25)=2.309$, $p=0.0295$, two-tailed t-test) (Figure 5.2C).

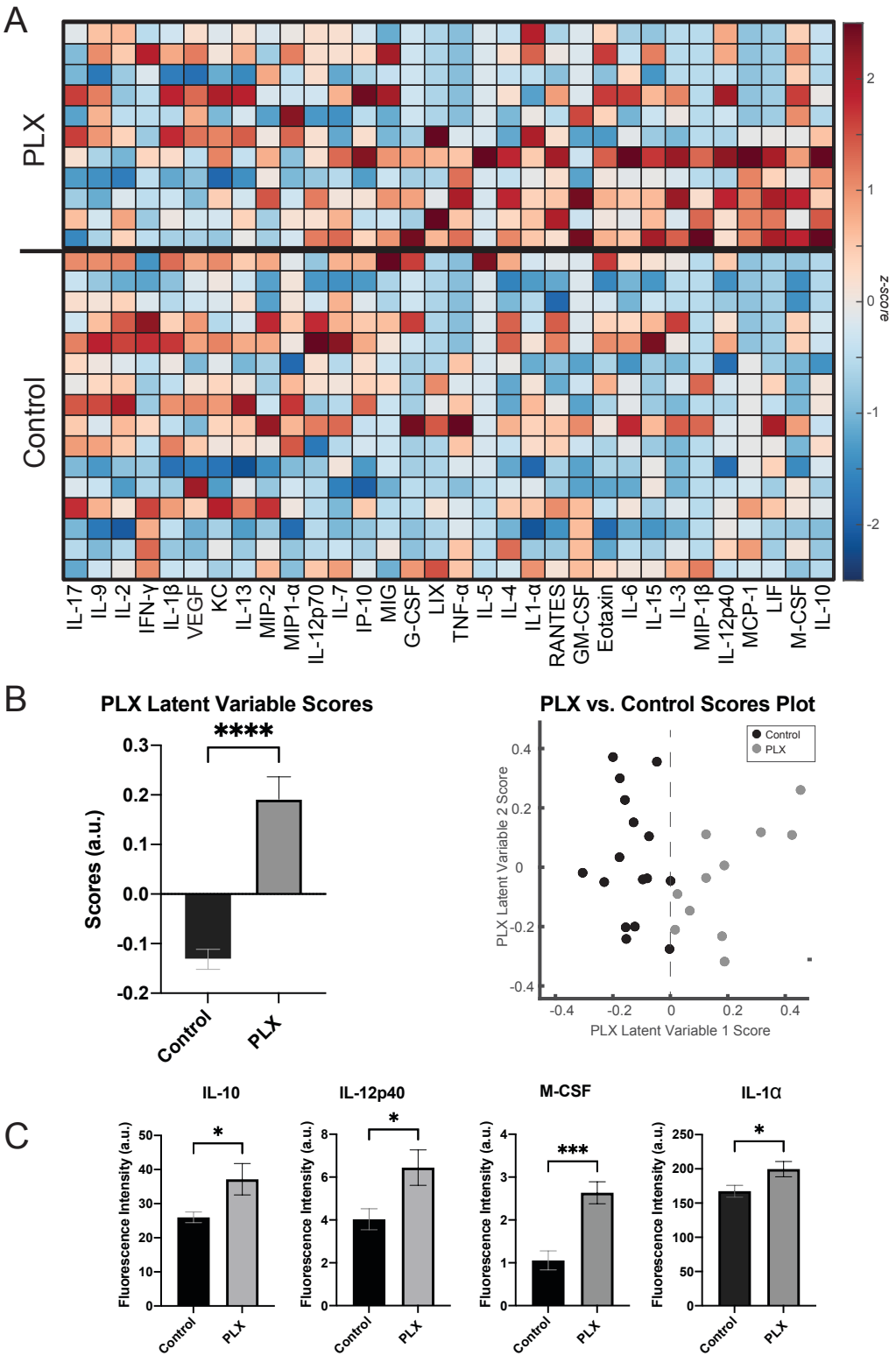
A
PLX
Control
z-score
2
1
0
-1
-2
IL-17
IL-9
IL-2
IFN-γ
IL-1β
VEGF
KC
IL-13
MIP-2
MIP1-α
IL-12p70
IL-7
IP-10
MIG
G-CSF
LIX
TNF-α
IL-5
IL-4
IL1-α
RANTES
GM-CSF
Eotaxin
IL-6
IL-15
IL-3
MIP-1β
IL-12p40
MCP-1
LIF
M-CSF
IL-10
B
PLX Latent Variable Scores
****
Scores (a.u.)
0.3
0.2
0.1
0.0
-0.1
-0.2
Control
PLX
PLX vs. Control Scores Plot
Control
PLX
PLX Latent Variable 2 Score
0.4
0.2
0
-0.2
-0.4
-0.4
-0.2
0
0.2
0.4
PLX Latent Variable 1 Score
C
IL-10
IL-12p40
M-CSF
IL-1α
Fluorescence Intensity (a.u.)
*
*
***
*
Control
PLX

Figure 5.2: Cytokines Persist in the Absence of Microglia.

***A**, Cytokine expression in visual cortices of mice fed PLX3397 or control diet for three weeks. Each row represents one animal. Cytokines (columns) are arranged in the order of their weights on the LV1. Color indicates z-scored expression levels for each cytokine. **B**, (right) PLSDA identified LV1, the axis that separated animals fed PLX3397 and a control diet, (left) LV1 scores were significantly different between the two groups of animals (mean ± SEM; t(25)=7.297, p<0.0001, unpaired, two-tailed t-test). **C**, Cytokines with significant differences in expression between both groups, IL-10: t(25)=2.647, p=0.0139; , IL-12p40: t(25)=2.665, p=0.0133; M-CSF: t(25)=4.608, p=0.0001; IL-1α: t(25)=2.309, p=0.0295.SEM, standard error of the mean.*

5.2.3 Microglia are not necessary for all 40Hz gamma flicker-induced cytokines

After finding cytokines are still produced in a brain absent of microglia, we next asked if 40Hz-flicker induced cytokines were still present after microglia depletion. We fed mice either a control diet or the PLX diet for three weeks followed by one hour of 40Hz flicker stimulation, or 20Hz flicker stimulation, for a comparison. We found a unique cytokine expression profile in each of the three groups (Figure 5.3A). A PLSDA showed that latent variable 1, termed 40Hz LV, best separated animals exposed to 40Hz versus 20Hz (Figure 5.3B). A one-way ANOVA showed a significant difference between group scores on this variable ($F(2,33)=7.747$, $p=0.0017$). Post-hoc Dunnett's multiple comparison test showed the differences along this 40Hz LV variable were between animals fed control diets and exposed to 40Hz versus 20Hz ($p=0.0043$). There was no significant different between microglia-depleted animals and control animals exposed to 40Hz stimulation along this variable ($p=0.9773$) (Figure 5.3C).

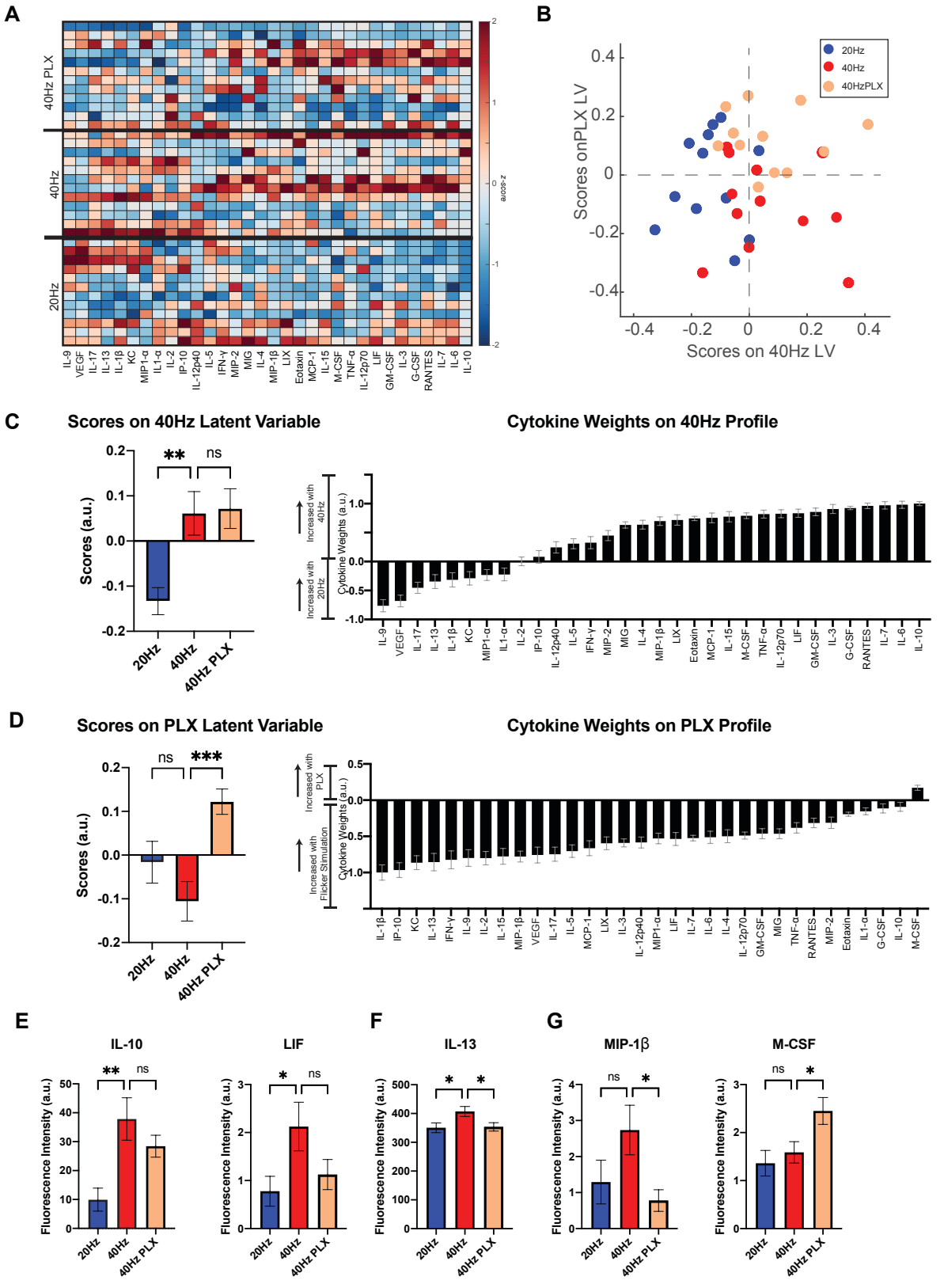
A
40Hz PLX
40Hz
20Hz
IL-9 VEGF IL-17 IL-13 IL-1β KC MIP1-α IL1-α IL-2 IP-10 IL-12p40 IL-5 IFN-γ MIP-2 MIG IL-4 MIP-1β LIX Eotaxin MCP-1 IL-15 M-CSF TNF-α IL-12p70 LIF GM-CSF IL-3 G-CSF RANTES IL-7 IL-6 IL-10
B
20Hz
40Hz
40HzPLX
Scores onPLX LV
Scores on 40Hz LV
C
Scores on 40Hz Latent Variable
Scores (a.u.)
**
ns
20Hz
40Hz
40Hz PLX
Cytokine Weights on 40Hz Profile
Cytokine Weights (a.u.)
Increased with 40Hz
Increased with 20Hz
IL-9 VEGF IL-17 IL-13 IL-1β KC MIP1-α IL1-α IL-2 IP-10 IL-12p40 IL-5 IFN-γ MIP-2 MIG IL-4 MIP-1β LIX Eotaxin MCP-1 IL-15 M-CSF TNF-α IL-12p70 LIF GM-CSF IL-3 G-CSF RANTES IL-7 IL-6 IL-10
D
Scores on PLX Latent Variable
Scores (a.u.)
ns
***
20Hz
40Hz
40Hz PLX
Cytokine Weights on PLX Profile
Cytokine Weights (a.u.)
Increased with PLX
Increased with Flicker Stimulation
IL-1β IP-10 KC IL-13 IFN-γ IL-9 IL-2 IL-15 MIP-1β VEGF IL-17 IL-5 MCP-1 LIX IL-3 IL-12p40 MIP1-α LIF IL-7 IL-6 IL-4 IL-12p70 GM-CSF MIG TNF-α RANTES MIP-2 Eotaxin IL1-α G-CSF IL-10 M-CSF
E
IL-10
LIF
F
IL-13
G
MIP-1β
M-CSF
Fluorescence Intensity (a.u.)
20Hz
40Hz
40Hz PLX

Figure 5.3: 40Hz-Induced Cytokines Persist in the Absence of Microglia.

***A**, Cytokine expression in visual cortices of mice fed PLX or control diet then exposed to one hour of visual stimulation. Cytokines (columns) are arranged in the order of their weights on the LV1. Color indicates z-scored expression levels for each cytokine. **B**, PLSDA identified LV1, the axis that separated 40Hz flicker-exposed animals (red and beige) to the right and 20Hz flicker (blue)-exposed animals to the left (dots indicate individual animals for all graphs in this figure). LV2 separated animals treated with PLX before 40Hz flicker (beige) on top versus control treated animals before 40Hz flicker exposure (red) on the bottom. **C**, left, LV1 (termed 40Hz Latent Variable) scores were significantly different between groups (mean ± SEM ;F(2,33)=7.747, p=0.0017, one-way ANOVA) post-hoc analysis revealed significant differences between animals treated with control diet and exposed to 40Hz flicker versus 20Hz (p=0.0043); right, the weighted profile of cytokines that make up LV1 based on which cytokines best correlated with separation of 40Hz (positive) versus 20Hz flicker control (negative) (mean ± SD from a leave-one-out cross-validation). **D**, left, LV2 (termed PLX Latent Variable) scores were significantly different between groups (mean ± SEM ;F(2,33)=7.630, p=0.0019, one-way ANOVA) post-hoc analysis revealed significant differences between animals exposed to 40Hz flicker and pretreated with PLX diet or control diet (p=0.0010). right, the weighted profile of cytokines that make up LV2 based on which cytokines best correlated with separation of animals treated with PLX (positive) versus flicker stimulation (negative) (mean ± SD from a leave-one-out cross-validation). **E**, There were significant differences in expression of IL-10 across the three comparison groups (mean ± SEM; F(2,33)=7.195, p=0.0026, one-way ANOVA), with a significant increase in expression in animals exposed to 40Hz control versus 20Hz control (mean ± SEM; IL-10: p=0.0014;LIF: p=0.0362). **F**, IL-13 had significantly different expression across groups (mean ± SEM ; F(2,33)=3.840, p=0.0317, one-way ANOVA). A post-hoc comparison test shows significant differences between 20Hz and 40Hz stimulation exposed animals (p=0.0345) and between 40Hz stimulation control and PLX pretreated animals (p=0.0479). **G**, There are significant differences across groups in MIP-1β (mean ± SEM; F(2,33)=3.315, p=0.0488, one-way ANOVA) and M-CSF(mean ± SEM; F(2,33)=4.959, p=0.0131, one-way ANOVA).Post-hoc multiple comparisons analysis*

shows significant differences between animals exposed to 40Hz and pretreated with a control diet versus PLX (MIP-1β: (p=0.0339); M-CSF: (p=0.0445)).

Through this analysis, we also saw differences in cytokine expression in animals fed PLX or the control diet. The second latent variable (PLX LV) separated microglia depleted animals versus not (Figure 5.3B). A one-way ANOVA found a significant difference between groups on scores along this variable ($F(2,33)=7.630$, $p=0.0019$). Post-hoc Dunnett's multiple comparisons tests showed a significant difference in scores between animals exposed to 40Hz stimulation with microglia depleted versus non-depleted ($p=0.0010$) and not between non-depleted animals exposed to 40Hz versus 20Hz stimulation ($p=0.2352$) (Figure 5.3D). This difference was mostly driven by increase M-CSF expression by the PLX drug (Figure 5.3D, right).

We next examined individual cytokines that showed significant differences between groups and found some cytokines were uniquely regulated by each condition. Animals exposed to 40Hz expressed significantly more IL-10 than animals exposed to 20Hz (mean difference= 27.89, $p=0.0014$) (Figure 5.3E, left). The two groups exposed to 40Hz flicker stimulation, regardless of PLX or control diet administered (mean difference= 9.402, $p=0.3581$) (Figure 5.3E, left). Similar effects were seen for LIF, with a significant difference in LIF expression between animals fed control diet and exposed to 40Hz versus 20Hz (mean difference= 1.3447, $p=0.0362$), and no significant difference in expression between animals exposed to 40Hz flicker and fed PLX versus a control diet (mean difference= 1.00, $p=0.1368$) (Figure 5.3E, right). IL-13 expression was significantly increased in animals exposed to 40Hz flicker versus 20Hz, both fed control diets, (mean difference=56.79, $p=0.0354$), and microglial depletion led to a significant decrease in IL-13 expression after 40Hz flicker exposure (mean difference=53.71, $p=0.0479$) (Figure 5.3F). Last, we show two cytokines that were not significantly different between

stimulation types but significantly differed with PLX pretreatment. MIP-1β expression showed a significant decrease in microglia-depleted animals exposed to 40Hz flicker when compared to microglia-intact animals exposed to 40Hz flicker (mean difference= 1.958, p=0.0339). M-CSF had increased expression in microglia-depleted exposed to 40Hz flicker compared to microglia-intact (mean difference=-0.8623, p=0.0445). Through this study, we found that microglia are not necessary for the increased expression of some cytokines after gamma flicker, while others did depend on microglia for expression.

5.2.4 pNFκB Expression After Gamma Flicker Occurs in Neurons

We previously found that 40Hz flicker leads to increased phosphorylation of the NFκB pathway. Next, to identify the cellular source of this increased phosphorylation pattern, we used immunohistochemistry to co-label phosphorylated NFκB (pNFκB) with cell markers for three of the main cells in the brain, neurons (NeuN), microglia (IBA1), and astrocytes (GFAP). We found that, after 40Hz flicker stimulation, pNFκB colocalizes with NeuN specifically, and not microglial or astrocytic markers (Figure 5.4A-C).

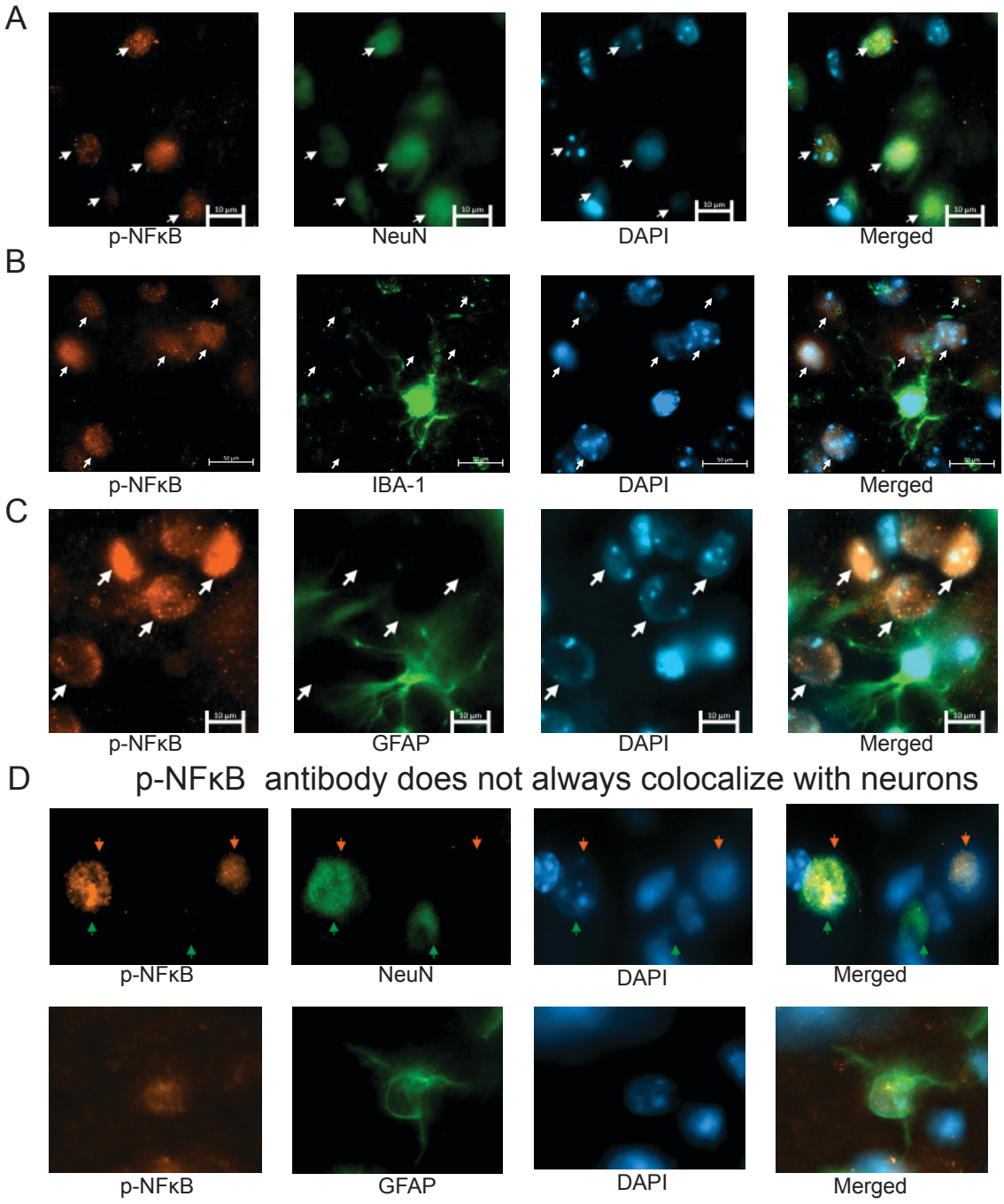

Figure 5.4: pNFκB Induced after 40Hz Flicker Colocalizes with NeuN.

A*, Representative IHC co-labeling of pNFκB (orange) with neuronal marker, NeuN, (green), and DAPI (blue) shows colocalization of pNFκB with neurons after 40Hz 15 minutes of flicker exposure (scale*

bar= 10 μm) ***B****, Representative IHC colabeling pNFκB (orange) with microglial marker, IBA1, (green), and DAPI (blue) shows pNFκB does not colocalize with microglia after 40Hz flicker exposure (scale bar= 50 μm)* ***C****, Representative IHC colabeling of pNFκB (orange) with astrocyte marker, GFAP, (green), and DAPI (blue) shows pNFκB does not colocalize with astrocytes after 40Hz flicker exposure (scale bar= 10 μm)* ***D****, Representative baseline (no flicker) IHC colabeling of pNFκB (orange) with neuronal marker, NeuN, (top) and astrocyte marker, GFAP (bottom) shows our pNFκB antibody does not always colocalize only with NeuN. Note, D images are not after 40Hz flicker.*

Because we saw such clear colocalization between pNFκB and NeuN only, we wanted to ensure there were no indirect interactions occurring between the pNFκB antibody and the NeuN antibody used that caused them to always visualize together. We showed that the pNFκB antibody used does not always colocalize with the NeuN antibody used and can, in fact, colocalize with other cells types, such as glial fibrillary acidic protein (GFAP) (Figure 5.4D).

5.2.4 M-CSF Expressed after Gamma Flicker is Expressed Neurons

After finding pNFκB was expressed in neurons after 40Hz flicker stimulation and previous findings showing pNFκB is necessary for downstream cytokine expression after gamma flicker, we speculated the flicker-induced cytokines are also expressed in neurons. To test this, we used immunohistochemistry to test if M-CSF did colocalize with neuronal marker, NeuN. We chose M-CSF because it was the top cytokine differentiating 40Hz Flicker versus the controls (Figure 3.1). We found M-CSF does colocalize with neurons after 40Hz flicker exposure (Figure 5.5).

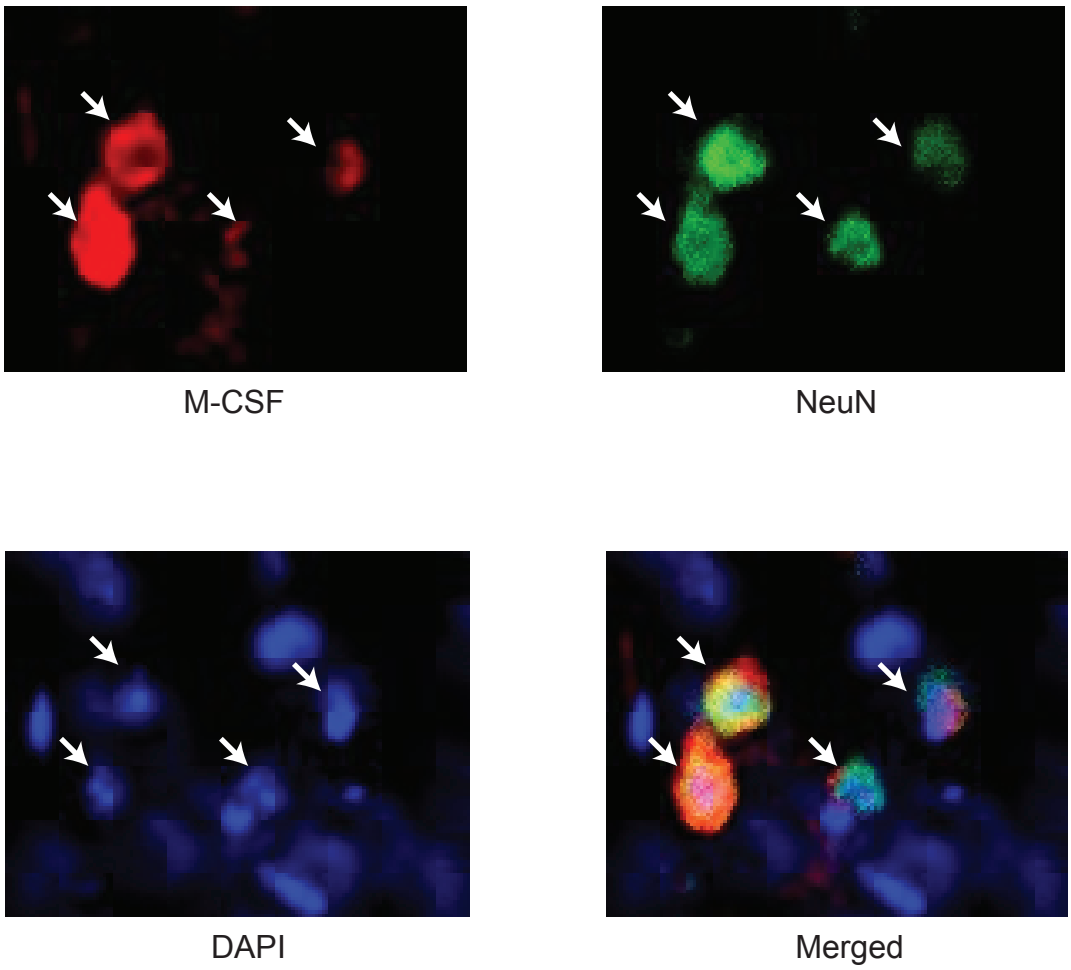

Figure 5.5: M-CSF Induced after 40Hz Flicker Colocalizes with NeuN.

Representative IHC co-labeling of M-CSF (red) with neuronal marker, NeuN, (green), and DAPI (blue) shows colocalization of M-CSF with neurons after 40Hz flicker exposure

5.3 Discussion

5.3.1 Confirmation of Microglial Depletion

To create a neural environment devoid of microglia, we used a CSF1 receptor (CSF1R) inhibitor, PLX3397 (PLX). PLX has previously been used to reduce microglia in the brain, with very little off-target impacts [72,160]. Previous uses of this drug in chow have been used for both one week and three-week durations [160,161]. We first confirmed our drug + diet combination worked as expected. We also used this experiment to establish a duration of feeding for the drug diet. While some previous research has established one-week of drug feeding as enough to deplete microglia, we found that one week of PLX diet feeding did significantly reduce microglia in the brain, but it was not enough to establish a full depletion [161] (Figure 5.1C). Further, we found that the microglia remaining after PLX treatment had altered morphology, specifically soma volume. We speculate this is due to remaining microglia reacting to the rapid decrease in microglial cells. Microglial soma volume is used as a measure of microglial reactivity, and reactive microglia have different properties than microglia at rest [162,163]. We felt that while one week of PLX treatment did significantly reduce microglia number, the remaining microglia were altered and could potentially impact the neural environment. For this reason, we decided three weeks of PLX treatment was the best experimental protocol to follow for our question of interest.

5.3.2 Cytokines Persist in the Brain in the Absence of Microglia

Microglia are the resident immune cells in the brain. Because of this, they are thought to be the main cytokine-producing cells [145]. Before using the depletion paradigm to examine the effects after gamma stimulation, we wondered if/how the microglia depletion would impact the

cytokine environment at a baseline, without stimulation. To answer this question, we fed mice the PLX chow for three weeks. After, mice were sacrificed, the visual cortex was extracted, and we used a multi-plex Luminex assay to measure the cytokines in the brain after microglia depletion.

While previous research has examined the brain's immune profile after depletion, we wanted to examine a baseline profile, without any sensory or inflammatory stimulation, using our proteomics assays. Previous research examine mRNA expression after 7 days of a PLX chow diet, and found a robust decrease in many cytokines after LPS stimulation [72]. This research was used to establish that microglial elimination itself does not produce an inflammatory response [72]. Under baseline conditions, we found that the PLX chow produces a unique profile of cytokine expression, which are separated from the cytokine profile of animals fed a control chow (Figure 5.2B). To our knowledge, this is the first characterization of cytokine expression after microglia depletion at baseline conditions. Interestingly, most cytokine expression did not significantly differ in animals fed the PLX chow versus not. The separation was mostly driven by the changed expression of four cytokines, IL-10, IL-12p40, M-CSF, and IL-1α. We suspect these changes in cytokine expression are the brain's response to decreased microglia in the environment.

Of these cytokines, we observed M-CSF to be continually increased in response to PLX. The main receptor for M-CSF is CSF1R, the receptor that the PLX drug is inhibiting. CSF1R regulates microglial activity in the brain [164]. We suspect there is a feedback loop occurring, where the blockade of CSF1R, along with the absence of microglia, leads the brain to release more M-CSF, in an attempt recruit microglia. As IL-12p40 is a proliferative and regulatory cytokine, we suspect it is also involved in the stability and recruitment of other cell types in a

microglia-depleted brain [165]. Il-12p40 also has roles as a pro-inflammatory cytokine, as does IL-1α. Microglia depletion producing pro-inflammatory cytokines is unlike previous findings using this drug [72]. However, it is likely that these cytokines are part of an attempted restoration process in the brain, as IL-1 has been known to play a role in microglial repopulation [166]. In contrast to IL-1, IL-10 is a known anti-inflammatory cytokine. In a microglial-depleted brain environment, there is a need to promote survival of neurons and other glial cells, a function which IL-10 is known to be involved in. IL-10 also leads to the release of neurotrophins and inhibits cell death [167]. IL-10 could be acting to promote a healthy brain environment after the death of microglial cells induced by PLX.

Importantly here, there were no cytokines that were significantly lowered in expression after PLX administration, which told us that microglia depletion in itself would not lead to a significant decrease in overall cytokine expression.

5.3.3 Microglia are not necessary for all 40Hz flicker-induced cytokines

After ensuring cytokines are still produced in a microglia-depleted environment, we next used this approach to ask if microglia are necessary for the increased cytokine expression after 40Hz flicker stimulation. Using a PLSDA, we found a clear separation between animals exposed to 40Hz flicker versus 20Hz, validating our previous experiments. This finding suggests that microglia are not necessary for the complete cytokine expression profile produced after 40Hz flicker exposure. Specifically, IL-10 and LIF are two cytokines that significantly differed between 20Hz and 40Hz stimulation but not between 40Hz-control- and 40Hz PLX-fed mice. IL-10 and LIF are two cytokines specifically upregulated by 40Hz that are not dependent on microglia. This finding is intriguing as IL-10 is a traditionally anti-inflammatory cytokine, providing further support that neurons, stimulated with 40Hz flicker, are protective for the

neuronal environment [168]. LIF is especially interesting as an upregulated cytokine not reduced by microglial depletion, as there is evidence that LIF is only expressed in neurons, as opposed to other important regulatory cell types in the brain, like astrocytes [169].

We next examined IL-13, a cytokine that is upregulated by 40Hz flicker, and this upregulation is attenuated with microglia depletion (Figure 5.3F). This finding shows that IL-13 is dependent on microglia. IL-13 is associated with microglial death and neuronal- specific survival, making it a key cytokine involved in both processes we were modulating [170]. It's role in neuronal survival could also be indicative of a potential protective effect of 40Hz flicker.

Last, both MIP-1β and M-CSF were found to be uniquely regulated by the PLX drug only. We suspect M-CSF was upregulated for reasons stated earlier, as it is a microglial recruiting cytokine that is involved in the recruitment and growth of microglia [171,172] . Therefore, we suspect it is being overly produced in a microglial-depleted environment. MIP-1β decreased in expression after PLX treatment (Figure 5.3G). However, this is not a trend we saw following PLX treatment alone (Figure 5.2A). While the difference in MIP-1β between 20Hz and 40Hz was not significant, 40Hz flicker exposed animals did seem to have a trending increase in MIP-1β expression (Figure 5.3G). Therefore, it is possible that 40Hz flicker does indeed lead to an increase in MIP-1β that is dependent on microglia.

This cytokine represents an overall trend we saw in our data. While microglia are not required for all cytokine expression after 40Hz, it is clear that their absence has some effects after 40Hz flicker. The PLX treated group did separate along a second latent variable (PLX LV), clearly differentiating it from 40Hz control treated animals (Figure 5.3B, D). We speculate this separation is because microglia are recruited after a disruption to the brain's usual environment. 40Hz flicker is altering the neural environment, and there is evidence that shows microglia react

to this stimulation [12]. Therefore, while our data shows that microglia are not necessary for all 40Hz flicker-induced cytokine expression, they do play a role in expression of some cytokines after flicker. We hypothesize that upon stimulation from 40Hz flicker, neurons release cytokines that recruit microglia, which then release cytokines themselves and perpetuate the effect, as microglia are known to be both sources and targets of cytokines [145] .

While we focus on specific cytokines because they show significant differences between groups, the profile of the combined cytokines is most important in these studies. It is possible that there is not a single cytokine primarily responsible for the effect seen after 40Hz flicker. Instead, our evidence shows that 40Hz flicker is modulating the immune environment, evident by the overall increased expression in cytokines after 40Hz flicker (Figure 3.1, Figure 5.3). For this reason, we focus on the overall pattern seen after microglial depletion. While some cytokines differed, microglia depletion did not fully reduce the increased expression of cytokines after 40Hz flicker exposure. We expect this altered immune environment is more important than any individual cytokine difference, as cytokine signaling pathways constitute an intertwined network, where cytokines signal and respond to each other.

5.3.4 Phosphorylated NFκB Gamma Flicker Localizes to Neurons

We identified that microglia are not necessary for the cytokine effect produced after 40Hz flicker. We established that the NFκB phosphoprotein pathway precedes and is necessary for cytokine production after 40Hz flicker (Chapter 4). So, to determine where these signals are originating, we used immunohistochemistry to determine where NFκB was phosphorylated after 40Hz flicker.

We focused on neurons because previous research has shown gamma visual flicker modulates neuronal activity [12,23]. Also, because phosphorylation of protein pathways happens

within minutes of flicker exposure, the time course is consistent with neuron modulation after flicker [173]. We, therefore, hypothesized that the signals were originating in the cells being modulated (Figure 4.1). We used pNFκB as a representative marker for NFκB pathway phosphorylation. We found that our pNFκB antibody colocalized specifically with neuronal marker, NeuN, and not with markers for microglia or astrocytes, which aligned with our hypothesis.

We found that our antibody strictly colocalized only with neurons after 40Hz flicker, which made us question the dynamics of the antibody and any biochemical interactions it is having with NeuN antibody. Antibodies are known to have non-specific binding, so we wanted to ensure our findings of pNFκB colocalization with NeuN were not an error. We used immunohistochemistry to visualize pNFκB in brains of animals at a baseline condition (not exposed to flicker). Using these brains, we found that the pNFκB antibody we used does not only colocalize with NeuN, as there are cases of it colocalizing with GFAP as well as examples of it not colocalizing with NeuN (Figure 5.4D).

5.3.5 M-CSF Induced after 40Hz Flicker Colocalizes with NeuN

We found evidence to support that pNFκB induced after 40Hz flicker is occurring in neurons. This finding, along with our previous findings showing that cytokines after 40Hz flicker persist even in the absence of microglia, lead us to hypothesize that flicker-induced cytokines are originating in neurons. We used a similar approach as above and conducted immunohistochemistry for M-CSF and NeuN to assess colocalization. We chose M-CSF as it is a key cytokine of interest expressed after 40Hz flicker, is still present after microglia depletion, and has routinely shown its importance throughout this thesis.

We found that M-CSF did colocalize with NeuN, showing that it is indeed possible for M-CSF to be originating in neurons. Usually, cytokines are thought to be derived from more traditional immune cells, such as microglia. Using our microglia-depletion study, we were able to conclude microglia are not necessary for cytokine expression. However, a limitation in our study is that we are not able to fully deplete all non-neuronal brain cells to accurately conclude the cellular origin of flicker-induced cytokines. It is important to note that it is possible other cells are responsible for increased cytokine expression after flicker, such as astrocytes, dendritic cells, and other antigen-presenting cells in the brain parenchyma.

Previous research does support a role of neurons as possible cytokine producers. M-CSF specifically is present in post-natal neurons as well as post-injury sensory neurons [174,175]. Neurons have also shown expression of other cytokines, especially after a modulation to the neuronal environment. For example, both TNF-α an IL-1α have been shown to be expressed in neurons after an induced surgical ablation [156,176]. IL-6 is expressed in cortical and hippocampal neurons following a forebrain ischemia [154]. These findings even extend to humans, as evidence for neuronal M-CSF has been seen in AD patients[159]. Based on this literature, the idea of neurons expressing cytokines is not novel. However, it has not garnered much attention. Further research is necessary to understand the roles of neurons as immunomodulators.

While our data shows these signals are not microglia-dependent and provides support that both flicker-induced phosphoproteins and cytokines are originating in neurons, future studies should further examine this with more conclusive techniques. For testing phosphoprotein origin after flicker, the use of a specific pNFκB knock-out transgenic mice would be beneficial. For

examining cytokine expression, we suggest techniques such as in-situ hybridization, RNAscope, or single-cell RNA sequencing.

Chapter 6: General Discussion

6.1 Summary

The overall objective of this thesis was to investigate the effect of flicker stimulation on the brain's immune environment. We tested the hypothesis that 40Hz gamma flicker recruits the brains immune system through phosphoprotein pathways and cytokine expression in neurons. We demonstrated that one hour of 40Hz visual flicker leads to an increase expression profile of cytokines in the mouse brain which differed from traditional models of inflammation (Chapter 3). We showed that phosphorylation of the NFκB and MAPK pathways is increased within minutes of 40Hz flicker exposure, and that these pathways are necessary for the increased cytokine observation after an hour of flicker (Chapter 4). We found that NFκB and M-CSF colocalize with neurons and some cytokines expression is not microglia dependent following 40Hz flicker, suggesting that these signals are originating in neurons (Chapter 5).

6.2 Major Contributions

Research underling gamma sensory stimulation has been enriched in the past decade. From observing the decreased gamma band activity in models of AD to using previously established techniques to induce gamma entrainment, a seminal 2014 paper reignited this field of study [12].This paper established the recruitment of microglia and decrease in amyloid beta in a mouse model of AD, highlighting the use of flicker as a potential therapeutic [12]. Further studies explored gamma stimulation, through flicker, does indeed rescue behavioral memory impairments in mouse models of AD, aligning with other similar work done through optogenetic stimulation [18,23]. Behavioral learning and memory as well as pathological rescue was seen in multiple models of neurodegeneration [50][50]. Similar studies show that after long term sensory flicker exposure, there is an upregulation in genes involved in immune response and synaptic

function [50]. These past studies have been crucial in defining the importance of gamma sensory flicker and its impact on the brain. We learned from these studies that gamma sensory flicker recruits multiple cell types, ameliorates pathological symptoms, and improves learning and memory behavior. Because of these more long-term impacts, it is clear that gamma sensory flicker is impacting the brain's immune environment, however, before this thesis, there was no knowledge on the immediate neuroimmune impact of gamma sensory flicker.

The work in this thesis contribute to the field in four major ways. First, we showed flicker begins to impact the immune environment within minutes of stimulation, previously the shortest duration of flicker's impact was two hours. Second, while most research on flicker has focused on 40Hz stimulation, our work shows, for the first time, that different flicker frequencies impact the immune environment in unique ways. Third, through our inhibition experiments, we provide a direct mechanism for how flicker elicits cytokine production. Last, we show microglia, a key immune cell in the brain, are not necessary for the effect of 40Hz flicker on increased cytokine production.

6.3 Flicker's Dynamic Effect on the Neuro-Immune System

Findings from this thesis show gamma visual flicker impacts immune signaling pathways in the brain. We specifically showed the impact on phosphoprotein pathways and cytokine signaling, and that these signals differ from pathological neuroimmune impacts. Because there was little background information on the interaction between neural activity and the neuro-immune environment, we began our experiments using a multi-plex approach, where we examined the expression of 32 different cytokines after flicker stimulation. This allowed us to understand how flicker is impacting the neuroimmune environment as a whole, and we therefore,

focused on the entire profile of cytokine expression in our studies. We feel this was an important first approach to characterize this effect. Still, our studies showed that some cytokines such as M-CSF, consistently increased in expression after gamma visual flicker. We hypothesized M-CSF was particularly present in our work because M-CSF is responsible for recruiting microglia [171]. It would benefit the field to further explore questions about the roles of specific cytokines in the flicker process.

Exploring the role of specific cytokine signal's role after flicker will prove beneficial, and this thesis also discussed the potential roles of individual cytokines in chapter discussions. However, we would like to acknowledge the findings of this thesis reflect an overall activation of the immune system. This is an important finding because many immune signals play different roles, depending on the situation and/or environment affecting the brain, and cytokines also regulate and impact each other's functions. One example of many is IL-6, which has pro- and anti-inflammatory properties, each elicited in response to different situations [177]. A unique balance of cytokines in the brain is crucial to keep a brain healthy, especially to prevent pathology. We believe flicker induces a unique and dynamic changing immune cytokine profile, and the exact expression of certain cytokines is not as important as the overall immune environment created.

Another key component of neuroimmune signaling is feedback mechanisms within signaling pathways. In Chapter 4, we focused on the NFκB and MAPK pathways' role in regulating cytokine expression. Another key component to this system is that cytokines also regulate expression of these phosphoprotein pathways. Further, we focused on the neuronal origin of our observed signals. It is highly possible that neurons elicit these immune signals, recruit glial cells, which then start expressing immune proteins themselves. While our studies

were not timed to detect these components, examining the feedback impacts of cytokines on phosphoprotein pathways as well as the role of other cell types in producing immune signals is an important consideration. As the use of longer, more chronic sensory flicker is gaining attention, it will be crucial to understand the dynamics of how the neuroimmune system responds after flicker.

6.4 Proposed Mechanism

This work lays crucial ground for establishing a mechanism of action for flicker as a therapeutic. So far, we have established flicker-induced phosphoprotein pathways followed by cytokine production. This pathway aligns well with previous research on these signals. We incorporated our research findings with previous literature on the subject to hypothesize a proposed mechanism for how flicker is changing the brain's immune system.

6.4.1 The Calcium Hypothesis

Our hypothesis centers on the impact of neuronal activity on calcium and vice versa. When a neuron is stimulated past threshold, an action potential is enacted. The action potential leads to a change in the electrochemical makeup of the cell and its surrounding, leading to an increased voltage inside the cell. This depolarization activates voltage-gate calcium channels, which allow for an influx of calcium into the cell. Gamma entrainment modulates action potential spikes, therefore leading to changes in calcium concentrations inside a neuron [23]. Once inside the cell, calcium acts as a second messenger and impacts many signaling pathways. Oscillations actually reduce the calcium threshold for activation of transcription factors, making

it more likely to transmit cellular signals [178]. These calcium-induced cellular signals include both the NFκB and MAPK pathways.

6.4.2 Calcium and the NFκB Pathway

We show phosphorylation of the NFκB pathway is necessary for downstream cytokine changes after gamma flicker exposure. The ability for NFκB to activate and drive transcription changes to cytokine expression after a stimulus is calcium dependent [179,180]. These findings lead to our hypothesis that gamma visual flicker leads to changes in NFκB through calcium signaling. A possible mechanism of action for how this could be happening is outlined in Figure 6.1. Briefly, increases in calcium concentrations after gamma-modulated neuronal spiking could bind to calmodulin, a calcium-binding protein. In fact, antagonizing calmodulin blocks NFκB activation [180]. Further, inhibition of calcium- responsive protein kinase C (PKCs) also reduces NFκB activity [180]. PKCs is hypothesized to also interact with calmodulin, providing another providing another possible mechanism linking calcium fluctuations to the NFκB pathway. PKC then phosphorylates IKK, which will then follow the canonical NFκB phosphorylation pathway (Figure 1.2).

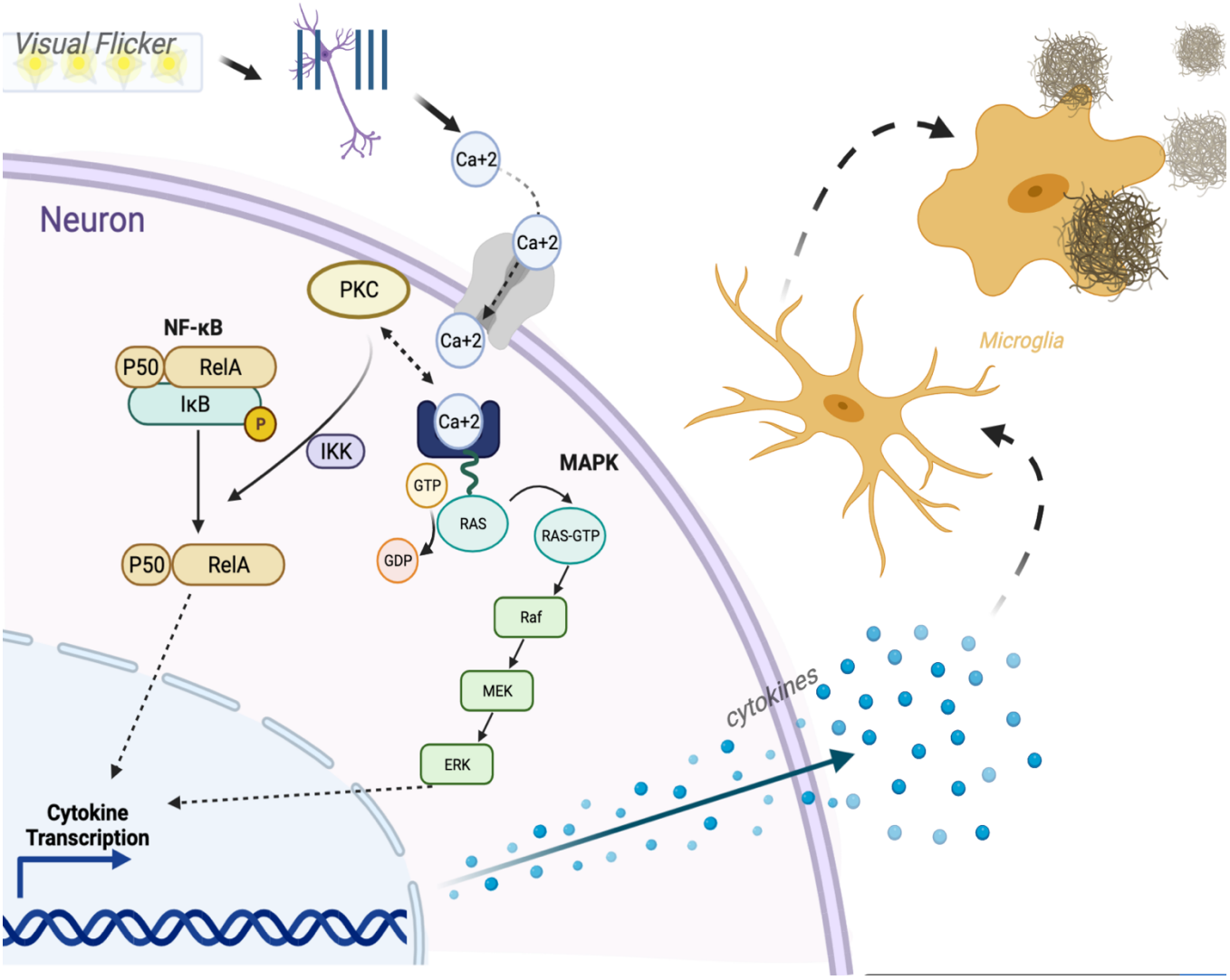

Figure 6.1: Propose mechanism of action for how gamma sensory flicker impacts the brain's immune environment.

In this thesis, we showed gamma visual flicker activates the NFκB and MAPK pathways, which are necessary for an increased cytokine expression profile after gamma flicker. To fit this into the current literature, we propose gamma flicker's modulation of neuronal activity drives changes in calcium levels that are responsible for the increased activity in the phosphoprotein pathways. We hypothesize the induced cytokines after gamma flicker recruit microglia and lead to the decrease in amyloid beta levels.

6.4.3 Calcium and the MAPK Pathway

While we showed stronger activity in the NFκB pathway following gamma visual flicker, the MAPK pathway is also involved in flicker-induced cytokine expression. Activation of the MAPK pathway after flicker aligns well with our proposed mechanism for calcium's involvement in gamma visual flicker, as calcium also acts as a second messenger in the MAPK pathway [181,182]. Our proposed mechanism for how gamma flicker activates the MAPK pathway is diagramed in Figure 6.1. Incorporating previously published work with work from this thesis presented above, we hypothesize flicker leads to increase in intercellular neuronal calcium, which binds to the calcium-sensory protein calmodulin, known to bind to RAS- GRF, a guanine nucleotide exchange factor that increases activity with elevated calcium levels [183].RAS-GRF catalyzes the conversion of RAS GDP to GTP, allowing RAS to act as a molecular switch on to the MAPK pathway diagramed in Figure 1.2.

6.4.4 Microglia and Amyloid Beta

After our hypothesized calcium- induced activation, both NFκB and MAPK pathways terminate in the activation of transcription factors that are known to regulate cytokine expression, which we show are upregulated by 40Hz flicker. As outlined in Chapter 3, we hypothesize that a key role of these increased cytokines is to recruit microglia. After gamma visual flicker, these microglia colocalize with amyloid beta and correlate with the ultimate decrease in amyloid beta pathology in a mouse model of AD. Interestingly, calcium deficits are also common in AD patients and AD mouse models, adding a potential connection between our proposed flicker mechanism and using flicker as a therapeutic for AD [184].

A precise mechanism of action for how gamma sensory flicker improves disease pathology has yet to be established. However, the work from this thesis provides key components of this pathway. The proposed mechanism outlined here is offered as a potential explanation and future research should use experimental manipulations to explore each causal component of this hypothesized pathway.

6.5 Flicker as a Therapeutic

Due to work done in this field in the past decade, using flicker sensory stimulation as a therapeutic is now more possible. The work of this thesis established a neuroimmune pathway induced after gamma visual stimulation. Other work has found multi-sensory stimulation, rather than visual alone, reaches deeper brain regions more likely to be impacted by disease, such as the hippocampus [23]. We specifically focused on one modality of sensory stimulation in our work to enable us to establish a mechanism of action on a simpler system. However, we anticipate our established pathway after visual flicker persists after multi-modal flicker simulation, and we hypothesize similar effects are occurring in the sensory cortices of other modalities stimulated.

6.5.1 Alzheimer's Disease

Expanding flicker to more brain regions allows it to have a more pronounced therapeutic effect. Using gamma flicker as a clinical therapy has mostly focused on Alzheimer's disease. Alzheimer's disease was a starting point in analyzing the impacts of gamma flicker on a disease model because there are clear neural activity deficits that correlate with cell and molecular pathology in AD.

The field has made strides since first studying gamma flicker in the context of AD. For example, seven days of visual and/or audio flicker reduces amyloid levels in a 5XFAD mouse model and tau phosphorylation in the P301S tauopathy model, showing a wide range of

pathological recovery potential [12,23]. A longer duration of 22 days of visual flicker rescues neuronal and synaptic marker loss, tau phosphorylation and markers of damage [50]. Last, weeks of flicker reduces ventricular expansion and neuroinflammation in a CK-p25 mouse model [50,185]. These studies allude to flicker's potential to rescue, alleviate, or perhaps prevent AD pathology in humans.

While examining pathological symptoms is promising, the ultimate test for a clinical therapeutic for AD is its ability to alleviate behavioral learning and memory deficits. Studies examining the effects of sensory flicker have established it also improves behavioral deficits of AD. Using the 5XFAD mouse model, 7 days of auditory flicker has been shown to improve spatial recognition memory in the Morris Water Maze [23]. This finding has also been replicated in other models of pathology [50]. It is important to note that this work was all done in models of AD, and translation to humans is still necessary.

The established effects in animal models provide scientific justification for testing the effects of flicker in humans. Previous work has shown that auditory sensory stimulus, caused by auditory sound beats, leads to entrainment in humans [186]. More recent work has taken important steps in applying a more similar gamma sensory flicker approach in humans. Preliminary, non-yet published work is showing that that audio/visual sensory flicker can indeed entrain deep brain regions in humans, taking an important step toward using this paradigm as a therapeutic.

These studies show great potential for the translation of sensory flicker into humans with AD. However, there is a lack of consistency with the uni- vs multi-modal sensory stimulations used as well as the amount of time that is optimal for improvements in both pathology and behavior. For this reason, we view our short-term studies exploring the dynamic environment

almost immediately after flicker exposure as a unifying, basic mechanism. More research will have to be done to optimize the therapeutic impact of flicker on humans, and we feel that an understanding of the basic mechanism of action happening after flicker exposure will be helpful knowledge to implement into the optimization of flicker as a therapeutic in humans.

6.5.2 Implications for other disease types

The latest work exploring sensory flicker as a therapeutic has focused on Alzheimer's disease. The findings from this dissertation that show the effect of gamma flicker on the neuro-immune system provide further justification for exploring the use of flicker in other brain diseases. Specifically, the multiple immune effects after different flicker stimulations provides a key foundation for modulating the impacts of multiple types of disorders. The field of neuro-immunology has seen a sharp rise in research showing many neurological and neuropsychiatric brain disorders/diseases involve malfunctions in the brain's immune system. While the cause and effects of the role of the immune system on disorders of the brain presents a metaphorical chicken versus egg conundrum, it is clear that the ability to manipulate the brain's immune system presents huge therapeutic potential for many brain diseases.

This potential stems from recent research elucidating the role of the immune system in brain diseases which were originally thought to be related more to other deficits. For example, the monoamine hypothesis, suggesting a decrease in key monoamines is responsible for depression, prevailed for many years as the prominent mechanism behind the disease. This hypothesis has dominated medical treatment for depression and is even suggested to have initiated modern psychopharmacology [187]. More recent work showing an inflammatory component to depression has opened up new avenues for therapies. For example, social defeat, one of the most well-established models for depression, recruits immune cells and signals in the

brain, which also correlated with increased anxiety in mice [188,189]. Further, a meta-analysis of clinical trials in humans shows that pharmacological manipulation of the cytokine environment improves depressive symptoms [190]. While cytokine inhibitors could be helpful, they can have unwanted side effects and has shown variability in response. Further, alterations in gamma rhythms have also been correlated with depressive-like symptoms [191]. A therapy like sensory flicker is a more reliable, easy-to-use, and cost-effective way to manipulate or perhaps prevent depression by allowing for a two-pronged approach that targets the neuroimmune system and neural activity, two components of depression.

Many other brain disorders have been shown to be modulated by the neuroimmune system. For example, schizophrenia is associated with increased expression of immune genes in the prefrontal cortex, an area which is entrained with gamma sensory flicker [23,192]. Other disorders display similar potential for flicker treatment, such as PTSD, bipolar disorder, autism spectrum disorder, and many other diseases involving the neuroimmune system [193].

6.6 Future Directions

Our work sets a foundation for future studies to examine how sensory flicker impacts and is impacted by the neuroimmune environment. Through our work in this space, we have opened the door to asking many more questions to both further dive into understanding the mechanism of action of sensory flicker as well as to translate sensory flicker for human therapeutic use.

6.6.1 In Vivo Experiments

Earlier in this chapter, we presented a hypothesized a potential mechanism incorporating the findings from this thesis with previous literature on the subject. In this section, we proposed a dynamic system involving flicker-induced calcium, leading to changes in immune proteins,

followed by microglial recruitment (Figure 6.1). Future experiments aiming to understand this pathway would benefit from *in vivo* experiments. A major limitation to our experiments was the importance of timing. In order to observe some of the changes we were able to see, we had to conduct highly time sensitive experimental procedures. Conducting *in vivo* imaging during sensory flicker would bypass this limitation as well as offer key insights into sensory flicker-induced changes in the brain.

6.6.1.1 Calcium Imaging

After the observed changes in neuronal electrophysiological activity that follow sensory flicker, we hypothesize there is a change in internal cellular calcium levels. We expect this increase to occur shortly after flicker onset. While the precise method used for calcium imaging will require further research and planning, as there are a plethora of possible protocols to follow, similar studies have shown it is indeed feasible to get single-cell resolution in a live, awake animal recording during a sensory flicker stimulation [194,195]. The use of two-photon microscopy with calcium imaging could also allow for the localization of calcium to specific neuronal sub-compartments. For example, after confirming an increase in calcium signaling during sensory flicker, it is possible to look specifically at dendritic and spine calcium signals following both visual and auditory stimulation [196,197]. This kind of application could have implications further than the role of calcium in sensory induced flicker, as dendritic spine activity is a crucial component to learning and memory mechanisms. Visualizing calcium in dendritic spines has the potential to provide another avenue in understanding sensory gamma flicker as a possible therapeutic for Alzheimer's disease.

6.6.1.2 Microdialysis

Our hypothesized mechanism proposes calcium leads to increase phosphorylation in the NFκB and MAPK pathways, which we show are responsible for increased cytokine production after gamma sensory flicker. As stated earlier, we found the time dynamics of this pathway to be highly sensitive, and we predict this sensitivity led to the variability observed in our studies. One way to circumvent this time sensitivity and variability is through *in vivo* analysis of cytokine expression changes. Microdialysis during sensory flicker in the visual cortex would allow for a more precise view of what is happening to neuroimmune signals during flicker. Microdialysis for cytokine analysis during flicker is a feasible approach, as studies have shown success with similar methods [198]. When examining other types of neuropeptides, microdialysis is a relatively minimally invasive procedure. However, the invasiveness of this procedure has higher significance when the output measure is immune proteins, as the stab wound inflected from the microdialysis probe would lead to a production of cytokines [199]. The implanted probe could also change the surrounding tissue, which could potentially impact cellular response to flicker [200]. For these reasons, proper execution of microdialysis cytokine analysis during sensory flicker will require careful study design and planning.

Microdialysis would be a key method for visualizing changes in cytokines during flicker. Another advantageous use for microdialysis in this setting would be the possibility of detecting changes in neurotransmitters. In working on this thesis, we noticed similarities between researched effects of norepinephrine and flicker. Both norepinephrine and flicker increase NFκB pathway phosphorylation, expression of cytokines, like MCP-1, microglia-mediated phagocytosis of amyloid, trigger brain inflammatory changes, and help reverse learning and memory deficits [12,23,201–204]. Because of this evidence, we asked if flicker induced a change

in norepinephrine through a small pilot study (Figure A2.1). We used high-performance liquid chromatography to assess the expression of multiple neurotransmitters after gamma sensory flicker. Our preliminary results revealed there were no differences in neurotransmitter levels in gamma flicker than control stimulation (Figure A2.1). However, these results were from one pilot experiment. There are multiple reasons to examine this question again. For one, to ensure proper scientific outcome, it is important to replicate experimental results, and our results were from one preliminary study. Second, there is ample research suggesting a connection between neurotransmitters and sensory flicker and finding a possible link between these two could increase the therapeutic relevance of sensory flicker. A third reason to further explore this question is that the timing for detecting changes in neurotransmitters is sensitive, and more rapid, *in vivo* methods would show different results. For these reasons, using microdialysis to analyze changes in neurotransmitter concentrations following gamma flicker is an important future direction.

6.6.2 The Role of Akt phospho-signaling in Gamma Flicker

Our studies found an increase in NFκB and MAPK pathway activity following gamma sensory flicker. We also fund these pathways were responsible for the increased cytokine expression following 1 hour of sensory flicker. The NFκB and MAPK pathways are two crucial pathways to explore in this setting, and there is much more research needed to fully understand the impact sensory flicker has on these pathways. However, the Akt pathway is also of interest to this paradigm. We have preliminary data which suggests gamma visual flicker induces an increase in Akt pathway activity, when compare to 20Hz visual stimulation. The Akt pathway is responsible for cell growth and survival, with implications toward neurodegenerative diseases, such as Alzheimer's disease [45]. This pathway is also involved in neuronal function and

transcriptional regulation of genes involved in plasticity [205]. Last, there is evidence that the Akt pathway plays an important role in neuroinflammation [206]. For these reasons, as well as our preliminary data, we think it would be wise to further explore the role of the Akt pathway on gamma sensory flicker and vice versa.

6.6.3 Brain Cells and Gamma Sensory Flicker

6.6.3.1 Neurons

This thesis focuses on the possibility of neurons as immune modulators after gamma sensory flicker. Future studies should further investigate this idea through more targeted approaches, such as single-cell RNA sequencing or knock-out transgenic mouse line that allows for neuronal elimination of specific proteins.

After determining the role neurons play on the effect of gamma flicker on the neuro-immune environment, future directions should study specific neuronal subtypes. We know that gamma entrainment is driven by a network of pyramidal and parvalbumin interneuron interactions [147]. Identifying immune signaling pathways in the cells we already know are implicated in gamma entrainment would be further support for our hypothesis that neurons elicit immune signals in response to gamma entrainment. While the role of neurons in this process is important and discussed in Chapter 5, it is crucial to not ignore the possible roles of glial cells during gamma sensory flicker.

6.6.3.2 Microglia

As the resident immune cells of the brain, microglia play a large role in brain health and disease. Gamma sensory flicker recruits microglia and increases colocalization with amyloid beta [12]. We hypothesize this flicker-induced microglia recruitment is what ultimately leads to the decreased pathological symptoms in mice models of AD. It is clear that microglia are involved in

the post-flicker immune effects. Still, there are potential roles microglia might play during and/or after flicker that are still unknown.

In Chapter 5, we depleted microglia to ask if microglia were responsible for flicker-induced cytokine expression. This experiment taught us that some cytokines are still increased after flicker exposure, even in the absence of microglia. When we conducted this experiment, we did so under the assumption that microglia themselves were not involved in gamma entrainment. However, this has not yet been directly tested. Microglia are involved in network synchronization, and new research shows that microglia respond to changes in neuronal activity and are necessary for feedback control of neuronal activity [207,208]. Therefore, is it possible that microglia play a role in gamma entrainment, especially in relation to chronic flicker exposure. Future experiments should plan to examine gamma entrainment during sensory flicker in a microglia-depleted environment.

Through our experiments, we found that microglia were not solely responsible for cytokine production following gamma sensory flicker. The profile of cytokines elicited after microglia depletion still did not exactly match that of non-depleted animals after flicker. We discussed some possible reasons for this in Chapter 5. To further this discussion, it is possible that microglia do elicit cytokines after flicker, but perhaps just not the first cell type to do so. We know cytokines lead to the recruitment of microglia cells. These cytokines activate phosphoprotein pathways that further lead to the production of more cytokines [145]. Based on previously published work, there is evidence to support these microglia are responsible for amyloid beta clearance [12]. So, it is possible that microglia are responsible for cytokine release after flicker, and their involvement is even more critical for the effects of long-term flicker exposure.

6.6.3.3 Astrocytes

This thesis focused mainly on the effects of gamma flicker on neurons and microglia. We focused on these cells because neurons are the main cells known to drive gamma entrainment, and microglia are the resident immune cells in the brain, with previous research showing they are impacted by sensory flicker. However, this research has left out an important glial cell, astrocytes. While compromising up to 40% of the cells in the brain, astrocytes were long thought to be simply support for neurons. More recently, research has elucidated the role of astrocytes in many crucial brain functions, such as learning and memory, with implications for health and disease [209].

Still, the potential role of astrocytes in gamma sensory flicker has not received much attention. Astrocytes communicate with neurons via gap junctions, playing a crucial role in maintaining neuronal activity. In fact, research suggests that astrocytes do in fact contribute to gamma oscillations, and astrocytes both respond to and produce cytokines [210,211]. Because of this research, it follows that gamma sensory stimulation does indeed significantly increase astrocyte numbers [23]. We know that astrocytes are involved in gamma oscillations, in the neuroimmune system, and increase in number after sensory flicker, so research should examine the role of astrocytes in the neuroimmune signaling mechanism following gamma sensory flicker.

6.7 Concluding Remarks

This thesis uncovered crucial components in the mechanism of action for gamma sensory flicker's impact on the brain's immune system. We found that gamma visual flicker leads to a quick increase in phosphorylation of the NFκB and MAPK pathways. Through inhibiting these pathways, we discovered the increased activity in these pathways is responsible

for an increase in cytokine expression seen after one hour of gamma visual stimulation. We showed this increased cytokine profile differed from pathological cytokine profiles. Along the way, we found that other patterns of stimulation, traditionally thought of as control stimulations, impact the neuroimmune environment in unique ways. Last, we show these signals are not microglial dependent, and we provide evidence to suggest these signals are arising from neurons. There is a lot of work still needed to be done to fully elucidate the effect of gamma sensory stimulation on the brain and to use this research to translate this preclinical work to a possible therapeutic, with the potential to impact a wide range of diseases, and the work from this thesis provides an original contribution to this progress. Sensory flicker has been referred to as "the poor man's optogenetics", however, through past work, our work, and work still to be done, it may one day be the rich [wo]man's therapeutic.

Appendix

Appendix 1: Gamma visual flicker does not change cytokine levels in the periphery

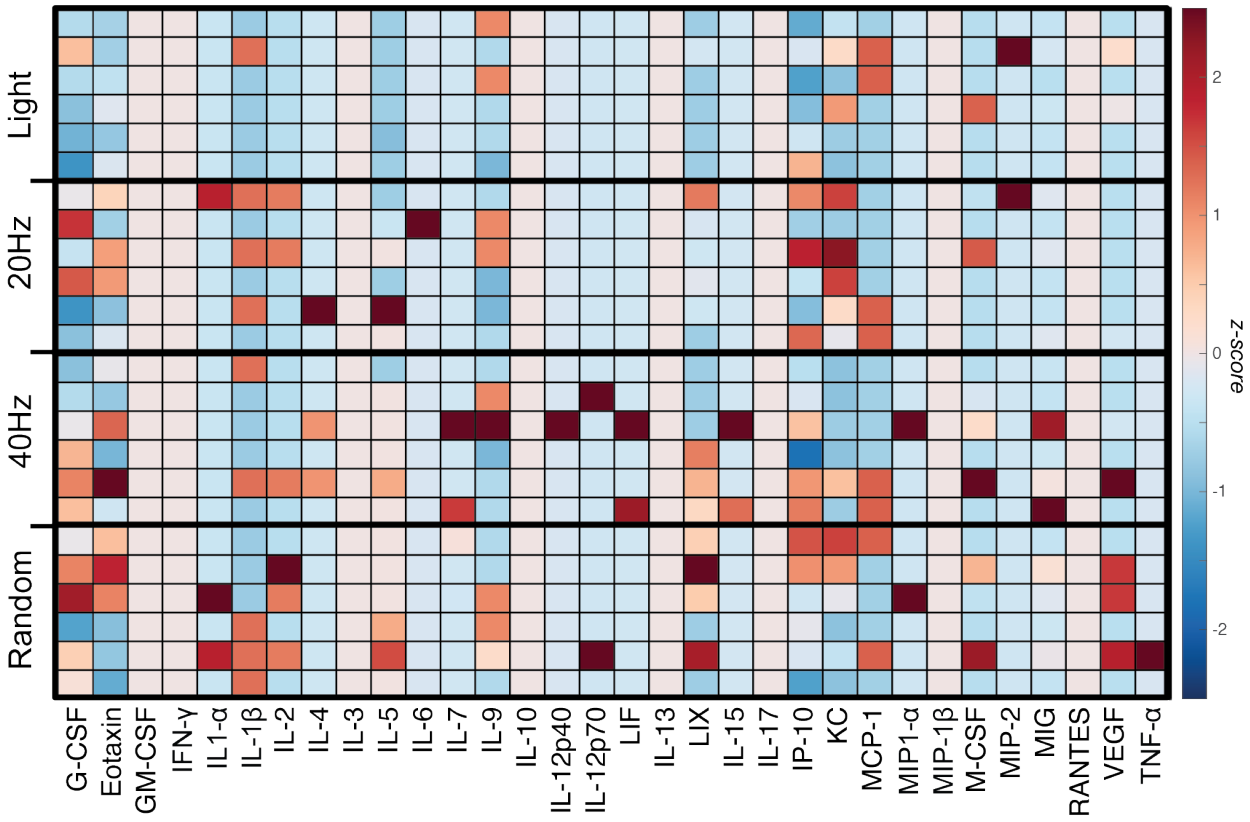

Figure A1: Gamma visual flicker does not alter peripheral cytokine levels

One hour of gamma visual flicker does not affect cytokine levels in the blood differently than control visual flicker stimulations.

Appendix 2: Gamma visual flicker and Monoamines

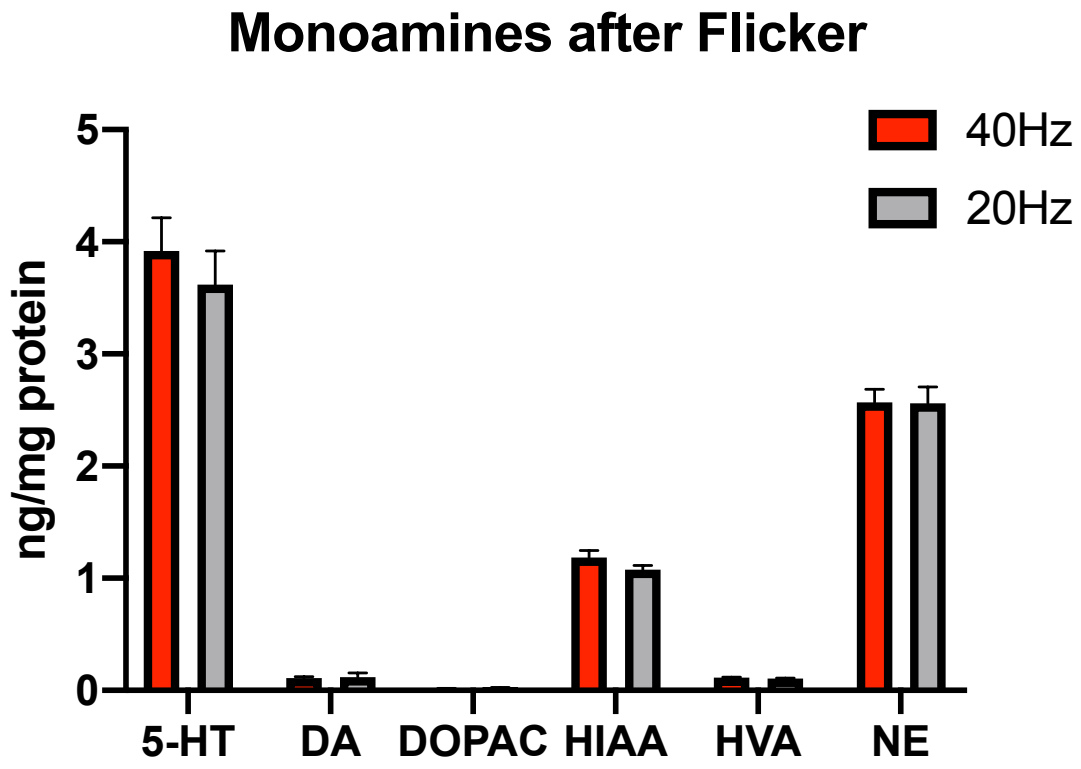

Figure A2.1: Monoamine Expression after gamma visual flicker

Key monoamines and their metabolites measured from visual cortex samples of animals exposed to one hour of visual flicker revealed no differences between animals exposed to 40Hz versus 20Hz stimulation. Samples were measured using high performance liquid chromatography (HPLC). 5HT: Serotonin, DA: Dopamine, DOPAC: 3,4-Dihydroxyphenylacetic acid, HIAA: Hydroxyindoleacetic Acid, HVA: homovanillic acid, NE: Norepinephrine

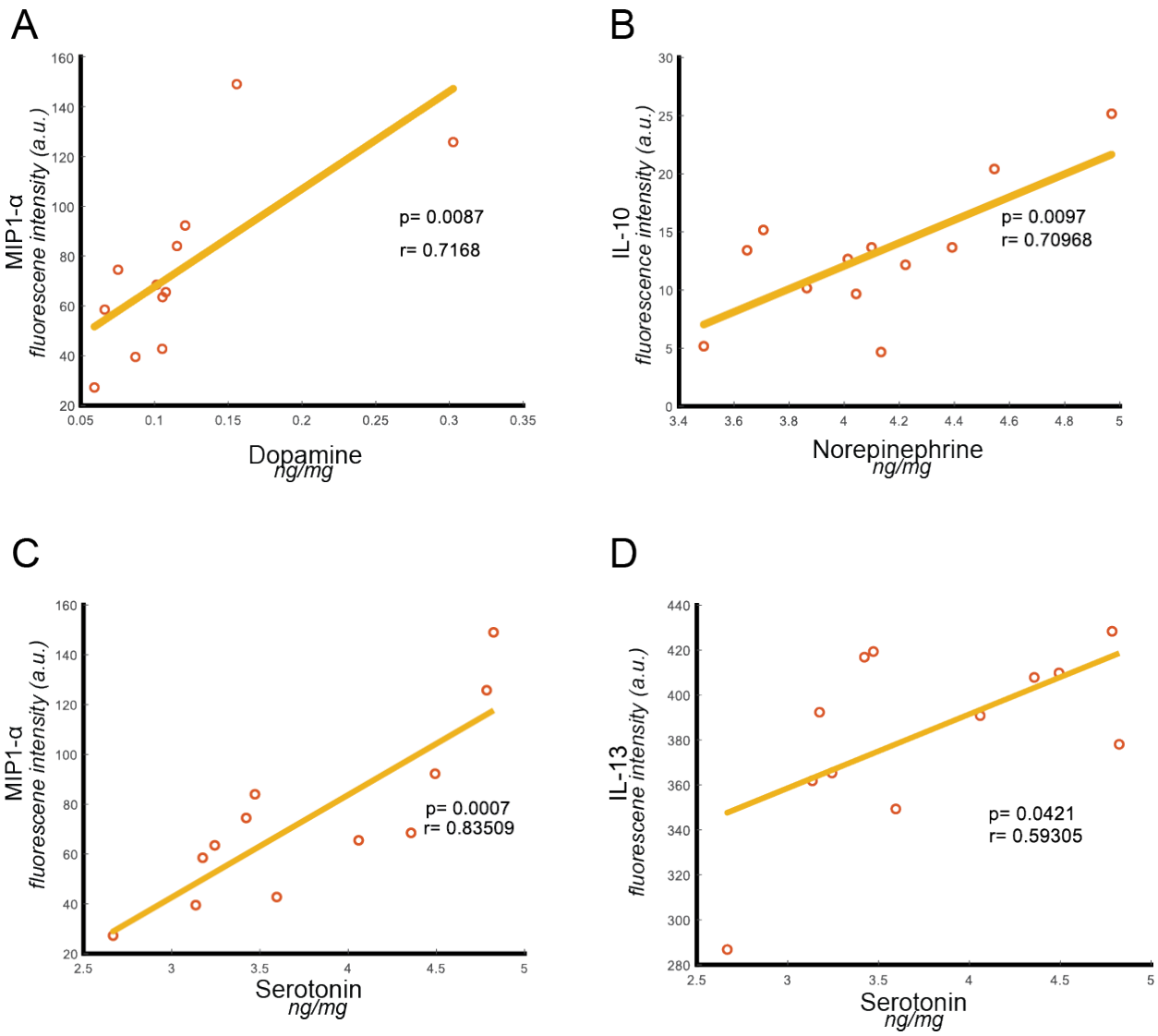

Figure A2.2: Monoamines Correlate to Cytokine Expression

A, MIP-1α correlates with dopamine expression after one hour of visual flicker stimulation, independent of frequency of stimulation, p-value and Pearson correlation coefficient displayed on figure. B, As in A for IL-10 and Norepinephrine. C, As in A for MIP-1α and serotonin. D, As in A for IL-13 and Serotonin

References

1. Gray CM, König P, Engel AK, Singer W. Oscillatory responses in cat visual cortex exhibit inter-columnar synchronization which reflects global stimulus properties. Nature. 1989 Mar;338(6213):334–7.

2. Rager G, Singer W. The response of cat visual cortex to flicker stimuli of variable frequency. 1998;10(i):1856–77.

3. Rodriguez E, George N, Lachaux JP, Martinerie J, Renault B, Varela FJ. Perception's shadow: Long-distance synchronization of human brain activity. Nature [Internet]. 1999 Feb 4 [cited 2020 Oct 12];397(6718):430–3. Available from: www.nature.com

4. Jensen O, Kaiser J, Lachaux JP. Human gamma-frequency oscillations associated with attention and memory. Vol. 30, Trends in Neurosciences. Elsevier Current Trends; 2007. p. 317–24.

5. Böttger D, Herrmann CS, Von Cramon DY. Amplitude differences of evoked alpha and gamma oscillations in two different age groups. Int J Psychophysiol. 2002 Sep 1;45(3):245–51.

6. Murty DVPS, Manikandan K, Kumar WS, Ramesh RG, Purokayastha S, Javali M, et al. Gamma oscillations weaken with age in healthy elderly in human EEG. Neuroimage [Internet]. 2020 Jul 15 [cited 2021 Jan 12];215. Available from: https://pubmed-ncbi-nlm-nih-gov.proxy.library.emory.edu/32276055/

7. Stam CJ, Van Cappellen van Walsum AM, Pijnenburg YAL, Berendse HW, De Munck JC, Scheltens P, et al. Generalized synchronization of MEG recordings in Alzheimer's disease: Evidence for involvement of the gamma band. J Clin Neurophysiol. 2002;

8. Başar E, Emek-Savaş DD, Güntekin B, Yener GG. Delay of cognitive gamma responses in Alzheimer's disease. NeuroImage Clin. 2016 Jan 1;11:106–15.

9. Van Deursen JA, Vuurman EFPM, Verhey FRJ, Van Kranen-Mastenbroek VHJM, Riedel WJ. Increased EEG gamma band activity in Alzheimer's disease and mild cognitive impairment. J Neural Transm. 2008;

10. van Deursen JA, Vuurman EFPM, van Kranen-Mastenbroek VHJM, Verhey FRJ, Riedel WJ. 40-Hz steady state response in Alzheimer's disease and mild cognitive impairment. Neurobiol Aging. 2011 Jan 1;32(1):24–30.

11. Gillespie AK, Jones EA, Lin YH, Karlsson MP, Kay K, Yoon SY, et al. Apolipoprotein E4 Causes Age-Dependent Disruption of Slow Gamma Oscillations during Hippocampal Sharp-Wave Ripples. Neuron [Internet]. 2016 May 18 [cited 2021 Jan 12];90(4):740–51. Available from: http://dx.doi.org/10.1016/j.neuron.2016.04.009

12. Iaccarino HF, Singer AC, Martorell AJ, Rudenko A, Gao F, Gillingham TZ, et al. Gamma frequency entrainment attenuates amyloid load and modifies microglia. Nature [Internet]. 2016;540(7632):230–5. Available from: http://dx.doi.org/10.1038/nature20587

13. Castano-Prat P, Perez-Mendez L, Perez-Zabalza M, Sanfeliu C, Giménez-Llort L, Sanchez-Vives M V. Altered slow (<1 Hz) and fast (beta and gamma) neocortical oscillations in the 3xTg-AD mouse model of Alzheimer's disease under anesthesia. Neurobiol Aging [Internet]. 2019 Jul 1 [cited 2021 Jan 12];79:142–51. Available from: https://pubmed-ncbi-nlm-nih-gov.proxy.library.emory.edu/31103943/

14. Nakazono T, Lam TN, Patel AY, Kitazawa M, Saito T, Saido TC, et al. Impaired in vivo gamma oscillations in the medial entorhinal cortex of knock-in Alzheimer model. Front

Syst Neurosci [Internet]. 2017 Jun 30 [cited 2021 Jan 12];11. Available from: https://pubmed.ncbi.nlm.nih.gov/28713250/

15. Mably AJ, Gereke BJ, Jones DT, Colgin LL. Impairments in spatial representations and rhythmic coordination of place cells in the 3xTg mouse model of Alzheimer's disease. Hippocampus [Internet]. 2017 Apr 1 [cited 2021 Jan 12];27(4):378–92. Available from: https://pubmed.ncbi.nlm.nih.gov/28032686/

16. Herrmann CS, Munk MHJ, Engel AK. Cognitive functions of gamma-band activity: Memory match and utilization. Trends Cogn Sci. 2004 Aug 1;8(8):347–55.

17. Howard MW. Gamma Oscillations Correlate with Working Memory Load in Humans. Cereb Cortex [Internet]. 2003 Dec 1 [cited 2021 Jan 12];13(12):1369–74. Available from: https://academic.oup.com/cercor/article-lookup/doi/10.1093/cercor/bhg084

18. Etter G, van der Veldt S, Manseau F, Zarrinkoub I, Trillaud-Doppia E, Williams S. Optogenetic gamma stimulation rescues memory impairments in an Alzheimer's disease mouse model. Nat Commun [Internet]. 2019 Dec 1 [cited 2021 Jan 12];10(1):1–11. Available from: https://doi.org/10.1038/s41467-019-13260-9

19. Sederberg PB, Schulze-Bonhage A, Madsen JR, Bromfield EB, McCarthy DC, Brandt A, et al. Hippocampal and neocortical gamma oscillations predict memory formation in humans. Cereb Cortex. 2007;

20. Goutagny R, Gu N, Cavanagh C, Jackson J, Chabot JG, Quirion R, et al. Alterations in hippocampal network oscillations and theta-gamma coupling arise before Aβ overproduction in a mouse model of Alzheimer's disease. Eur J Neurosci. 2013;37(12):1896–902.

21. Jacobs J, Miller J, Lee SA, Coffey T, Watrous AJ, Sperling MR, et al. Direct Electrical Stimulation of the Human Entorhinal Region and Hippocampus Impairs Memory. Neuron [Internet]. 2016 Dec 7 [cited 2021 Jan 12];92(5):983–90. Available from: http://dx.doi.org/10.1016/j.neuron.2016.10.062

22. Suthana N, Haneef Z, Stern J, Mukamel R, Behnke E, Knowlton B, et al. Memory Enhancement and Deep-Brain Stimulation of the Entorhinal Area. N Engl J Med [Internet]. 2012 Feb 9 [cited 2021 Jan 12];366(6):502–10. Available from: https://www.nejm.org/doi/full/10.1056/NEJMoa1107212

23. Martorell AJ, Paulson AL, Suk HJ, Abdurrob F, Drummond GT, Guan W, et al. Multi-sensory Gamma Stimulation Ameliorates Alzheimer's-Associated Pathology and Improves Cognition. Cell. 2019 Apr 4;177(2):256-271.e22.

24. Rao JS, Rapoport SI, Kim HW. Altered neuroinflammatory, arachidonic acid cascade and synaptic markers in postmortem Alzheimers disease brain. Translational Psychiatry. 2011.

25. Fitzgerald PJ, Watson BO. Gamma oscillations as a biomarker for major depression: an emerging topic. Transl Psychiatry [Internet]. 2018 Dec 1 [cited 2021 Mar 3];8(1). Available from: /pmc/articles/PMC6123432/

26. Woo TUW, Spencer K, McCarley RW. Gamma oscillation deficits and the onset and early progression of schizophrenia [Internet]. Vol. 18, Harvard Review of Psychiatry. NIH Public Access; 2010 [cited 2021 Mar 3]. p. 173–89. Available from: /pmc/articles/PMC2860612/

27. Maes M. Evidence for an immune response in major depression: A review and hypothesis. Vol. 19, Progress in Neuropsychopharmacology and Biological Psychiatry. Elsevier;

1995. p. 11–38.

28. Tomasik J, Rahmoune H, Guest PC, Bahn S. Neuroimmune biomarkers in schizophrenia. Vol. 176, Schizophrenia Research. Elsevier B.V.; 2016. p. 3–13.

29. Doyle KP, Cekanaviciute E, Mamer LE, Buckwalter MS. TGFβ signaling in the brain increases with aging and signals to astrocytes and innate immune cells in the weeks after stroke. J Neuroinflammation [Internet]. 2010 Oct 11 [cited 2021 Jan 17];7. Available from: https://pubmed.ncbi.nlm.nih.gov/20937129/

30. Stoll G, Jander S, Schroeter M. Inflammation and glial responses in ischemic brain lesions. Prog Neurobiol [Internet]. 1998 [cited 2021 Jan 17];56(2):149–71. Available from: https://pubmed-ncbi-nlm-nih-gov.proxy.library.emory.edu/9760699/

31. Ransohoff RM. A polarizing question: Do M1 and M2 microglia exist [Internet]. Vol. 19, Nature Neuroscience. Nature Publishing Group; 2016 [cited 2021 Jan 16]. p. 987–91. Available from: http://www.limes-institut-bonn.de/en/research/

32. Ji K, Miyauchi J, Tsirka SE. Microglia: An active player in the regulation of synaptic activity. Neural Plast. 2013;2013.

33. Paresce DM, Chung H, Maxfield FR. Slow degradation of aggregates of the Alzheimer's disease amyloid β- protein by microglial cells. J Biol Chem. 1997 Nov 14;272(46):29390–7.

34. Ard MD, Cole GM, Wei J, Mehrle AP, Fratkin JD. Scavenging of Alzheimer's amyloid ?-protein by microglia in culture. J Neurosci Res [Internet]. 1996 Jan 15 [cited 2021 Jan 18];43(2):190–202. Available from:

https://onlinelibrary.wiley.com/doi/10.1002/(SICI)1097-4547(19960115)43:2%3C190::AID-JNR7%3E3.0.CO;2-B

35. Szepesi Z, Manouchehrian O, Bachiller S, Deierborg T. Bidirectional Microglia–Neuron Communication in Health and Disease [Internet]. Vol. 12, Frontiers in Cellular Neuroscience. Frontiers Media S.A.; 2018 [cited 2021 Jan 17]. Available from: https://pubmed.ncbi.nlm.nih.gov/30319362/

36. Heneka MT, Kummer MP, Latz E. Innate immune activation in neurodegenerative disease [Internet]. Vol. 14, Nature Reviews Immunology. Nature Publishing Group; 2014 [cited 2021 Jan 16]. p. 463–77. Available from: www.nature.com/reviews/immunol

37. Terai K, Matsuo A, McGeer PL. Enhancement of immunoreactivity for NF-κB in the hippocampal formation and cerebral cortex of Alzheimer's disease. Brain Res. 1996 Sep 30;735(1):159–68.

38. Valerio A, Boroni F, Benarese M, Sarnico I, Ghisi V, Bresciani LG, et al. NFkB pathway: A target for preventing beta-amyloid-induced neuronal damage and Abeta42 production. Eur J Neurosci. 2006;23(7):1711–20.

39. Ferrer I, Martí E, López E, Tortosa A. NF-κB immunoreactivity is observed in association with βA4 diffuse plaques in patients with Alzheimer's disease. Neuropathol Appl Neurobiol [Internet]. 1998 [cited 2021 Jan 18];24(4):271–7. Available from: https://pubmed.ncbi.nlm.nih.gov/9775392/

40. O'Neill LAJ, Kaltschmidt C. NF-κB: A crucial transcription factor for glial and neuronal cell function. Trends Neurosci. 1997 Jun 1;20(6):252–8.

41. Ho GJ, Drego R, Hakimian E, Masliah E. Mechanisms of cell signaling and inflammation in Alzheimer's disease [Internet]. Vol. 4, Current Drug Targets: Inflammation and Allergy. Curr Drug Targets Inflamm Allergy; 2005 [cited 2021 Jan 18]. p. 247–56. Available from: https://pubmed-ncbi-nlm-nih-gov.proxy.library.emory.edu/15853747/

42. Peng S, Zhang Y, Zhang J, Wang H, Ren B. ERK in learning and memory: A review of recent research [Internet]. Vol. 11, International Journal of Molecular Sciences. Int J Mol Sci; 2010 [cited 2021 Jan 18]. p. 222–32. Available from: https://pubmed-ncbi-nlm-nih-gov.proxy.library.emory.edu/20162012/

43. Qiu Z, Lu P, Wang K, Zhao X, Li Q, Wen J, et al. Dexmedetomidine Inhibits Neuroinflammation by Altering Microglial M1/M2 Polarization Through MAPK/ERK Pathway. Neurochem Res [Internet]. 2020 Feb 1 [cited 2021 Jan 18];45(2):345–53. Available from: https://doi.org/10.1007/s11064-019-02922-1

44. Kirouac L, Rajic AJ, Cribbs DH, Padmanabhan J. Activation of Ras-ERK signaling and GSK-3 by amyloid precursor protein and amyloid beta facilitates neurodegeneration in Alzheimer's disease. eNeuro [Internet]. 2017 [cited 2021 Jan 18];4(2). Available from: https://pubmed-ncbi-nlm-nih-gov.proxy.library.emory.edu/28374012/

45. Rai SN, Dilnashin H, Birla H, Singh S Sen, Zahra W, Rathore AS, et al. The Role of PI3K/Akt and ERK in Neurodegenerative Disorders [Internet]. Vol. 35, Neurotoxicity Research. Springer New York LLC; 2019 [cited 2021 Jan 18]. p. 775–95. Available from: https://pubmed-ncbi-nlm-nih-gov.proxy.library.emory.edu/30707354/

46. Akiyama H, Barger S, Barnum S, Bradt B, Bauer J, Cole GM, et al. Inflammation and Alzheimer's disease. Vol. 21, Neurobiology of Aging. Elsevier Inc.; 2000. p. 383–421.

47. Griffin WST, Stanley LC, Ling C, White L, MacLeod V, Perrot LJ, et al. Brain interleukin 1 and S-100 immunoreactivity are elevated in Down syndrome and Alzheimer disease. Proc Natl Acad Sci U S A [Internet]. 1989 Oct 1 [cited 2021 Jan 18];86(19):7611–5. Available from: https://www.pnas.org/content/86/19/7611

48. Strauss S, Bauer J, Ganter U, Jonas U, Berger M, Volk B. Detection of interleukin-6 and α2-macroglobulin immunoreactivity in cortex and hippocampus of Alzheimer's disease patients. Lab Investig [Internet]. 1992 Feb 1 [cited 2021 Jan 18];66(2):223–30. Available from: https://europepmc.org/article/med/1370967

49. Patel NS, Paris D, Mathura V, Quadros AN, Crawford FC, Mullan MJ. Inflammatory cytokine levels correlate with amyloid load in transgenic mouse models of Alzheimer's disease. J Neuroinflammation [Internet]. 2005 Mar 11 [cited 2021 Jan 18];2(1):1–10. Available from: https://link.springer.com/articles/10.1186/1742-2094-2-9

50. Adaikkan C, Middleton SJ, Marco A, Pao PC, Mathys H, Kim DNW, et al. Gamma Entrainment Binds Higher-Order Brain Regions and Offers Neuroprotection. Neuron. 2019 Jun 5;102(5):929-943.e8.

51. Singer AC, Martorell AJ, Douglas JM, Abdurrob F, Attokaren MK, Tipton J, et al. Noninvasive 40-Hz light flicker to recruit microglia and reduce amyloid beta load. Nat Protoc. 2018 Aug 2;13(8):1850–68.

52. Eriksson, L.; Byrne, T.; Johansson, E.; Trygg, J.; Vikström C. Multi- and Megavariate Data Analysis. Basic principles and applications. Umetrics Academy. 2006.

53. Golland P, Liang F, Mukherjee S, Panchenko D. Permutation Tests for Classification. In 2010.

54. Calsolaro V, Edison P. Neuroinflammation in Alzheimer's disease: Current evidence and future directions. Alzheimers Dement [Internet]. 2016;12(6):719–32. Available from: http://www.ncbi.nlm.nih.gov/pubmed/27179961

55. Wohleb ES, Franklin T, Iwata M, Duman RS. Integrating neuroimmune systems in the neurobiology of depression. Nat Rev Neurosci [Internet]. 2016;17(8):497–511. Available from: http://www.ncbi.nlm.nih.gov/pubmed/27277867

56. Iaccarino HF, Singer AC, Martorell AJ, Rudenko A, Gao F, Gillingham TZ, et al. Gamma frequency entrainment attenuates amyloid load and modifies microglia. Nature [Internet]. 2016 Dec 7 [cited 2019 Apr 26];540(7632):230–5. Available from: http://www.nature.com/doifinder/10.1038/nature20587

57. Adaikkan C, Middleton SJ, Marco A, Pao P-C, Mathys H, Kim DN-W, et al. Gamma Entrainment Binds Higher-Order Brain Regions and Offers Neuroprotection. Neuron [Internet]. 2019; Available from: https://www.sciencedirect.com/science/article/pii/S0896627319303460

58. Hanisch U-K. Microglia as a source and target of cytokines. Glia [Internet]. 2002 Nov;40(2):140–55. Available from: http://www.ncbi.nlm.nih.gov/pubmed/12379902

59. Prieto GA, Cotman CW. Cytokines and cytokine networks target neurons to modulate long-term potentiation [Internet]. Vol. 34, Cytokine and Growth Factor Reviews. 2017. p. 27–33. Available from: http://www.ncbi.nlm.nih.gov/pubmed/28377062

60. Sheridan GK, Murphy KJ. Neuron-glia crosstalk in health and disease: Fractalkine and CX3CR1 take centre stage [Internet]. Vol. 3, Open Biology. 2013. p. 130181. Available from: http://rsob.royalsocietypublishing.org/cgi/doi/10.1098/rsob.130181

61. Goshen I, Kreisel T, Ounallah-Saad H, Renbaum P, Zalzstein Y, Ben-Hur T, et al. A dual role for interleukin-1 in hippocampal-dependent memory processes. Psychoneuroendocrinology [Internet]. 2007 Sep;32(8–10):1106–15. Available from: https://linkinghub.elsevier.com/retrieve/pii/S0306453007002120

62. Stellwagen D, Malenka RC. Synaptic scaling mediated by glial TNF-alpha. Nature [Internet]. 2006 Apr 20;440(7087):1054–9. Available from: http://www.ncbi.nlm.nih.gov/pubmed/16547515

63. Neniskyte U, Vilalta A, Brown GC. Tumour necrosis factor alpha-induced neuronal loss is mediated by microglial phagocytosis. FEBS Lett [Internet]. 2014 Aug 25;588(17):2952–6. Available from: http://www.ncbi.nlm.nih.gov/pubmed/24911209

64. Gray CM, König P, Engel AK, Singer W. Oscillatory responses in cat visual cortex exhibit inter-columnar synchronization which reflects global stimulus properties. Nature [Internet]. 1989 Mar 23;338(6213):334–7. Available from: http://www.ncbi.nlm.nih.gov/pubmed/2922061

65. Gabellec MM, Griffais R, Fillion G, Haour F. Expression of interleukin 1α, interleukin 1β and interleukin 1 receptor antagonist mRNA in mouse brain: regulation by bacterial lipopolysaccharide (LPS) treatment. Mol Brain Res. 1995;

66. Qin L, Wu X, Block ML, Liu Y, Breese GR, Hong JS, et al. Systemic LPS causes chronic neuroinflammation and progressive neurodegeneration. Glia. 2007;

67. Meneses G, Rosetti M, Espinosa A, Florentino A, Bautista M, Díaz G, et al. Recovery from an acute systemic and central LPS-inflammation challenge is affected by mouse sex and genetic background. PLoS One. 2018;

68. Rangaraju S, Dammer EB, Raza SA, Rathakrishnan P, Xiao H, Gao T, et al. Identification and therapeutic modulation of a pro-inflammatory subset of disease-associated-microglia in Alzheimer's disease. Mol Neurodegener [Internet]. 2018 Dec 21;13(1):24. Available from: https://molecularneurodegeneration.biomedcentral.com/articles/10.1186/s13024-018-0254-8

69. Gourmaud S, Thomas P, Thomasseau S, Tible M, Abadie C, Paquet C, et al. Brimapitide Reduced Neuronal Stress Markers and Cognitive Deficits in 5XFAD Transgenic Mice. J Alzheimers Dis [Internet]. 2018;63(2):665–74. Available from: http://www.ncbi.nlm.nih.gov/pubmed/29660941

70. Mitrasinovic OM, Murphy GM. Microglial overexpression of the M-CSF receptor augments phagocytosis of opsonized Abeta. Neurobiol Aging [Internet]. 2003 Oct;24(6):807–15. Available from: http://www.ncbi.nlm.nih.gov/pubmed/12927763

71. Imai Y, Kohsaka S. Intracellular signaling in M-CSF-induced microglia activation: role of Iba1. Glia [Internet]. 2002 Nov;40(2):164–74. Available from: http://www.ncbi.nlm.nih.gov/pubmed/12379904

72. Elmore MRP, Najafi AR, Koike MA, Dagher NN, Spangenberg EE, Rice RA, et al. Colony-stimulating factor 1 receptor signaling is necessary for microglia viability, unmasking a microglia progenitor cell in the adult brain. Neuron [Internet]. 2014 Apr 16;82(2):380–97. Available from: http://www.ncbi.nlm.nih.gov/pubmed/24742461

73. Ringheim GE, Szczepanik AM, Petko W, Burgher KL, Zhu SZ, Chao CC. Enhancement of beta-amyloid precursor protein transcription and expression by the soluble interleukin-6 receptor/interleukin-6 complex. Brain Res Mol Brain Res [Internet]. 1998 Mar

30;55(1):35–44. Available from: http://www.ncbi.nlm.nih.gov/pubmed/9645958

74. Decourt B, Lahiri DK, Sabbagh MN. Targeting Tumor Necrosis Factor Alpha for Alzheimer's Disease. Curr Alzheimer Res [Internet]. 2017;14(4):412–25. Available from: http://www.ncbi.nlm.nih.gov/pubmed/27697064

75. Barroeta-Espar I, Weinstock LD, Perez-Nievas BG, Meltzer AC, Siao Tick Chong M, Amaral AC, et al. Distinct cytokine profiles in human brains resilient to Alzheimer's pathology. Neurobiol Dis [Internet]. 2019 Jan 1;121:327–37. Available from: https://www.sciencedirect.com/science/article/pii/S0969996118307137

76. Bowen KK, Dempsey RJ, Vemuganti R. Adult interleukin-6 knockout mice show compromised neurogenesis. Neuroreport [Internet]. 2011 Feb 16;22(3):126–30. Available from: http://www.ncbi.nlm.nih.gov/pubmed/21266900

77. Donegan JJ, Girotti M, Weinberg MS, Morilak DA. A novel role for brain interleukin-6: facilitation of cognitive flexibility in rat orbitofrontal cortex. J Neurosci [Internet]. 2014 Jan 15;34(3):953–62. Available from: http://www.ncbi.nlm.nih.gov/pubmed/24431453

78. Baier PC, May U, Scheller J, Rose-John S, Schiffelholz T. Impaired hippocampus-dependent and -independent learning in IL-6 deficient mice. Behav Brain Res [Internet]. 2009 Jun 8;200(1):192–6. Available from: http://www.ncbi.nlm.nih.gov/pubmed/19378383

79. Wang GY, Taylor T, Sumich A, Merien F, Borotkanics R, Wrapson W, et al. Associations between immunological function and memory recall in healthy adults. Brain Cogn [Internet]. 2017;119:39–44. Available from: http://www.ncbi.nlm.nih.gov/pubmed/29020639

80. Rappert A. CXCR3-Dependent Microglial Recruitment Is Essential for Dendrite Loss after Brain Lesion. J Neurosci [Internet]. 2004 Sep 29;24(39):8500–9. Available from: http://www.ncbi.nlm.nih.gov/pubmed/15456824

81. Ghersa P, Gelati M, Colinge J, Feger G, Power C, Ghersa P, et al. MIG--differential gene expression in mouse brain endothelial cells. Neuroreport [Internet]. 2002 Jan 21;13(1):9–14. Available from: http://www.ncbi.nlm.nih.gov/pubmed/11924901

82. Ure DR, Lane TE, Liu MT, Rodriguez M. Neutralization of chemokines RANTES and MIG increases virus antigen expression and spinal cord pathology during Theiler's virus infection. Int Immunol. 2005 May 1;17(5):569–79.

83. De Filippo K, Dudeck A, Hasenberg M, Nye E, Van Rooijen N, Hartmann K, et al. Mast cell and macrophage chemokines CXCL1/CXCL2 control the early stage of neutrophil recruitment during tissue inflammation. Blood [Internet]. 2013 Jun 13;121(24):4930–7. Available from: http://www.bloodjournal.org.proxy.library.emory.edu/content/121/24/4930.long?sso-checked=true

84. Johnson EA, Dao TL, Guignet MA, Geddes CE, Koemeter-Cox AI, Kan RK. Increased expression of the chemokines CXCL1 and MIP-1α by resident brain cells precedes neutrophil infiltration in the brain following prolonged soman-induced status epilepticus in rats. J Neuroinflammation [Internet]. 2011 May 2;8(1):41. Available from: http://jneuroinflammation.biomedcentral.com/articles/10.1186/1742-2094-8-41

85. Fenn AM, Hall JCE, Gensel JC, Popovich PG, Godbout JP. IL-4 signaling drives a unique arginase+/IL-1β+ microglia phenotype and recruits macrophages to the inflammatory

CNS: consequences of age-related deficits in IL-4Rα after traumatic spinal cord injury. J Neurosci [Internet]. 2014 Jun 25;34(26):8904–17. Available from: http://www.ncbi.nlm.nih.gov/pubmed/24966389

86. Latta CH, Sudduth TL, Weekman EM, Brothers HM, Abner EL, Popa GJ, et al. Determining the role of IL-4 induced neuroinflammation in microglial activity and amyloid-β using BV2 microglial cells and APP/PS1 transgenic mice. J Neuroinflammation. 2015 Mar 4;12:41.

87. Lee YH, Kim SH, Kim Y, Lim Y, Ha K, Shin SY. Inhibitory effect of the antidepressant imipramine on NF-κB-dependent CXCL1 expression in TNFα-exposed astrocytes. Int Immunopharmacol [Internet]. 2012 Apr 1;12(4):547–55. Available from: https://www.sciencedirect.com/science/article/pii/S1567576912000318?via%3Dihub

88. Cai KC, van Mil S, Murray E, Mallet JF, Matar C, Ismail N. Age and sex differences in immune response following LPS treatment in mice. Brain Behav Immun. 2016;

89. Arakawa K, Arakawa H, Hueston CM, Deak T. Effects of the estrous cycle and ovarian hormones on central expression of interleukin-1 evoked by stress in female rats. Neuroendocrinology. 2014;

90. Ishikawa I, Kitamura H, Kimura K, Saito M. Brain interleukin-1 is involved in blood interleukin-6 response to immobilization stress in rats. Jpn J Vet Res [Internet]. 2001;49(1):19–25. Available from: https://pdfs.semanticscholar.org/8bb2/c97825f035ce2736ee52717042a3494b40dd.pdf

91. Minami M, Kuraishi Y, Yamaguchi T, Nakai S, Hirai Y, Satoh M. Immobilization stress induces interleukin-1β mRNA in the rat hypothalamus. Neurosci Lett [Internet]. 1991 Feb

25;123(2):254–6. Available from: https://www.sciencedirect.com/science/article/abs/pii/030439409190944O

92. Martorell AJ, Paulson AL, Suk H-J, Abdurrob F, Drummond GT, Guan W, et al. Multi-sensory Gamma Stimulation Ameliorates Alzheimer's-Associated Pathology and Improves Cognition. Cell [Internet]. 2019 Apr 4;177(2):256-271.e22. Available from: http://www.ncbi.nlm.nih.gov/pubmed/30879788

93. Crawley JN, Goodwin FK. Preliminary report of a simple animal model for the behavioral actions of benzodiazepines. Pharmacol Biochem Behav. 1980;13:167–70.

94. Kiyota T, Machhi J, Lu Y, Dyavarshetty B, Nemati M, Yokoyama I, et al. Granulocyte-macrophage colony-stimulating factor neuroprotective activities in Alzheimer's disease mice. J Neuroimmunol. 2018;

95. Bhattacharya P, Budnick I, Singh M, Thiruppathi M, Alharshawi K, Elshabrawy H, et al. Dual Role of GM-CSF as a Pro-Inflammatory and a Regulatory Cytokine: Implications for Immune Therapy. Journal of Interferon and Cytokine Research. 2015.

96. Alves S, Churlaud G, Audrain M, Michaelsen-Preusse K, Fol R, Souchet B, et al. Interleukin-2 improves amyloid pathology, synaptic failure and memory in Alzheimer's disease mice. Brain. 2017;

97. Baiocchi RA, Ward JS, Carrodeguas L, Eisenbeis CF, Peng R, Roychowdhury S, et al. GM-CSF and IL-2 induce specific cellular immunity and provide protection against Epstein-Barr virus lymphoproliferative disorder. J Clin Invest. 2001;

98. Stagg J, Wu JH, Bouganim N, Galipeau J. Granulocyte-macrophage colony-stimulating

factor and interleukin-2 fusion cDNA for cancer gene immunotherapy. Cancer Res. 2004;

99. Elias EG, Zapas JL, Beam SL, Brown SD. GM-CSF and IL-2 combination as adjuvant therapy in cutaneous melanoma: early results of a phase II clinical trial. Oncology (Williston Park). 2005;

100. Saadoun D, Rosenzwajg M, Joly F, Six A, Carrat F, Thibault V, et al. Regulatory T-cell responses to low-dose interleukin-2 in HCV-induced vasculitis. N Engl J Med. 2011;

101. Shachar I, Karin N. The dual roles of inflammatory cytokines and chemokines in the regulation of autoimmune diseases and their clinical implications. J Leukoc Biol. 2013;

102. Sgadari C, Angiolillo AL, Tosato G. Inhibition of angiogenesis by interleukin-12 is mediated by the interferon-inducible protein 10. Blood. 1996;

103. Oakley H, Cole SL, Logan S, Maus E, Shao P, Craft J, et al. Intraneuronal beta-Amyloid Aggregates, Neurodegeneration, and Neuron Loss in Transgenic Mice with Five Familial Alzheimer's Disease Mutations: Potential Factors in Amyloid Plaque Formation. J Neurosci [Internet]. 2006 Oct 4;26(40):10129–40. Available from: http://www.jneurosci.org/cgi/doi/10.1523/JNEUROSCI.1202-06.2006

104. Hillmann A, Hahn S, Schilling S, Hoffmann T, Demuth HU, Bulic B, et al. No improvement after chronic ibuprofen treatment in the 5XFAD mouse model of Alzheimer's disease. Neurobiol Aging [Internet]. 2012 Apr 1;33(4):833.e39-833.e50. Available from: https://www.sciencedirect.com/science/article/pii/S0197458011003216#bib24

105. Heppner FL, Ransohoff RM, Becher B. Immune attack: the role of inflammation in

Alzheimer disease. Nat Rev Neurosci. 2015 Jun 20;16(6):358–72.

106. Buckwalter MS, Wyss-Coray T. Modelling neuroinflammatory phenotypes in vivo. Vol. 1, Journal of Neuroinflammation. BioMed Central; 2004. p. 10.

107. Chen Z, Jalabi W, Shpargel KB, Farabaugh KT, Dutta R, Yin X, et al. Lipopolysaccharide-Induced Microglial Activation and Neuroprotection against Experimental Brain Injury Is Independent of Hematogenous TLR4. J Neurosci [Internet]. 2012 Aug 22;32(34):11706–15. Available from: http://www.ncbi.nlm.nih.gov/pubmed/22915113

108. Herber DL, Mercer M, Roth LM, Symmonds K, Maloney J, Wilson N, et al. Microglial activation is required for Aβ clearance after intracranial injection of lipopolysaccharide in APP transgenic mice. J Neuroimmune Pharmacol [Internet]. 2007 Apr 23 [cited 2019 May 21];2(2):222–31. Available from: http://link.springer.com/10.1007/s11481-007-9069-z

109. DiCarlo G, Wilcock D, Henderson D, Gordon M, Morgan D. Intrahippocampal LPS injections reduce Aβ load in APP+PS1 transgenic mice. Neurobiol Aging [Internet]. 2001 Nov 1;22(6):1007–12. Available from: https://www.sciencedirect.com/science/article/abs/pii/S0197458001002925

110. Liu T, Zhang L, Joo D, Sun S-C. NF-κB signaling in inflammation. Signal Transduct Target Ther [Internet]. 2017;2. Available from: http://www.ncbi.nlm.nih.gov/pubmed/29158945

111. Cloutier A, Ear T, Blais-Charron E, Dubois CM, McDonald PP. Differential involvement of NF-κB and MAP kinase pathways in the generation of inflammatory cytokines by human neutrophils. J Leukoc Biol [Internet]. 2007 Feb;81(2):567–77. Available from:

http://www.ncbi.nlm.nih.gov/pubmed/17062602

112. Hommes DW, Peppelenbosch MP, van Deventer SJH. Mitogen activated protein (MAP) kinase signal transduction pathways and novel anti-inflammatory targets. Gut [Internet]. 2003 Jan;52(1):144–51. Available from: http://www.ncbi.nlm.nih.gov/pubmed/12477778

113. Sweatt JD. The neuronal MAP kinase cascade: a biochemical signal integration system subserving synaptic plasticity and memory. J Neurochem [Internet]. 2001 Jan;76(1):1–10. Available from: http://www.ncbi.nlm.nih.gov/pubmed/11145972

114. Kaltschmidt B, Ndiaye D, Korte M, Pothion S, Arbibe L, Prüllage M, et al. NF-kappaB regulates spatial memory formation and synaptic plasticity through protein kinase A/CREB signaling. Mol Cell Biol. 2006 Apr;26(8):2936–46.

115. Mattson MP, Meffert MK. Roles for NF-κB in nerve cell survival, plasticity, and disease [Internet]. Vol. 13, Cell Death and Differentiation. Nature Publishing Group; 2006. p. 852–60. Available from: http://www.nature.com/articles/4401837

116. Chen T, Wu Y, Wang Y, Zhu J, Chu H, Kong L, et al. Brain-Derived Neurotrophic Factor Increases Synaptic Protein Levels via the MAPK/Erk Signaling Pathway and Nrf2/Trx Axis Following the Transplantation of Neural Stem Cells in a Rat Model of Traumatic Brain Injury. Neurochem Res [Internet]. 2017 Nov 5;42(11):3073–83. Available from: http://link.springer.com/10.1007/s11064-017-2340-7

117. Sugita A, Ogawa H, Azuma M, Muto S, Honjo A, Yanagawa H, et al. Antiallergic and Anti-Inflammatory Effects of a Novel I B Kinase Inhibitor, IMD-0354, in a Mouse Model of Allergic Inflammation. Int Arch Allergy Immunol [Internet]. 2009;148:186–98. Available from: www.karger.com

118. Wang ZQ, Wu DC, Huang FP, Yang GY. Inhibition of MEK/ERK 1/2 pathway reduces pro-inflammatory cytokine interleukin-1 expression in focal cerebral ischemia. Brain Res. 2004 Jan 16;996(1):55–66.

119. Rylski M, Kaczmarek L. AP-1 targets in the brain [Internet]. Vol. 9, Frontiers in Bioscience. Frontiers in Bioscience; 2004 [cited 2020 Oct 28]. p. 8–23. Available from: https://pubmed-ncbi-nlm-nih-gov.proxy.library.emory.edu/14766339/

120. Duncia J V., Santella JB, Higley CA, Pitts WJ, Wityak J, Frietze WE, et al. MEK inhibitors: The chemistry and biological activity of U0126, its analogs, and cyclization products. Bioorganic Med Chem Lett. 1998;

121. Bloom MJ, Saksena SD, Swain GP, Behar MS, Yankeelov TE, Sorace AG. The effects of IKK-beta inhibition on early NF-kappa-B activation and transcription of downstream genes. Cell Signal. 2019 Mar 1;55:17–25.

122. Munoz L, Ammit AJ. Neuropharmacology Targeting p38 MAPK pathway for the treatment of Alzheimer ' s disease. Neuropharmacology [Internet]. 2010;58(3):561–8. Available from: http://dx.doi.org/10.1016/j.neuropharm.2009.11.010

123. Janes KA, Albeck JG, Gaudet S, Sorger PK, Lauffenburger DA, Yaffe MB. Cell signaling: A systems model of signaling identifies a molecular basis set for cytokine-induced apoptosis. Science (80-). 2005 Dec 9;310(5754):1646–53.

124. Eisen MB, Spellman PT, Brown PO, Botstein D. Cluster analysis and display of genome-wide expression patterns. Proc Natl Acad Sci U S A [Internet]. 1998 Dec 8;95(25):14863–8. Available from: http://www.ncbi.nlm.nih.gov/pubmed/9843981

125. Kanonidis EI, Roy MM, Deighton RF, Le Bihan T. Protein Co-Expression Analysis as a Strategy to Complement a Standard Quantitative Proteomics Approach: Case of a Glioblastoma Multiforme Study. PLoS One [Internet]. 2016;11(8):e0161828. Available from: http://www.ncbi.nlm.nih.gov/pubmed/27571357

126. Gierut JJ, Wood LB, Lau KS, Lin Y-J, Genetti C, Samatar AA, et al. Network-level effects of kinase inhibitors modulate TNF-α-induced apoptosis in the intestinal epithelium. Sci Signal [Internet]. 2015 Dec 15;8(407):ra129. Available from: http://www.ncbi.nlm.nih.gov/pubmed/26671150

127. Lake D, Corrêa SAL, Müller J. Negative feedback regulation of the ERK1/2 MAPK pathway [Internet]. Vol. 73, Cellular and Molecular Life Sciences. 2016. p. 4397–413. Available from: http://www.ncbi.nlm.nih.gov/pubmed/27342992

128. Hutti JE, Turk BE, Asara JM, Ma A, Cantley LC, Abbott DW. I B Kinase Phosphorylates the K63 Deubiquitinase A20 To Cause Feedback Inhibition of the NF- B Pathway. Mol Cell Biol [Internet]. 2007 Nov 1;27(21):7451–61. Available from: https://mcb.asm.org/content/27/21/7451.short

129. Varley CL, Armitage S, Hassanshahiraviz G, Dickson AJ. Regulation of the C-X-C chemokine, mob-1, gene expression in primary rat hepatocytes. Cytokine [Internet]. 2003 Aug 7 [cited 2020 Oct 28];23(3):64–75. Available from: https://pubmed.ncbi.nlm.nih.gov/12906869/

130. Anisowicz A, Messineo M, Lee SW, Sager R. An NF-kappa B-like transcription factor mediates IL-1/TNF-alpha induction of gro in human fibroblasts. J Immunol. 1991;147(2).

131. Ohtsuka T, Kubota A, Hirano T, Watanabe K, Yoshida H, Tsurufuji M, et al.

Glucocorticoid-mediated gene suppression of rat cytokine-induced neutrophil chemoattractant CINC/gro, a member of the interleukin-8 family, through impairment of NF-κB activation. J Biol Chem [Internet]. 1996 Jan 19 [cited 2020 Oct 28];271(3):1651–9. Available from: https://pubmed.ncbi.nlm.nih.gov/8576166/

132. Yeruva S, Ramadori G, Raddatz D. NF-κB-dependent synergistic regulation of CXCL10 gene expression by IL-1β and IFN-γ in human intestinal epithelial cell lines. Int J Colorectal Dis [Internet]. 2008 Mar [cited 2020 Oct 28];23(3):305–17. Available from: /pmc/articles/PMC2225996/?report=abstract

133. Lavoie H, Gagnon J, Therrien M. ERK signalling: a master regulator of cell behaviour, life and fate [Internet]. Vol. 21, Nature Reviews Molecular Cell Biology. Nature Research; 2020 [cited 2020 Oct 28]. p. 607–32. Available from: www.nature.com/nrm

134. Shah S, King EM, Chandrasekhar A, Newton R. Roles for the Mitogen-activated Protein Kinase (MAPK) Phosphatase, DUSP1, in Feedback Control of Inflammatory Gene Expression and Repression by Dexamethasone * □ S. 2014 [cited 2020 Oct 28]; Available from: http://www.jbc.org/

135. Yi A-K, Yoon J-G, Yeo S-J, Hong S-C, English BK, Krieg AM. Role of Mitogen-Activated Protein Kinases in CpG DNA-Mediated IL-10 and IL-12 Production: Central Role of Extracellular Signal-Regulated Kinase in the Negative Feedback Loop of the CpG DNA-Mediated Th1 Response. J Immunol [Internet]. 2002 May 1 [cited 2020 Oct 28];168(9):4711–20. Available from: http://www.jimmunol.org/content/168/9/4711http://www.jimmunol.org/content/168/9/4711.full#ref-list-1

136. Kreutzberg GW. Microglia: a sensory for pathological events in the CNS. TiNS [Internet]. 1996;19
(8):312-318
. Available from: http://www.sciencedirect.com/science/article/pii/0166223696100497

137. Zha Z, Bucher F, Nejatfard A, Zheng T, Zhang H, Yea K, et al. Interferon-γ is a master checkpoint regulator of cytokine-induced differentiation. Proc Natl Acad Sci U S A [Internet]. 2017 Aug 15 [cited 2020 Oct 28];114(33):E6867–74. Available from: https://www.pnas.org/content/114/33/E6867

138. Zhu Y, Culmsee C, Klumpp S, Krieglstein J. Neuroprotection by transforming growth factor-β1 involves activation of nuclear factor-κB through phosphatidylinositol-3-OH kinase/Akt and mitogen-activated protein kinase-extracellular-signal regulated kinase1,2 signaling pathways. Neuroscience. 2004 Jan 1;123(4):897–906.

139. Madrid L V, Wang C-Y, Guttridge DC, Schottelius AJG, Baldwin AS, Mayo MW. Akt Suppresses Apoptosis by Stimulating the Transactivation Potential of the RelA/p65 Subunit of NF-B Downloaded from [Internet]. Vol. 20, MOLECULAR AND CELLULAR BIOLOGY. 2000 [cited 2020 Oct 29]. Available from: http://mcb.asm.org/

140. Blum S, Moore AN, Adams F, Dash PK. A Mitogen-Activated Protein Kinase Cascade in the CA1/CA2 Subfield of the Dorsal Hippocampus Is Essential for Long-Term Spatial Memory [Internet]. 1999. Available from: http://www.jneurosci.org/content/jneuro/19/9/3535.full.pdf

141. C. AB, P. MM. Evidence for the involvement of TNF and NF-κB in hippocampal synaptic plasticity. Synapse. 1999;35(2):151–9.

142. Meffert MK, Chang JM, Wiltgen BJ, Fanselow MS, Baltimore D. NF-κB functions in

synaptic signaling and behavior. Nat Neurosci [Internet]. 2003 Oct 31;6(10):1072–8. Available from: http://www.nature.com/articles/nn1110

143. Tiedje C, Holtmann H, Gaestel M. The role of mammalian MAPK signaling in regulation of cytokine mRNA stability and translation [Internet]. Vol. 34, Journal of Interferon and Cytokine Research. Mary Ann Liebert Inc.; 2014 [cited 2021 Mar 4]. p. 220–32. Available from: https://www.liebertpub.com/doi/abs/10.1089/jir.2013.0146

144. Tak PP, Firestein GS. NF-κB: A key role in inflammatory diseases [Internet]. Vol. 107, Journal of Clinical Investigation. The American Society for Clinical Investigation; 2001 [cited 2021 Mar 4]. p. 7–11. Available from: /pmc/articles/PMC198552/

145. Hanisch UK. Microglia as a source and target of cytokines. Glia. 2002;40(2):140–55.

146. Bartos M, Vida I, Jonas P. Synaptic mechanisms of synchronized gamma oscillations in inhibitory interneuron networks [Internet]. Vol. 8, Nature Reviews Neuroscience. Nature Publishing Group; 2007 [cited 2021 Mar 4]. p. 45–56. Available from: https://www.nature.com/articles/nrn2044

147. Buzsáki G, Wang X-J. Mechanisms of Gamma Oscillations. Annu Rev Neurosci [Internet]. 2012 Jul 21 [cited 2021 Jan 25];35(1):203–25. Available from: http://www.annualreviews.org/doi/10.1146/annurev-neuro-062111-150444

148. Parrish RR, Codadu NK, Racca C, Trevelyan AJ. Pyramidal cell activity levels affect the polarity of activity-induced gene transcription changes in interneurons. J Neurophysiol [Internet]. 2018 Nov 1 [cited 2021 Jan 25];120(5):2358–67. Available from: /pmc/articles/PMC6295532/?report=abstract

149. Salles A, Romano A, Freudenthal R. Synaptic NF-kappa B pathway in neuronal plasticity and memory. Vol. 108, Journal of Physiology Paris. Elsevier Masson SAS; 2014. p. 256–62.

150. Alonso M, Medina JH, Pozzo-Miller L. ERK1/2 Activation Is Necessary for BDNF to Increase Dendritic Spine Density in Hippocampal CA1 Pyramidal Neurons. Learn Mem [Internet]. 2004 [cited 2021 Jan 25];11(2):172–8. Available from: http://www.learnmem.org/cgi/doi/10.1101/

151. Wang X, Zhou Z, Yang C, Xu J, Yang J. Nuclear factor-κB is involved in the phenotype loss of parvalbumin-interneurons in vitro. Neuroreport [Internet]. 2011 Apr 20 [cited 2021 Jan 25];22(6):264–8. Available from: http://journals.lww.com/00001756-201104200-00002

152. Meberg PJ, Kinney WR, Valcourt EG, Routtenberg A. Gene expression of the transcription factor NF-κB in hippocampus: Regulation by synaptic activity. Mol Brain Res. 1996 Jun 1;38(2):179–90.

153. Fann DYW, Lim YA, Cheng YL, Lok KZ, Chunduri P, Baik SH, et al. Evidence that NF-κB and MAPK Signaling Promotes NLRP Inflammasome Activation in Neurons Following Ischemic Stroke. Mol Neurobiol [Internet]. 2018 Feb 1 [cited 2021 Jan 25];55(2):1082–96. Available from: https://link.springer.com/article/10.1007/s12035-017-0394-9

154. Suzuki S, Tanaka K, Nagata E, Ito D, Dembo T, Fukuuchi Y. Cerebral neurons express interleukin-6 after transient forebrain ischemia in gerbils. Neurosci Lett. 1999 Mar 5;262(2):117–20.

155. Orzyłowska O, Oderfeld-Nowak B, Zaremba M, Januszewski S, Mossakowski M. Prolonged and concomitant induction of astroglial immunoreactivity of interleukin-1beta and interleukin-6 in the rat hippocampus after transient global ischemia. Neurosci Lett. 1999 Mar 1;263(1):72–6.

156. Tchelingerian JL, Vignais L, Jacque C. Tnfα gene expression is induced in neurones after a hippocampal lesion. Neuroreport [Internet]. 1994 [cited 2021 Jan 25];5(5):585–8. Available from: https://pubmed.ncbi.nlm.nih.gov/8025249/

157. Breder CD, Tsujimoto M, Terano Y, Scott DW, Saper CB. Distribution and characterization of tumor necrosis factor-α-like immunoreactivity in the murine central nervous system. J Comp Neurol [Internet]. 1993 [cited 2021 Jan 25];337(4):543–67. Available from: https://pubmed.ncbi.nlm.nih.gov/8288770/

158. Gong C, Qin Z, Betz AL, Liu XH, Yang GY. Cellular localization of tumor necrosis factor alpha following focal cerebral ischemia in mice. Brain Res [Internet]. 1998 Aug 10 [cited 2021 Jan 25];801(1–2):1–8. Available from: https://pubmed.ncbi.nlm.nih.gov/9729236/

159. Du Yan S, Zhu H, Fu J, Fang Yan S, Roher A, Tourtellotte WW, et al. Amyloid-peptide-Receptor for Advanced Glycation Endproduct interaction elicits neuronal expression of macrophage-colony stimulating factor: A proinflammatory pathway in Alzheimer disease (microglianeuronscerebrospinal f luid) [Internet]. Vol. 94, Medical Sciences Health Sciences. 1997. Available from: www.pnas.org.

160. Elmore MRP, Lee RJ, West BL, Green KN. Characterizing newly repopulated microglia in the adult mouse: Impacts on animal behavior, cell morphology, and neuroinflammation. PLoS One. 2015;

161. Fu H, Zhao Y, Hu D, Wang S, Yu T, Zhang L. Depletion of microglia exacerbates injury and impairs function recovery after spinal cord injury in mice. Cell Death Dis [Internet]. 2020 Jul 1 [cited 2021 Feb 11];11(7):1–12. Available from: https://doi.org/10.1038/s41419-020-2733-4

162. Kozlowski C, Weimer RM. An Automated Method to Quantify Microglia Morphology and Application to Monitor Activation State Longitudinally In Vivo. Tansey MG, editor. PLoS One [Internet]. 2012 Feb 28 [cited 2021 Feb 11];7(2):e31814. Available from: https://dx.plos.org/10.1371/journal.pone.0031814

163. Hefendehl JK, Neher JJ, Sühs RB, Kohsaka S, Skodras A, Jucker M. Homeostatic and injury-induced microglia behavior in the aging brain. Aging Cell [Internet]. 2014 Feb 1 [cited 2021 Feb 11];13(1):60–9. Available from: http://doi.wiley.com/10.1111/acel.12149

164. Sawada M, Suzumura A, Yamamoto H, Marunouchi T. Activation and proliferation of the isolated microglia by colony stimulating factor-1 and possible involvement of protein kinase C. Brain Res. 1990 Feb 12;509(1):119–24.

165. Aloisi F, Penna G, Cerase J, Menéndez Iglesias B, Adorini L. IL-12 production by central nervous system microglia is inhibited by astrocytes. J Immunol. 1997;159(4).

166. Bruttger J, Karram K, Wörtge S, Regen T, Marini F, Hoppmann N, et al. Genetic Cell Ablation Reveals Clusters of Local Self-Renewing Microglia in the Mammalian Central Nervous System. Immunity [Internet]. 2015 Jul 21 [cited 2021 Feb 11];43(1):92–106. Available from: https://pubmed.ncbi.nlm.nih.gov/26163371/

167. Garcia JM, Stillings SA, Leclerc JL, Phillips H, Edwards NJ, Robicsek SA, et al. Role of interleukin-10 in acute brain injuries [Internet]. Vol. 8, Frontiers in Neurology. Frontiers

Media S.A.; 2017 [cited 2021 Feb 11]. p. 244. Available from: www.frontiersin.org

168. Brewer KL, Bethea JR, Yezierski RP. Neuroprotective effects of interleukin-10 following excitotoxic spinal cord injury. Exp Neurol. 1999 Oct 1;159(2):484–93.

169. Lemke R, Gadient RA, Schliebs R, Bigl V, Patterson PH. Neuronal expression of leukemia inhibitory factor (LIF) in the rat brain. Neurosci Lett [Internet]. 1996 Sep 13 [cited 2021 Feb 12];215(3):205–8. Available from: https://pubmed.ncbi.nlm.nih.gov/8899749/

170. Shin WH, Lee D-Y, Park KW, Kim SU, Yang M-S, Joe E-H, et al. Microglia expressing interleukin-13 undergo cell death and contribute to neuronal survival in vivo. Glia [Internet]. 2004 Apr 15 [cited 2021 Feb 12];46(2):142–52. Available from: http://doi.wiley.com/10.1002/glia.10357

171. Imai Y, Kohsaka S. Intracellular signaling in M-CSF-induced microglia activation: Role of Iba1. Glia [Internet]. 2002 Nov 1 [cited 2021 Feb 12];40(2):164–74. Available from: http://doi.wiley.com/10.1002/glia.10149

172. Théry C, Hétier E, Evrard C, Mallat M. Expression of macrophage colony-stimulating factor gene in the mouse brain during development. J Neurosci Res [Internet]. 1990 May 1 [cited 2021 Feb 12];26(1):129–33. Available from: http://doi.wiley.com/10.1002/jnr.490260117

173. Maguire O, O'Loughlin K, Minderman H. Simultaneous assessment of NF-κB/p65 phosphorylation and nuclear localization using imaging flow cytometry. J Immunol Methods [Internet]. 2015 Aug 1 [cited 2021 Mar 7];423:3–11. Available from: /pmc/articles/PMC4522232/

174. Guan Z, Kuhn JA, Wang X, Colquitt B, Solorzano C, Vaman S, et al. Injured sensory neuron-derived CSF1 induces microglial proliferation and DAP12-dependent pain. Nat Neurosci [Internet]. 2015 Dec 29 [cited 2021 Feb 12];19(1):94–101. Available from: /pmc/articles/PMC4703328/

175. Nandi S, Gokhan S, Dai XM, Wei S, Enikolopov G, Lin H, et al. The CSF-1 receptor ligands IL-34 and CSF-1 exhibit distinct developmental brain expression patterns and regulate neural progenitor cell maintenance and maturation. Dev Biol. 2012 Jul 15;367(2):100–13.

176. Tchelingerian JL, Quinonero J, Booss J, Jacque C. Localization of TNFα and IL-1a immunoreactivities in striatal neurons after surgical injury to the hippocampus. Neuron. 1993 Feb 1;10(2):213–24.

177. Scheller J, Chalaris A, Schmidt-Arras D, Rose-John S. The pro- and anti-inflammatory properties of the cytokine interleukin-6. Vol. 1813, Biochimica et Biophysica Acta - Molecular Cell Research. Elsevier; 2011. p. 878–88.

178. Dolmetsch RE, Xu K, Lewis RS. Calcium oscillations increase the efficiency and specificity of gene expression. Nature [Internet]. 1998 Apr 30 [cited 2021 Feb 17];392(6679):933–6. Available from: https://pubmed-ncbi-nlm-nih-gov.proxy.library.emory.edu/9582075/

179. Gewirtz AT, Rao AS, Simon PO, Merlin D, Carnes D, Madara JL, et al. Salmonella typhimurium induces epithelial IL-8 expression via Ca2+- mediated activation of the NF-κb pathway. J Clin Invest [Internet]. 2000 [cited 2021 Feb 17];105(1):79–92. Available from: https://pubmed.ncbi.nlm.nih.gov/10619864/

180. Lilienbaum A, Israël A. From Calcium to NF-κB Signaling Pathways in Neurons. Mol Cell Biol [Internet]. 2003 Apr 15 [cited 2021 Feb 17];23(8):2680–98. Available from: /pmc/articles/PMC152563/

181. Rosen LB, Ginty DD, Greenberg ME, Weber MJ. Membrane Depolarization and Calcium Influx Stimulate MEK and MAP Kinase via Activation of Ras. 1994;12:1207–21.

182. Agell N, Bachs O, Rocamora N, Villalonga P. Modulation of the Ras/Raf/MEK/ERK pathway by Ca2+, and Calmodulin [Internet]. Vol. 14, Cellular Signalling. Cell Signal; 2002 [cited 2021 Feb 18]. p. 649–54. Available from: https://pubmed-ncbi-nlm-nih-gov.proxy.library.emory.edu/12020764/

183. Farnsworth CL, Freshney NW, Rosen LB, Ghosh A, Greenberg ME, Feig LA. Calcium activation of Ras mediated by neuronal exchange factor Ras-GRF. Nature [Internet]. 1995 [cited 2021 Feb 18];376(6540):524–7. Available from: https://pubmed.ncbi.nlm.nih.gov/7637786/

184. LaFerla FM. Calcium dyshomeostasis and intracellular signalling in alzheimer's disease. Nat Rev Neurosci [Internet]. 2002 [cited 2021 Feb 27];3(11):862–72. Available from: https://www.nature.com/articles/nrn960

185. Adaikkan C, Tsai LH. Gamma Entrainment: Impact on Neurocircuits, Glia, and Therapeutic Opportunities [Internet]. Vol. 43, Trends in Neurosciences. Elsevier Ltd; 2020 [cited 2021 Feb 22]. p. 24–41. Available from: https://doi.org/10.1016/j.tins.2019.11.001

186. Becher AK, Höhne M, Axmacher N, Chaieb L, Elger CE, Fell J. Intracranial electroencephalography power and phase synchronization changes during monaural and

binaural beat stimulation. Eur J Neurosci. 2015;

187. Mulinari S. Monoamine Theories of Depression: Historical Impact on Biomedical Research. J Hist Neurosci [Internet]. 2012 Oct 1 [cited 2021 Feb 23];21(4):366–92. Available from: http://www.tandfonline.com/doi/abs/10.1080/0964704X.2011.623917

188. Sawicki CM, McKim DB, Wohleb ES, Jarrett BL, Reader BF, Norden DM, et al. Social defeat promotes a reactive endothelium in a brain region-dependent manner with increased expression of key adhesion molecules, selectins and chemokines associated with the recruitment of myeloid cells to the brain. Neuroscience. 2015 Aug 7;302:151–64.

189. Wohleb ES, Powell ND, Godbout JP, Sheridan JF. Stress-induced recruitment of bone marrow-derived monocytes to the brain promotes anxiety-like behavior. J Neurosci [Internet]. 2013 Aug 21 [cited 2021 Feb 23];33(34):13820–33. Available from: https://www.jneurosci.org/content/33/34/13820

190. Kappelmann N, Lewis G, Dantzer R, Jones PB, Khandaker GM. Antidepressant activity of anti-cytokine treatment: A systematic review and meta-analysis of clinical trials of chronic inflammatory conditions. Mol Psychiatry [Internet]. 2018 Feb 1 [cited 2021 Feb 23];23(2):335–43. Available from: www.nature.com/mp

191. Fitzgerald PJ, Watson BO. Gamma oscillations as a biomarker for major depression: an emerging topic. Transl Psychiatry [Internet]. 2018;8(1). Available from: http://dx.doi.org/10.1038/s41398-018-0239-y

192. Arion D, Unger T, Lewis DA, Levitt P, Mirnics K. Molecular Evidence for Increased Expression of Genes Related to Immune and Chaperone Function in the Prefrontal Cortex in Schizophrenia. Biol Psychiatry. 2007 Oct 1;62(7):711–21.

193. Radtke FA, Chapman G, Hall J, Syed YA. Modulating neuroinflammation to treat neuropsychiatric disorders [Internet]. Vol. 2017, BioMed Research International. Hindawi Limited; 2017 [cited 2021 Feb 24]. Available from: /pmc/articles/PMC5664241/

194. Stosiek C, Garaschuk O, Holthoff K, Konnerth A. In vivo two-photon calcium imaging of neuronal networks. Proc Natl Acad Sci U S A [Internet]. 2003 Jun 10 [cited 2021 Feb 26];100(12):7319–24. Available from: www.pnas.orgcgidoi10.1073pnas.1232232100

195. Yang W, Yuste R. In vivo imaging of neural activity [Internet]. Vol. 14, Nature Methods. Nature Publishing Group; 2017 [cited 2021 Feb 26]. p. 349–59. Available from: https://www.nature.com/articles/nmeth.4230

196. Chen X, Leischner U, Rochefort NL, Nelken I, Konnerth A. Functional mapping of single spines in cortical neurons in vivo. Nature [Internet]. 2011 Jul 28 [cited 2021 Feb 26];475(7357):501–5. Available from: https://www.nature.com/articles/nature10193

197. Jia H, Rochefort NL, Chen X, Konnerth A. Dendritic organization of sensory input to cortical neurons in vivo. Nature [Internet]. 2010 Apr 29 [cited 2021 Feb 26];464(7293):1307–12. Available from: https://www.nature.com/articles/nature08947

198. Vasicek TW, Jackson MR, Poseno TM, Stenken JA. In vivo microdialysis sampling of cytokines from rat hippocampus: Comparison of cannula implantation procedures. ACS Chem Neurosci [Internet]. 2013 May 15 [cited 2021 Feb 26];4(5):737–46. Available from: /pmc/articles/PMC3656755/

199. Ghirnikar RS, Lee YL, He TR, Eng LF. Chemokine expression in rat stab wound brain injury. J Neurosci Res [Internet]. 1996 Dec 15 [cited 2021 Feb 26];46(6):727–33. Available from: https://onlinelibrary.wiley.com/doi/10.1002/(SICI)1097-

4547(19961215)46:6%3C727::AID-JNR9%3E3.0.CO;2-H

200. Clapp-Lilly KL, Roberts RC, Duffy LK, Irons KP, Hu Y, Drew KL. An ultrastructural analysis of tissue surrounding a microdialysis probe. J Neurosci Methods [Internet]. 1999 Aug 15 [cited 2021 Feb 26];90(2):129–42. Available from: https://pubmed.ncbi.nlm.nih.gov/10513596/

201. Heneka MT, Gavrilyuk V, Landreth GE, O'Banion MK, Weinberg G, Feinstein DL. Noradrenergic depletion increases inflammatory responses in brain: Effects on IκB and HSP70 expression. J Neurochem [Internet]. 2003 [cited 2021 Feb 26];85(2):387–98. Available from: https://pubmed-ncbi-nlm-nih-gov.proxy.library.emory.edu/12675915/

202. Chalermpalanupap T, Kinkead B, Hu WT, Kummer MP, Hammerschmidt T, Heneka MT, et al. Targeting norepinephrine in mild cognitive impairment and Alzheimer's disease [Internet]. Vol. 5, Alzheimer's Research and Therapy. Alzheimers Res Ther; 2013 [cited 2021 Feb 26]. Available from: https://pubmed.ncbi.nlm.nih.gov/23634965/

203. Scullion GA, Kendall DA, Marsden CA, Sunter D, Pardon MC. Chronic treatment with the α 2-adrenoceptor antagonist fluparoxan prevents age-related deficits in spatial working memory in APP × PS1 transgenic mice without altering β-amyloid plaque load or astrocytosis. Neuropharmacology. 2011 Feb 1;60(2–3):223–34.

204. Garza KM, Zhang L, Borron B, Wood LB, Singer AC. Gamma visual stimulation induces a neuroimmune signaling profile distinct from acute neuroinflammation. J Neurosci [Internet]. 2020 Feb 5 [cited 2021 Feb 26];40(6):1211–25. Available from: https://doi.org/10.1523/JNEUROSCI.1511-19.2019

205. Sánchez-Alegría K, Flores-León M, Avila-Muñoz E, Rodríguez-Corona N, Arias C. PI3K

signaling in neurons: A central node for the control of multiple functions [Internet]. Vol. 19, International Journal of Molecular Sciences. MDPI AG; 2018 [cited 2021 Feb 26]. Available from: /pmc/articles/PMC6321294/

206. Cianciulli A, Porro C, Calvello R, Trotta T, Lofrumento DD, Panaro MA. Microglia mediated neuroinflammation: Focus on PI3K modulation [Internet]. Vol. 10, Biomolecules. MDPI AG; 2020 [cited 2021 Feb 26]. Available from: https://pubmed-ncbi-nlm-nih-gov.proxy.library.emory.edu/31947676/

207. Badimon A, Ayata P, Strasburger HJ, Chen X, Ikegami A, Graves SM, et al. Negative feedback control of neuronal activity by microglia. Nature. 2020;

208. Akiyoshi R, Wake H, Kato D, Horiuchi H, Ono R, Ikegami A, et al. Microglia enhance synapse activity to promote local network synchronization. eNeuro [Internet]. 2018 Sep 1 [cited 2021 Feb 26];5(5):88–106. Available from: /pmc/articles/PMC6220592/

209. Kol A, Adamsky A, Groysman M, Kreisel T, London M, Goshen I. Astrocytes contribute to remote memory formation by modulating hippocampal–cortical communication during learning. Nat Neurosci [Internet]. 2020 Oct 1 [cited 2021 Feb 26];23(10):1229–39. Available from: https://doi.org/10.1038/s41593-020-0679-6

210. Lee HS, Ghetti A, Pinto-Duarte A, Wang X, Dziewczapolski G, Galimi F, et al. Astrocytes contribute to gamma oscillations and recognition memory. Proc Natl Acad Sci U S A [Internet]. 2014 Aug 12 [cited 2021 Feb 26];111(32):E3343–52. Available from: www.pnas.org/cgi/doi/10.1073/pnas.1410893111

211. Dong Y, Benveniste EN. Immune function of astrocytes. Glia [Internet]. 2001 Nov 1 [cited 2021 Feb 26];36(2):180–90. Available from:

http://doi.wiley.com/10.1002/glia.1107